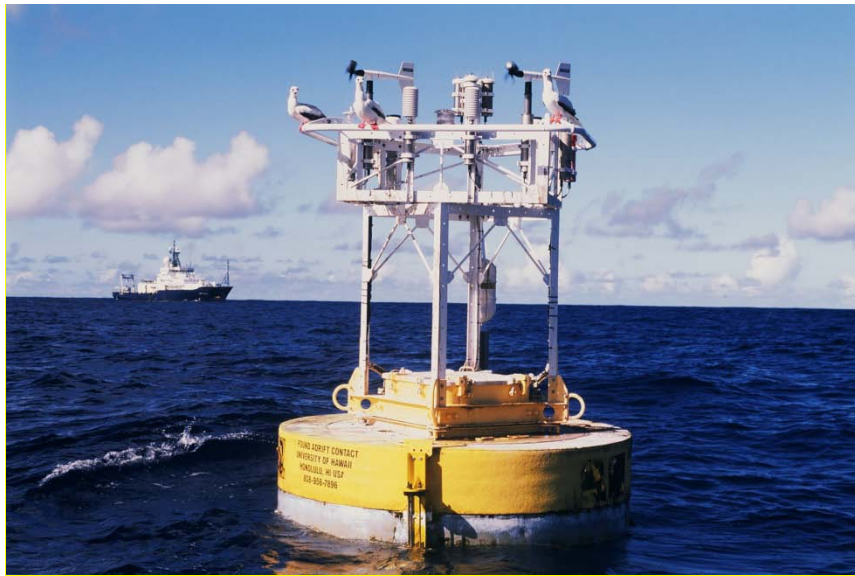


Hydrographic Observations at the
Woods Hole Oceanographic Institution
Hawaii Ocean Time-series Site:
2016 – 2017
Data Report #13

Fernando Santiago-Mandujano, Andrew King, Kellen Rosburg, Ksenia Trifonova, Daniel McCoy, R. Walter Deppe, Albert Plueddemann, Robert Weller, Roger Lukas, Jeffrey Snyder, and Nan Galbraith

January, 2019



SCHOOL OF OCEAN AND EARTH
SCIENCE AND TECHNOLOGY
UNIVERSITY OF HAWAII AT HONOLULU

SOEST Publication no. 10643

Acknowledgments

Many people participated in the WHOTS mooring deployment/recovery cruises. They are listed in Tables 2.1 and 2.4. We gratefully acknowledge their contributions and support. Thanks are due to all the personnel of the Upper Ocean Processes Group (UOP) at WHOI who prepared the WHOTS buoy's instrumentation and mooring; to Kelsey Maloney, Noah Howins, Garrett Hebert, and Svetlana Natarov, for their technical assistance with the moored and shipboard instrumentation; to Kellie Terada for her excellent project support. We gratefully acknowledge the support from the colleagues at Sea-Bird for helping us maintain the quality of the CTD data. We would also like to thank the captains and crew of the Ship *Hi'ialakai* and especially the University of Hawaii (UH) Marine Center staff for their efforts. The WHOTS project is funded in part by the Ocean Observing and Monitoring Division, Climate Program Office (FundRef number 100007298). National Oceanic and Atmospheric Administration, US Department of Commerce under grant NA14OAR4320158. This work is also supported by the National Science Foundation grant OCE12-60164.

Table of Contents

I.	Introduction.....	1
II.	Description of the WHOTS-13 Mooring Cruises	3
A.	WHOTS-13 Cruise: WHOTS-13 Mooring Deployment	3
B.	WHOTS-14 Cruise: WHOTS-13 Mooring Recovery.....	5
III.	Description of WHOTS-13 Mooring.....	8
IV.	WHOTS-13 and -14 cruise shipboard observations	11
A.	Conductivity, Temperature and Depth (CTD) profiling.....	11
1.	Data acquisition and processing.....	12
2.	CTD sensor calibration and corrections.....	13
Pressure	13	
Temperature/Conductivity	13	
Dissolved Oxygen.....	13	
B.	Water sampling and analysis	13
Salinity	13	
C.	Thermosalinograph data acquisition and processing	14
1.	WHOTS-13 Cruise.....	14
Temperature Calibration	15	
Nominal Conductivity Calibration.....	15	
Data Processing.....	15	
Bottle Salinity and CTD Salinity Comparisons	16	
CTD Temperature Comparisons	16	
2.	WHOTS-14 Cruise.....	16
Temperature Calibration	17	
Nominal Conductivity Calibration.....	17	
Data Processing.....	17	
Bottle Salinity and CTD Salinity Comparisons	18	
CTD Temperature Comparisons	18	
D.	Shipboard ADCP	19
1.	WHOTS-13 Deployment Cruise.....	19
2.	WHOTS-14 Deployment Cruise.....	19
V.	Moored Instrument Observations	20
A.	MicroCAT/SeaCAT data processing procedures.....	20
1.	Internal Clock Check and Missing Samples	21
2.	Pressure Drift Correction and Pressure Variability	21
3.	Temperature Sensor Stability.....	23
Comparisons with VMCM and ADCP temperature sensors	25	
4.	Conductivity Calibration.....	30
B.	Acoustic Doppler Current Profiler.....	40
1.	Compass Calibrations	40
2.	ADCP Configurations.....	43
3.	ADCP data processing procedures.....	44
C.	Vector Measuring Current Meter (VMCM)	54
D.	Global Positioning System Receiver and ARGOS Positions	60
VI.	Results.....	63
A.	CTD Profiling Data.....	65

B.	Thermosalinograph data.....	77
C.	MicroCAT/SeaCAT data	81
D.	Moored ADCP data.....	100
E.	Moored and Shipboard ADCP comparisons.....	107
F.	Next Generation Vector Measuring Current Meter data (VMCM)	114
G.	GPS data.....	116
H.	Mooring Motion.....	117
VII.	References	119
VIII.	Appendices.....	121
A.	Appendix 1: WHOTS-13 300 kHz ADCP Configuration	121
B.	Appendix 2: WHOTS-13 600 kHz ADCP Configuration	122

I. Introduction

In 2003, Robert Weller (Woods Hole Oceanographic Institution [WHOI]), Albert Plueddemann (WHOI), and Roger Lukas (University of Hawaii [UH]) proposed to establish a long-term surface mooring at the Hawaii Ocean Time-series (HOT) Station ALOHA (22°45'N, 158°W) to provide sustained, high-quality air-sea fluxes and the associated upper ocean response as a coordinated part of the HOT program, and as an element of the global array of ocean reference stations supported by the National Oceanic and Atmospheric Administration's (NOAA) Office of Climate Observation.

With support from NOAA and the National Science Foundation (NSF), the WHOI HOT Site (WHOTS) surface mooring has been maintained at Station ALOHA since August 2004. The objective of this project is to provide long-term, high-quality air-sea fluxes as a coordinated part of the HOT program and contribute to the goals of observing heat, fresh water, and chemical fluxes at a site representative of the oligotrophic North Pacific Ocean. The approach is to maintain a surface mooring outfitted for meteorological and oceanographic measurements at a site near Station ALOHA by successive mooring turnarounds. These observations are being used to investigate air-sea interaction processes related to climate variability and change.

The original mooring system is described in the mooring deployment/recovery cruise reports (Plueddemann et al., 2006; Whelan et al., 2007). Briefly, a Surlyn foam surface buoy is equipped with meteorological instrumentation including two complete Air-Sea Interaction Meteorological (ASIMET) systems (Hosom et al. (1995), Colbo and Weller (2009)), measuring air and sea surface temperatures, relative humidity, barometric pressure, wind speed and direction, incoming shortwave and longwave radiation, and precipitation. Complete surface meteorological measurements are recorded every minute, as required to compute air-sea fluxes of heat, freshwater, and momentum. Each ASIMET system also transmits hourly averages of the surface meteorological variables via the Argos satellite system and via iridium. The mooring line is instrumented in order to collect time series of upper ocean temperatures, salinities and velocities with the surface forcing record. This includes conductivity, salinity and temperature recorders, two Vector Measuring Current Meters (VMCMs), and two Acoustic Doppler current profilers (ADCPs). See the WHOTS-13 mooring diagram in Figure 1-1.

The subsurface instrumentation is located vertically to resolve the temporal variations of shear and stratification in the upper pycnocline to support study of mixed layer entrainment. Experience with moored profiler measurements near Hawaii suggests that Richardson number estimates over 10 m scales are adequate. Salinity is crucial to water mass stratification, as salt-stratified barrier layers are observed at HOT and in the region (Kara et al., 2000), thus Sea-Bird MicroCATs with vertical separation ranging from 5-20 m were used to measure temperature and salinity. A Teledyne RD Instruments (TRDI) ADCP obtains current profiles across the entrainment zone and another in the mixed layer. Both ADCPs are in an upward-looking configuration, one is at 125 m, using 4 m bins, and the other is a 47.5 m using 2 m bins. To provide near-surface velocity (where the ADCP estimates are less reliable) we deploy two VMCMs. The nominal mooring design is a balance between resolving extremes versus typical annual cycling of the mixed layer (see WHOTS Data Report 1-2, Santiago-Mandujano et al., 2007).

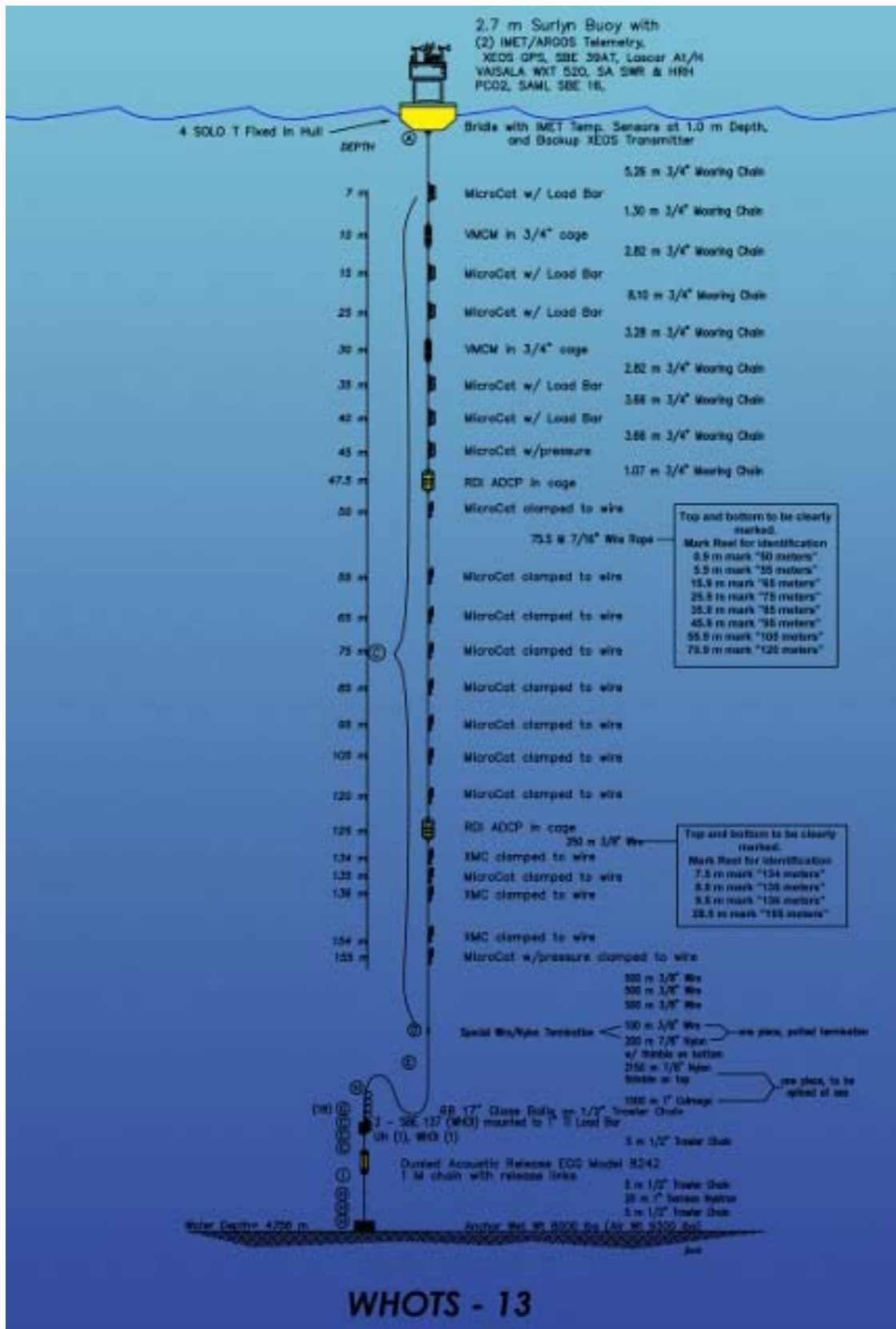


Figure 1-1. WHOTS-13 mooring design.

The 13th WHOTS mooring (WHOTS-13 mooring) was deployed on June 27th, 2016 during a seven-day cruise (WHOTS-13 cruise), and was recovered on August 1st, 2017 during a nine-day cruise (WHOTS-14 cruise); both cruises were aboard the NOAA Ship *Hi'ialakai*. A 14th mooring (WHOTS-14 mooring) was deployed during the WHOTS-14 cruise; to be recovered in September 2018.

This report documents and describes the oceanographic observations made on the 13th WHOTS mooring during a period of nearly one year, and from shipboard measurements during the two cruises when the mooring was deployed and recovered. Sections II and III include a detailed description of the cruises and the mooring, respectively. Sampling and processing procedures of the hydrographic casts, thermosalinograph, and shipboard ADCP data collected during these cruises are described in Section IV. Section V includes the processing procedures for the data collected by the moored instruments: SeaCATs, MicroCATs, VMCMs, and moored ADCPs. Plots of the resulting data and a preliminary analysis are presented in Section VI.

II. Description of the WHOTS-13 Mooring Cruises

A. WHOTS-13 Cruise: WHOTS-13 Mooring Deployment

The Woods Hole Oceanographic Institution Upper Ocean Processes Group (WHOI/UOP), with the assistance of the UH group conducted the 13th deployment of the WHOTS mooring on board the NOAA Ship *Hi'ialakai* during the WHOTS-13 cruise between June 25th and July 2nd, 2016. The WHOTS-13 mooring was deployed at HOT Station 50 on June 27th, 2016 and the anchor was dropped at 08:48 UTC at 22° 47.39'N, 157° 54.48'W. Scientific personnel who participated in the cruise are listed in Table 2-1.

Table 2-1. Scientific personnel on Ship *Hi'ialakai* during the WHOTS-13 deployment cruise.

Cruise	Name	Title or function	Affiliation
WHOTS-13	Plueddeman, Albert	Chief Scientist	WHOI
	Smith, Jason	Senior Engineering Assistant	WHOI
	Cole, Rick	Mooring Specialist	RDSea Inc.
	Snyder, Jeffrey	Marine Electronic's Technician	UH
	Santiago-Mandujano, Fernando	Research Associate	UH
	McCoy, Daniel	Research Associate	UH
	Deppe, Robert Walter	Research Associate	UH
	Rosburg, Kellen	Research Associate	UH
	Carter, Glenn	Research Scientist	UH
	Berry, Katrina	Technician	UH
	Meskhidze, Nicolas	Professor	NCSU
	Royalty, Taylor	Student	NCSU
	Harvey, Julia	Teacher	South Eugene High School

The shipboard oceanographic observations during the cruise were conducted by the UH group.

A Sea-Bird CTD (conductivity, temperature and depth) system was used to measure T, S, and O₂ profiles during CTD casts. The time, location, and maximum CTD pressure for each of the profiles are listed in Table 2-2. Ten CTD casts were conducted during the WHOTS-13 cruise. CTD profile data were collected at Station 50 (near the WHOTS-13 buoy), and Station 52 (near the WHOTS-12 buoy). A test cast was conducted at Station 20 (21°27.95'N 158°21.24'W) offshore of Makaha, HI to a depth of 1500 m in order to test three acoustic releases. Four 200 m yo-yo casts were conducted at Station 52 for comparison with subsurface instruments on the WHOTS-12 mooring prior to recovery. These casts each consisted of five up-down cycles between 5 and 200 dbar. Five more yo-yo casts were performed at Station 50 for comparison with subsurface instruments on the WHOTS-13 mooring just after deployment. These consisted of three hours of up-down cycling (approximately 14 cycles each). The last cycle of the fifth cast was to a depth of 2000 m to allow ship's engineers to grease the CTD wire on the up-cast. Four water samples were taken from each casts for salinity analysis at UH.

Table 2-2. CTD stations occupied during the WHOTS-13 cruise

Station/ cast	Date	Time (GMT)	Location (using NMEA data)	Maximum pressure (dbar)
20 / 1	06/26/16	04:07	21° 27.95' N, 158° 21.24' W	1510
52 / 1	06/28/16	00:13	22° 39.58' N, 157° 58.26' W	203
52 / 2	06/28/16	02:25	22° 39.48' N, 157° 58.86' W	208
52 / 3	06/28/16	05:02	22° 39.30' N, 157° 59.50' W	209
52 / 4	06/28/16	07:26	22° 39.48' N, 157° 58.31' W	208
50 / 1	07/02/16	20:07	22° 46.39' N, 157° 56.38' W	210
50 / 2	07/02/16	00:51	22° 46.26' N, 157° 56.46' W	211
50 / 3	07/02/16	05:53	22° 46.34' N, 157° 56.49' W	209
50 / 4	07/02/16	16:06	22° 45.89' N, 157° 56.41' W	209
50 / 5	07/02/16	19:52	22° 46.46' N, 157° 56.66' W	2010

In addition, continuous ADCP and near surface thermosalinograph data were obtained while underway.

The NOAA Ship *Hi'ialakai* was equipped with an RD Instruments Ocean Surveyor 75 kHz ADCP, set to function in broadband and narrowband configurations. The configuration information is shown in Table 2-3. The ADCP used input from a S.G. Brown gyrometer and a Furuno GP 90 GPS receiver to establish the heading and attitude of the ship, while an Applanix POSMV4 system archived attitude data for use in post-processing.

A description of these operations is available in the WHOTS-13 cruise report (Santiago-Mandujano *et al.*, 2016).

Table 2-3. Configuration of the Ocean Surveyor 75kHz ADCP on board the Ship *Hi'ialakai* during the WHOTS-13 cruise.

	OS75BB	OS75NB
Sample interval (s)	900	900
Number of bins	80	60
Bin Length (m)	8	16
Pulse Length (m)	8	16
Transducer depth (m)	5	5
Blanking length (m)	16	24

Near-surface temperature and salinity data during the WHOTS-13 cruise were acquired through the use of a thermosalinograph (TSG) system aboard Ship *Hi'ialakai*. The sensors were sampling water from the continuous seawater system running through the ship, and were comprised of one thermosalinograph model SBE-21 and a micro-thermosalinograph model SBE-45, both with (internal) temperature and conductivity sensors located in the ship's wet lab, about 67 m from separate hull intakes; and an SBE-38 external temperature sensor located at the entrance to one of the water intakes. The SBE-21 recorded data every 5 seconds, and the other two instruments recorded data every second. The water intake for the SBE-21 and SBE-38 is located at the bow of the ship, next to the starboard side bow thruster, at a depth of 2 m. The intake for the SBE-45 is located near the middle of the ship, also 2 m deep. The system's pressure gauge indicated 20 psi at the sampling spigot, however, pressure decreased to ~18 psi when the valve was opened for sampling.

Data from the SBE-45 exhibited numerous conductivity and temperature glitches, indicating a possible problem with the system; SBE-21 data and calculated salinities were of good quality (see Section VI-B). SBE-21 data did exhibit some large conductivity spikes, which often occur due to bubble entrainment from the surface, especially during bad weather or while the ship is pitching in transit. The records from the external and internal temperature sensors are also of good quality, the internal temperature from the SBE-21 appears to be consistently lower than the external temperature, probably due to cooling from the ship's A/C system while the water travels from the intake to the thermosalinograph. The SBE-45 micro-thermosalinograph uses a much smaller volume of water as compared to the SBE-21, and seems to be affected more significantly by the wet-lab's temperature changes than the SBE-21.

B. WHOTS-14 Cruise: WHOTS-13 Mooring Recovery

The WHOI/UOP group with the assistance of the UH group conducted the WHOTS-13 mooring turnaround operations during the WHOTS-14 cruise between July 26th and August 1st 2017. The WHOTS-13 mooring was recovered on June 31st, and the WHOTS-14 mooring was deployed at Station 52 on July 28th, 2017 02:19 UTC at 22° 40.02 'N, 157° 57.09 'W.

The scientific personnel that participated during the cruise are listed in Table 2-4.

Table 2-4. Scientific personnel on Ship *Hi'ialakai* during the WHOTS-14 cruise (WHOTS-13 mooring recovery).

Cruise	Name	Title or function	Affiliation
WHOTS-14	Weller, Robert	Chief Scientist	WHOI
	Hasbrouck, Emerson	Marine Technician	WHOI
	Adams, Samantha	Teacher	WHOI
	Clabaugh, Abby	Summer Fellow	WHOI
	Blomquist, Byron	ESRL Meteorologist	NOAA
	Snyder, Jeffrey	Marine Technician	UH
	Santiago-Mandujano, Fernando	Research Associate	UH
	Rosburg, Kellen	Research Associate	UH
	King, Andrew	Research Associate	UH
	Natarov, Svetlana	Research Associate	UH
	Maloney, Kelsey	Student	UH
	Howins, Noah	Student	UH
	Hebert, Garrett	Student	UH

The shipboard oceanographic observations during the cruise were conducted by the UH group. A description of these operations is available in the WHOTS-14 cruise report (Santiago-Mandujano *et al.*, 2017).

A Sea-Bird CTD system was used to measure T, S, and O₂ profiles during CTD casts. The time, location, and maximum CTD pressure for each of the profiles are listed in Table 2-5. Thirteen CTD casts were conducted during the WHOTS-14 cruise, from July 26th through August 1st, 2017. CTD profile data were collected Station 52 (near the WHOTS-14 buoy), and Station 50 (near the WHOTS-13 buoy). A test cast was conducted at Station 20 (21°30.76'N 158°22.70'W) offshore of Makaha, HI to an approximate depth of 1500 m in order to test three acoustic releases. Five CTD yo-yo casts were conducted to obtain profiles for comparison with subsurface instruments on the WHOTS-14 mooring after deployment, and five yo-yo casts were conducted for comparison with the WHOTS-13 mooring before recovery. These casts were started less than 0.5 nm from the buoys with varying drift during each cast, and consisted of 5 up-down cycles between near the surface and 210 m, except for S52C4 which was to 490 m in its last cycle. S50C1 showed conductivity and oxygen glitches at 70 dbar during the downcast of the 4th cycle, probably caused by some biology going through the plumbing. The conductivity and oxygen traces appeared to return to normal values soon after, and the secondary sensors did not show any anomaly during this event. Two 3500 m CTD casts were conducted near the WHOTS-13 and -14 buoys respectively (S50C6 and S52C6), to obtain deep Brunt-Väisälä frequency profiles. The CTD had a modulo error at 1275 dbar during the S50C6 downcast, the pumps went off momentarily, and the primary and secondary conductivity and oxygen traces showed large glitches. There was also one modulo error during S52C6 at 1210 dbar downcast, with glitches in primary and secondary oxygen. It is unknown what caused these errors, though it is suspected that one of the conductors was compromised.

Water samples were taken from all casts; 4 samples for each of them. These samples were to be analyzed for salinity at UH and used to calibrate the CTD conductivity sensors.

Table 2-5. CTD stations occupied during the WHOTS-14 cruise (WHOTS-13 mooring recovery).

Station/cast	Date	Time (UTC)	Location (using NMEA data)	Maximum pressure (dbar)
20 / 1	07/26/2017	04:32	21° 30.761' N, 158° 22.695' W	1525
52 / 1	07/28/2017	16:13	22° 38.835' N, 157° 59.132' W	215
52 / 2	07/28/2017	20:02	22° 39.229' N, 157° 58.849' W	207
52 / 3	07/29/2017	00:07	22° 39.199' N, 157° 58.856' W	214
52 / 4	07/29/2017	04:03	22° 39.087' N, 157° 59.061' W	490
52 / 5	07/29/2017	08:04	22° 39.328' N, 157° 58.950' W	213
50 / 1	07/29/2017	16:04	22° 46.002' N, 157° 55.804' W	215
50 / 2	07/29/2017	19:56	22° 46.072' N, 157° 55.782' W	215
50 / 3	07/29/2017	23:56	22° 46.048' N, 157° 56.767' W	211
50 / 4	07/30/2017	04:02	22° 45.763' N, 157° 56.389' W	214
50 / 5	07/30/2017	07:59	22° 45.961' N, 157° 56.594' W	215
50 / 6	07/30/2017	23:07	22° 45.608' N, 157° 55.934' W	3501
52 / 6	08/01/2017	23:29	22° 39.309' N, 158° 3.562' W	3206

In addition, continuous ADCP and near surface thermosalinograph data were obtained while underway.

The NOAA Ship *Hi'ialakai* was equipped with an TRDI Ocean Surveyor 75 kHz ADCP, set to function in broadband and narrowband configurations. The configuration information is shown in Table 2-6. The ADCP used input from a S.G. Brown gyrometer and a Furuno GP 90 GPS receiver to establish the heading and attitude of the ship, while an Applanix POSMV4 system archived attitude data for use in post-processing.

Table 2-6. Configuration of the Ocean Surveyor 75kHz ADCP on board the Ship *Hi'ialakai* during the WHOTS-14 cruise.

	OS75BB	OS75NB
Sample interval (s)	900	900
Number of bins	80	60
Bin Length (m)	8	16
Pulse Length (m)	8	16
Transducer depth (m)	5	5
Blanking length (m)	16	24

Near-surface temperature and salinity data during the WHOTS-14 cruise were acquired from the thermosalinograph (TSG) system installed on the NOAA Ship *Hi'ialakai*. The sensors were sampling water from the continuous seawater system running through the ship, and were comprised of one thermosalinograph model SBE-21 (SN 3155) and a micro-thermosalinograph model SBE-45 (SN 4540403-0150), both with (internal) temperature and conductivity sensors located in the ship's wet lab, about 67 m from separate hull intakes; and an SBE-38 (SN 215)

external temperature sensor located at the entrance to one of the water intakes. The SBE-21 recorded data every 5 seconds, and the other two instruments recorded data every second. The water intake for the SBE-21 and SBE-38 is located at the bow of the ship, next to the starboard side bow thruster, at a depth of 2 m. The intake for the SBE-45 is located near the middle of the ship, also 2 m deep. The system had a pressure gauge showing a flow pressure of about 20 psi, decreasing to 18 psi when the water intake was open. Both thermosalinograph systems had a debubbler.

Data from the SBE-45 records exhibited a number of very large conductivity and temperature glitches, which often occur due to bubble entrainment from the surface, especially during bad weather or while the ship is pitching in transit. However, temperature data comparisons between the SBE-45 and SBE-21 were within ± 0.05 °C outside these glitches. Conductivity and calculated salinity for the SBE-21 are of good quality (see Section VI-B). The records from the external and internal temperature sensors are also of good quality; however, temperature differences between the SBE-21 and SBE-38 cycle between ± 0.5 °C offset on a diurnal time scale (probably mostly due to ocean, but ship's temperatures also have diurnal cycle). Higher frequency cyclic temperature differences were also noted between the SBE-21 and SBE-38, typically close to 00:00 UTC.

III. Description of WHOTS-13 Mooring

The WHOTS-13 mooring, deployed on June 27th, 2016 from NOAA's Ship *Hi'ialakai*, was outfitted with two complete sets (L19 and L42) of ASIMET sensors on the buoy and underneath, and subsurface instruments from 7 to 155 m depth, and 36 m above the bottom (Figure 1-1). The WHOTS-13 recovery on July 31st, 2017 resulted in about 399 days on station.

The buoy tower also contains a radar reflector, two marine lanterns, and two independent Argos satellite transmission systems that provide continuous monitoring of buoy position. A Xeos Melo Global Positioning System (GPS) receiver, a SBE-39 temperature sensor adapted to measure air temperature and a Vaisala WXT-520 multi-variable (temperature, humidity, pressure, wind and precipitation) were also mounted on the tower. A fourth positioning system (SiS Argos transmitter) was mounted beneath the hull. Several other instruments were mounted on the buoy. A Battelle pCO₂ system, a pumped SBE-16 CTD and a SEAFET pH sensor were mounted to the underside of the buoy. The SHB-16 hosted turbidity and dissolved oxygen sensors. Three downlooking radiometers were mounted on the buoy. One hyperspectral sensor is mounted facing upward near the radiometers as a reference for the incoming spectral irradiance. A chlorophyll fluorometer was also mounted on the buoy hull.

Four internally-logging SBE-56 temperature sensors and two SBE-37 MicroCATs were bolted to the underside of the buoy hull measuring sea surface temperature (SST) and salinity. The SBE-56s measured SST once every 60 sec between 80-95 cm below the surface, and the MicroCATs were at 1.50 m (see Table 3-2). The buoy was deployed on 6/26/2016 at 19:30.

Instrumentation provided by UH for the WHOTS-13 mooring included 16 SBE-37 Microcats, and two RDI Workhorse ADCPs, transmitting in 300 kHz 600 kHz, respectively. The Microcats all measured temperature and conductivity, with 7 also measuring pressure. All MicroCATs were deployed with antifoulant capsules. In addition to the instrumentation on the buoy, WHOI provided two Vector Measuring Current Meters (VMCMs), two deep Microcats (SBE-37) installed near the bottom of the mooring, and all required subsurface mooring hardware.

Table 3-1 provides a listing of the WHOTS-13 subsurface instrumentation at their nominal depths on the mooring, along with serial numbers, sampling rates and other pertinent information. A cold water spike was induced to the UH MicroCATs before deployment and after recovery by placing an ice pack in contact with their temperature sensor to check for any drift in their internal clock. To produce a spike in the ADCP data each instrument’s transducer was rubbed gently by hand for 20 seconds before deployment and after recovery.

The RDI 300 kHz Workhorse Sentinel ADCP, SN 7637, with an additional external battery pack, was deployed at 125 m with transducers facing upwards. The instrument was set to ping at 4-second intervals for 160 seconds every 10 minutes. This burst sampling was designed to minimize aliasing by occasional large ocean swell orbital motions. Bin size was set for 4 m. This instrument also measured temperature.

The RDI 600 kHz Workhorse Sentinel ADCP, SN 13917, with an additional external battery pack, was deployed at 47.5 m with transducers facing upwards. The instrument was set to ping at 2-second intervals for 160 seconds every 10 minutes. This burst sampling was designed to minimize aliasing by occasional large ocean swell orbital motions. Bin size was set for 2 m. This instrument also measured temperature.

The two VMCMs, SN 2016 and 2075 (called here 16 and 75 respectively) were deployed at 10 m and 30 m depth , respectively. The instruments were prepared for deployment by the WHOI/UOP group and set to sample at 1-minute intervals. These instruments also measured temperature. The compass from instrument SN 16 failed and the instrument did not provide current direction data (see Sect. V-C).

Table 3-1. WHOTS-13 mooring subsurface instrument deployment information. All times are in UTC.

SN:	Instrument	Depth (m)	Pressure SN	Sample Interval (sec)	Start Logging Data		Cold Spike begin		Cold Spike end		Time in Water	
6892	MicroCAT	7	51324	75	6/23/16	0:00:00	6/24/16	22:16:00	6/24/16	22:46:00	6/26/16	18:33:00
2016	VMCM	10	N/A	60	6/19/16	20:58:00	N/A	N/A	N/A	N/A	6/26/16	18:33:00
3382	MicroCAT	15	N/A	180	6/23/16	0:00:00	6/24/16	22:16:00	6/24/16	22:46:00	6/26/16	18:29:00
4663	MicroCAT	25	N/A	180	6/23/16	0:00:00	6/24/16	22:16:00	6/24/16	22:46:00	6/26/16	18:20:00
2075	VMCM	30	N/A	60	6/19/16	22:05:00	N/A	N/A	N/A	N/A	6/26/16	18:19:00
3633	MicroCAT	35	N/A	180	6/23/16	0:00:00	6/24/16	22:16:00	6/24/16	22:46:00	6/26/16	18:15:00
3381	MicroCAT	40	N/A	180	6/23/16	0:00:00	6/24/16	22:16:00	6/24/16	22:46:00	6/26/16	18:10:00
3668	MicroCAT	45	5579	240	6/23/16	0:00:00	6/24/16	22:16:00	6/24/16	22:46:00	6/26/16	18:05:00
13917	600 kHz ADCP	47.5	N/A	600	6/23/16	0:00:00	6/25/16	00:49:54	6/25/16	00:51:00	6/26/16	19:37:00
3619	MicroCAT	50	N/A	180	6/23/16	0:00:00	6/24/16	22:16:00	6/24/16	22:46:00	6/26/16	19:37:00
3620	MicroCAT	55	N/A	180	6/23/16	0:00:00	6/24/16	22:16:00	6/24/16	22:46:00	6/26/16	19:39:00

3621	MicroCAT	65	N/A	180	6/23/16	0:00:00	6/24/16	22:16:00	6/24/16	22:46:00	6/26/16	19:40:00
3632	MicroCAT	75	N/A	180	6/23/16	0:00:00	6/24/16	22:16:00	6/24/16	22:46:00	6/26/16	19:42:00
4699	MicroCAT	85	10209	240	6/23/16	0:00:00	6/24/16	22:16:00	6/24/16	22:46:00	6/26/16	19:43:00
3791	MicroCAT	95	N/A	180	6/23/16	0:00:00	6/24/16	22:16:00	6/24/16	22:46:00	6/26/16	19:44:00
2769	MicroCAT	105	2949	240	6/23/16	0:00:00	6/24/16	22:16:00	6/24/16	22:46:00	6/26/16	19:45:00
4700	MicroCAT	120	9944	240	6/23/16	0:00:00	6/24/16	22:16:00	6/24/16	22:46:00	6/26/16	19:53:00
7637	300 kHz ADCP	125	N/A	600	6/23/16	0:00:00	6/25/16	00:10:05	6/25/16	01:00:40	6/26/16	19:54:00
2965	MicroCAT	135	3021	240	6/23/16	0:00:00	6/24/16	22:16:00	6/24/16	22:46:00	6/26/16	19:55:00
4701	MicroCAT	155	10211	240	6/23/16	0:00:00	6/24/16	22:16:00	6/24/16	22:46:00	6/26/16	19:57:00
12246	MicroCAT	36m off bottom	N/A	300	6/15/16	1:00:00	6/23/16	20:11:00	6/23/16	21:46:00	6/27/16	8:13:00
12247	MicroCAT	36m off bottom	N/A	300	6/15/16	1:00:00	6/23/16	20:11:00	6/23/16	21:46:00	6/27/16	8:13:00

Table 3-2. WHOTS-13 MicroCAT and SBE-56 Temperature Sensor Information.

Instrument	SN:	Depth (m)	Sample Interval (sec)
SBE-56	6150	0.80	60
SBE-56	6239	0.95	60
SBE-56	6410	0.80	60
SBE-56	6412	0.80	60
MicroCAT	1306	1.5	300
MicroCAT	1727	1.5	300

All WHOTS-13 instruments were successfully recovered; recovery information for the C-T instruments is shown in Table 3-3. Most of the instruments had some degree of biofouling, with the heaviest fouling near the surface. Fouling extended down to the ADCP at 125 m, although it was minor at that level.

All MicroCATs were in good condition after recovery. MicroCAT 3633 (35 m) had barnacles attached at the top end of its conductivity cell, possibly partially blocking the flow. The data from all instruments were downloaded on board the ship, and all instruments returned full data records. A post-cruise evaluation showed no missing samples in all the MicroCATs and both ADCPs. Table 3-3 has an initial evaluation of the data quality; more details are in Section V-A.

Table 3-3. WHOTS-13 MicroCAT Recovery Information. All times stated are in UTC.

Depth (m)	Sea-Bird Serial #	Time out of water	Time of Spike	Time Logging Stopped	Samples Logged	Data Quality
7	SBE 37-6892	8/01/17 02:13:00	8/01/17 05:15:00	8/01/17 06:12:30	465706	Good
15	SBE 37-3382	8/01/17 02:20:00	8/01/17 05:15:00	8/01/17 06:37:45	194052	Good
25	SBE 37-4663	8/01/17 02:25:00	8/01/17 05:15:00	8/02/17 03:15:00	194465	Good
35	SBE 37-3633	8/01/17 02:29:00	8/01/17 05:15:00	8/01/17 18:29:00	194289	Good
40	SBE 37-3381	8/01/17 02:30:00	8/01/17 05:15:00	8/01/17 06:31:00	194050	Good
45	SBE 37-3668	8/01/17 02:35:00	8/01/17 05:15:00	8/01/17 06:23:30	145535	Good
47.5	ADCP 13917	8/01/17 00:51:00	8/01/17 00:31:20	8/02/17 02:39:00	58336	Good
50	SBE 37-3619	8/01/17 00:51:00	8/01/17 05:15:00	8/01/17 06:50:15	194056	Good

55	SBE 37-3620	8/01/17 00:50:00	8/01/17 05:15:00	8/01/17 07:01:00	194060	Good
65	SBE 37-3621	8/01/17 00:49:00	8/01/17 05:15:00	8/01/17 07:06:00	194062	Good
75	SBE 37-3632	8/01/17 00:47:00	8/01/17 05:15:00	8/01/17 07:10:45	194064	Good
85	SBE 37-4699	8/01/17 00:46:00	8/01/17 05:15:00	8/1/17 18:01:15	145710	Good
95	SBE 37-3791	8/01/17 00:46:00	8/01/17 05:15:00	8/1/17 20:56:00	194338	Good
105	SBE 37-2769	8/01/17 00:45:00	8/01/17 05:15:00	8/01/17 18:31:30	145718	Good
120	SBE 37-4700	8/01/17 00:43:00	8/01/17 05:15:00	8/01/17 18:26:30	145717	Good
125	ADCP 7637	8/01/17 00:39:00	8/02/17 00:21:00	8/02/17 02:30:30	58334	Good
135	SBE 37-2965	8/01/17 00:38:00	8/01/17 05:15:00	8/01/17 18:09:30	145712	Good
155	SBE 37-4701	8/01/17 00:37:00	8/01/17 05:15:00	8/01/17 18:05:45	145711	Good
36 mab	SBE 37-12246	7/31/17 19:14:00	8/01/17 05:15:00	8/02/17 05:52:30	119003	Good
36 mab	SBE 37-12247	7/31/17 19:14:00	8/01/17 05:15:00	8/02/17 03:58:30	118981	Good

The data from the upward-looking 300 kHz ADCP at 125 m were good; the instrument was pinging upon recovery. There appears to be no obviously questionable data from this ADCP, apart from near-surface artifacts, more details are in Section V-B.

The data from the upward-looking 600 kHz ADCP at 47.5 m were good; the instrument was pinging upon recovery. There appears to be no obviously questionable data from this ADCP, apart from near-surface artifacts, more details are in Section V-B.

IV. WHOTS-13 and -14 cruise shipboard observations

The hydrographic profile observations made during the WHOTS cruises were obtained with a Sea-Bird CTD package with dual temperature, salinity and oxygen sensors. This CTD was installed on a rosette-sampler with 5-liter Niskin bottles for calibration water samples. In addition, the *Hi'ialakai* came equipped with a thermosalinograph system which provided a continuous depiction of temperature and salinity of the near-surface layer. Horizontal currents over the depth range of 30-1000 m were measured from the shipboard 75 kHz Ocean Surveyor (OS75) ADCP (narrowband) with a vertical resolution of 16m for the WHOTS-13 and WHOTS-14 cruises. Broadband mode for the OS75 provided additional current data over the range of 20-650 m with a vertical resolution of 8m.

A. Conductivity, Temperature and Depth (CTD) profiling

Continuous measurements of temperature, conductivity, dissolved oxygen and pressure were made with the UH Sea-Bird SBE-9/11Plus CTD underwater unit #09P43777-91361 (referred to as #91361) during the WHOTS-13 cruise, and #09P43777-0850 (referred to as #850) during

WHOTS-14 cruise. The CTD was equipped with an internal Digiquartz pressure sensor and pairs of external temperature, conductivity, and oxygen sensors.

Each of the temperature-conductivity sensor pairs used a Sea-Bird TC duct which circulated seawater through independent pump and plumbing installations. The CTD configuration also included two oxygen sensors, installed in the plumbing for each sensor set. In both cruises, the CTD was mounted in a vertical position in the lower part of a rosette sampler, with the sensors' water intakes located at the bottom of the rosette.

The package was deployed on a conducting cable, which allowed for real-time data acquisition and display. The deployment procedure consisted in lowering the package to approximately 10 dbar and waiting until the CTD pumps started operating. The CTD was then raised until the sensors were close to the surface to begin the CTD cast. The time and position of each cast was obtained via a GPS connection to the CTD deck box. Six Niskin bottles were used on the rosette. Four salinity samples were taken on each cast for calibration of the conductivity sensors.

1. Data acquisition and processing

CTD data were acquired at the instrument's highest sampling rate of 24 samples per second. Digital data were stored on a laptop computer and, for redundancy, the analog signal was recorded on VHS video tapes. Backups of CTD data were made onto USB storage cards.

The raw CTD data were quality controlled and screened for spikes as described in the WHOTS Data Report 1 (Santiago-Mandujano et al., 2007). Data alignment, averaging, correction and reporting were done as described in Tupas *et al.* (1993). Spikes in the data occur when the CTD samples the disturbed water of its wake. Therefore, samples from the downcast were rejected when the CTD was moving upward or when its acceleration exceeded 0.5 m s^{-2} in magnitude. The data were subsequently averaged into 2-dbar pressure bins after calibrating the CTD conductivity with the bottle salinities.

The data were additionally screened by comparing the T-C sensor pairs. These differences permitted identification of problems with the sensors. The data from only one T-C pair, whichever was deemed most reliable, is reported here. Only data from the downcast are reported, as upcast data are commonly contaminated by wake effects from the rosette.

Temperature is reported in the ITS-90 scale. Salinity and all derived units were calculated using the UNESCO (1981) routines; salinity is reported in the practical salinity scale (PSS-78). Oxygen is reported in $\mu\text{mol kg}^{-1}$.

2. CTD sensor calibration and corrections

Pressure

The pressure calibration strategy for CTD pressure transducers SN 75434 used during WHOTS-13 and SN 101430 used during WHOTS-14 cruises employed a high-quality quartz pressure transducer as a transfer standard. Periodic recalibrations of this lab standard were performed with a primary pressure standard. The only corrections applied to the CTD pressures were a constant offset determined at the time that the CTD first enters the water on each cast. In addition, a span correction determined from bench tests on the sensor against the transfer standard was applied. These procedures and corrections are thoroughly documented in the HOT-2016 and 2017 data reports (Fujieki et al. 2018, 2019)

Temperature/Conductivity

Sea-Bird SBE-3-Plus temperature and SBE 4C conductivity transducers were used during WHOTS-13 and -14 cruises. The history and performance of these sensors have been monitored during HOT cruises, and calibrations and drift corrections applied during WHOTS cruises are thoroughly documented in the HOT-2016 and 2017 data reports (Fujieki et al. 2018, 2019).

Dissolved Oxygen

Sea-Bird SBE-43 oxygen sensors were used during the WHOTS-13 and -14 cruises. Oxygen data from the WHOTS-13 cruise were calibrated using empirical calibration coefficients obtained during the HOT-284 cruise conducted on 27-31 May 2016, before the WHOTS-13 cruise, which used the same oxygen sensors. Similarly, the WHOTS-14 oxygen data were calibrated using calibration coefficients obtained during the HOT-294 cruise conducted on 19-23 June 2017, before the WHOTS-14 cruise, which used the same oxygen sensors. Fujieki, et al. (2018, 2019) have details on these calibrations. The CTD empirical calibration was conducted using oxygen water samples and the procedure from Owens and Millard (1985). See Tupas et al. (1997) for details on these calibrations procedures.

B. Water sampling and analysis

Salinity

Salinity samples were collected by a rosette sampler during CTD casts at selected depths during WHOTS-13 and -14, and sub-sampled in 250 ml glass bottles. The top of each bottle and thimble were thoroughly dried before being tightly capped to prevent water from being trapped between the cap or thimble and the bottle's mouth. It has been observed that residual water trapped in this way increases its salinity due to evaporation, and it can leak into the sample when the bottle is opened for measuring. Samples from each cruise were measured after the cruise in

the laboratory at the UH using a Guildline Autosol 8400B (SN 70168). IAPSO¹ standard seawater samples were measured to standardize the Autosol, and samples from a large batch of “secondary standard” (substandard) seawater were measured after every 24-48 samples to detect drift in the Autosol. Standard deviations of the secondary standard measurements were less than ± 0.001 for WHOTS-13 and -14 cruises (Table 4-1).

The substandard water was collected by a rosette sampler from 1020 m at station ALOHA during HOT cruises and drained into a 50-liter Nalgene plastic carboy. In the laboratory, the water was then thoroughly mixed in a glass carboy for 20 minutes by manually shaking, rolling and tilting the carboy vigorously, after which a 2-inch protective layer of white oil was added on top to deter evaporation. The substandard water was allowed to stand for approximately three days before it was used, and was stored in the same temperature controlled room as the Autosol, protecting it from the light with black plastic bags to inhibit biological growth. Substandard seawater batches #60 and #61 were prepared on 15 September 2015 and 9 June 2016, and used for WHOTS-13 and -14 samples, respectively.

Samples from WHOTS-13 cruise were measured during the same session as the HOT-285 samples. Samples from WHOTS-14 cruise were measured during the same session as the HOT-295 samples. The substandard statistics in Table 4-1 include the combined substandard samples measured for the WHOTS-13 and HOT-285 samples and the WHOTS-14 and HOT-295 samples, respectively.

Table 4-1. Precision of salinity measurements of secondary lab standards.

Cruise	Mean Salinity +/- SD	# Samples	Substandard Batch #	IAPSO Batch #
WHOTS-13 / HOT-285	34.5080 \pm 0.0001	5	60	P158
WHOTS-14 / HOT-295	34.4681 \pm 0.0009	4	61	P158

C. Thermosalinograph data acquisition and processing

1. WHOTS-13 Cruise

Near-surface temperature and salinity data during the WHOTS-13 cruise were acquired from the thermosalinograph (TSG) system installed on the NOAA Ship *Hi'ialakai*. The sensors were sampling water from the continuous seawater system running through the ship, and were comprised of one thermosalinograph model SBE-21 (SN 3155) and a micro-thermosalinograph model SBE-45 (SN 4537642-0121), both with (internal) temperature and conductivity sensors located in the ship's wet lab, about 67 m from separate hull intakes; and an SBE-38 external temperature sensor located at the entrance to one of the water intakes. The SBE-21 recorded data every 5 seconds, and the other two instruments recorded data every second. The water intake for

¹ International Association for Physical Sciences of the Ocean

the SBE-21 and SBE-38 (SN 215) is located at the bow of the ship, next to the starboard side bow thruster, at a depth of 2 m. The intake for the SBE-45 is located near the middle of the ship, also 2 m deep. The system had a pressure gauge showing a flow pressure of about 20 psi, decreasing to 18 psi when the valve was opened for sampling. Both systems were equipped with a de-bubbler.

Temperature Calibration

External temperature data from the SBE-38 sensor (last calibrated at Sea-Bird on 06 February 2016) were used as a measure of the seawater temperature. These data were compared to the data collected during CTD casts.

Nominal Conductivity Calibration

Data from the SBE-21 conductivity and temperature sensors were used to calculate the intake seawater salinity. These sensors were last calibrated at Sea-Bird on 09 February 2016. All conductivity data from the thermosalinograph were nominally calibrated with coefficients from this calibration. However, all the final salinity data reported here were calibrated against bottle data as explained below.

Data Processing

Daily files containing navigation data recorded every second were concatenated with the thermosalinograph data. The thermosalinograph data were then screened for gross errors, with upper and lower bounds of 18 °C and 35 °C for temperature and 3 Siemens m⁻¹ and 6 Siemens m⁻¹ for conductivity. There were no points outside the valid temperature range and no points outside the valid conductivity range.

A 5-point running median filter was used to detect one- or two-point temperature and conductivity glitches in the thermosalinograph data. Glitches in temperature and conductivity detected by the 5-point median filter were immediately replaced by the median. Threshold values of 0.3 °C for temperature and 0.1 Siemens m⁻¹ for conductivity were used for the median filter. After running the filter, there were no temperature or conductivity points replaced by the median. A 3-point triangular running mean filter was used to smooth the temperature and conductivity data after passing the glitch detection.

The thermosalinograph aboard the Ship *Hi'ialakai* was set to record data every five seconds, but occasionally, due to an error in the acquisition software rounding routine, a record is written at a longer interval. Only 369 timing errors occurred during this cruise; of these 364 were between 6 and 9 seconds, and 5 were greater than 10 seconds. One gap, however, lasted 169 seconds.

Data were visually scanned to flag spikes likely caused by contamination due to the introduction of bubbles to the flow-through system during transits or rough conditions. The *Hi'ialakai's* flow-through system was equipped with a de-bubbler. Hence, of a total of 121,686 data points, merely 235 conductivity data points (or 0.2%) were flagged as bad.

Bottle Salinity and CTD Salinity Comparisons

The thermosalinograph salinity was calibrated by comparing it to bottle salinity samples drawn from a water intake next to the thermosalinograph every 8 hours throughout the cruise. Of the 21 bottles sampled, one was considered an outlier and discarded from analysis. Samples were analyzed as described in Section IV-B. The comparison was made in conductivity in order to eliminate the effects of temperature. Conductivity of each bottle sample was computed using the salinity of the bottle, thermosalinograph temperature and a pressure of 3.44 dbar, which includes the pressure of the flowthrough system's pump.

Salinity samples were drawn from the flowthrough system, located less than 0.5 m from the SBE-21 and consequently there should be virtually no delay between when the water passes through the thermosalinograph and it being sampled. A 90 second average centered on the sample draw time was chosen for processing purposes.

The CTD salinity data at 2 dbar from the 10 casts conducted during the cruise was used for comparisons with the thermosalinograph conductivity. Using the thermosalinograph temperature data and a pressure of 3.44 dbar, the CTD conductivity was calculated for the 10 casts conducted while the thermosalinograph was running. Five CTD casts were excluded from processing as outliers. The SBE-21 conductivity sensor had a mean offset of 0.0009 Sm^{-1} with respect to the CTD data.

A cubic spline was fit to the time series of the differences between the bottle and TSG conductivity and a correction was obtained for the TSG conductivities. Salinity was calculated using these corrected conductivities, the thermosalinograph temperatures, and 3.44 dbar pressure. After correction, the mean difference between the bottle and thermosalinograph salinities was 0.0000 psu with a standard deviation of 0.0032 psu. The mean CTD - thermosalinograph difference was -0.0001 psu with a standard deviation of 0.0022 psu.

CTD Temperature Comparisons

There were 10 CTD casts conducted during the WHOTS-13 cruise. The 2 dbar CTD temperature data were used to compare with the thermosalinograph internal temperature. Five CTD casts were excluded from processing as obvious outliers. The mean difference between the internal sensor and the CTD was $-0.2320 \text{ }^\circ\text{C}$, with a standard deviation of $\pm 0.0327 \text{ }^\circ\text{C}$.

2. WHOTS-14 Cruise

Near-surface temperature and salinity data during the WHOTS-14 cruise were acquired from the thermosalinograph (TSG) system installed on the NOAA Ship *Hi'ialakai*. The sensors were sampling water from the continuous seawater system running through the ship, and were comprised of one thermosalinograph model SBE-21 (SN 3155) and a micro-thermosalinograph model SBE-45 (SN 4540403-0150), both with (internal) temperature and conductivity sensors located in the ship's wet lab, about 67 m from separate hull intakes; and an SBE-38 (SN 215) external temperature sensor located at the entrance to one of the water intakes. The SBE-21 recorded data every 5 seconds, and the other two instruments recorded data every second. The water intake for the SBE-21 and SBE-38 is located at the bow of the ship, next to the starboard side bow thruster, at a depth of 2 m. The intake for the SBE-45 is located near the middle of the ship, also 2 m deep. The system had a pressure gauge showing a flow pressure of about 20 psi, decreasing to 18 psi when the water intake was open. Both thermosalinograph systems had a de-bubbler.

Temperature Calibration

External temperature data from the SBE-38 sensor (last calibrated at Sea-Bird on 06 Feb. 2016) were used as a measure of the seawater temperature. These data were compared to the data collected during CTD casts.

Nominal Conductivity Calibration

Data from the SBE-21 conductivity and temperature sensors were used to calculate the intake seawater salinity. These sensors were last calibrated at Sea-Bird on 09 Feb. 2016. All conductivity data from the thermosalinograph were nominally calibrated with coefficients from this calibration. However, all the final salinity data reported here were calibrated against bottle data as explained below.

Data Processing

Daily files containing navigation data recorded every second were concatenated with the thermosalinograph data. The thermosalinograph data were then screened for gross errors, with upper and lower bounds of 18 °C and 35 °C for temperature and 3 Siemens m⁻¹ and 6 Siemens m⁻¹ for conductivity. There were no points outside the valid temperature range and no points outside the valid conductivity range.

A 5-point running median filter was used to detect one- or two-point temperature and conductivity glitches in the thermosalinograph data. Glitches in temperature and conductivity detected by the 5-point median filter were immediately replaced by the median. Threshold values of 0.3 °C for temperature and 0.1 Siemens m⁻¹ for conductivity were used for the median filter. After running the filter, there were no temperature or conductivity points replaced by the median.

A 3-point triangular running mean filter was used to smooth the temperature and conductivity data after passing the glitch detection.

The thermosalinograph aboard the Ship Hi'ialakai was set to record data every five seconds, but occasionally, due to an error in the acquisition software rounding routine, a record is written at a longer interval. Only 2 timing errors occurred during this cruise; both were greater than 20 seconds. The largest gap lasted 473 seconds.

Data were visually scanned to flag spikes likely caused by contamination due to the introduction of bubbles to the flow-through system during transits or rough conditions. Of a total of 754,531 data points, 6,773 conductivity data points (0.9%) were flagged as bad.

Bottle Salinity and CTD Salinity Comparisons

The thermosalinograph salinity was calibrated by comparing it to bottle salinity samples drawn from a water intake next to the thermosalinograph every 8 hours throughout the cruise. Of the 24 bottles sampled, six were considered outliers and discarded from analysis. Samples were analyzed as described in Section IV-B. The comparison was made in conductivity in order to eliminate the effects of temperature. Conductivity of each bottle sample was computed using the salinity of the bottle, thermosalinograph temperature and a pressure of 3.44 dbar, which includes the pressure of the flowthrough system's pump.

Salinity samples were drawn from the flowthrough system, located less than 0.5 m from the SBE-21 and consequently there should be virtually no delay between when the water passes through the thermosalinograph and it being sampled. A 90 second average centered on the sample draw time was chosen for processing purposes.

The CTD salinity data at 2 dbar from the 13 casts conducted during the cruise was used for comparisons with the thermosalinograph conductivity. Using the thermosalinograph temperature data and a pressure of 3.44 dbar, the CTD conductivity was calculated for the 13 casts conducted while the thermosalinograph was running. Six CTD casts were excluded from processing as outliers.

A cubic spline was fit to the time series of the differences between the bottle and TSG conductivity and a correction was obtained for the TSG conductivities. Salinity was calculated using these corrected conductivities, the thermosalinograph temperatures, and 3.44 dbar pressure. After correction, the mean difference between the bottle and thermosalinograph salinities was 0.000 psu with a standard deviation of 0.001 psu. The mean CTD - thermosalinograph difference was -0.002 psu with a standard deviation of 0.001 psu.

CTD Temperature Comparisons

There were 13 CTD casts conducted during the WHOTS-14 cruise. The 2 dbar CTD temperature data were used to compare with the thermosalinograph internal temperature. Six

CTD casts were excluded from processing as outliers. The mean difference between the internal sensor and the CTD was $-0.259\text{ }^{\circ}\text{C}$, with a standard deviation of $\pm 0.071\text{ }^{\circ}\text{C}$.

D. Shipboard ADCP

1. WHOTS-13 Deployment Cruise

Currents were measured for the duration of the cruise over the depth range of 30-1000 m with a 75 kHz RDI Ocean Surveyor (OS75) ADCP working in narrowband mode with a vertical resolution of 16 m, and in broadband mode with vertical resolution of 8 m. The system yielded good data (see cruise report). Periods of missing data between 300 and 450 m in the broadband ADCP are apparently due to the lack of scatter material in the water. The gaps in the data occurred when the system was shut down temporarily during communications with the acoustic releases used for the moorings. The long gap on June 28 from about 19:40 to 22:00 UTC was during triangulation of the WHOTS-13 anchor after deployment. The times of the datasets from the OS75 are shown in Table 4-2.

Table 4-2. ADCP record times (UTC) for the Narrow Band 75 kHz ADCP during the WHOTS-13 cruise.

WHOTS-13	OS75nb	OS75bb
File beginning time	25-Jun-2016 20:06:59	25-Jun-2016 20:06:59
File ending time	03-Jul-2016 17:22:24	03-Jul-2016 17:19:55

2. WHOTS-14 Deployment Cruise

Currents were measured for the duration of the cruise over the depth range of 30-1000 m with a 75 kHz RDI Ocean Surveyor (OS75) ADCP working in narrowband mode with a vertical resolution of 16 m, and in broadband mode with vertical resolution of 8 m. The system yielded good data (see cruise report). Periods of missing data between 300 and 450 m in the broadband ADCP are apparently due to the lack of scatter material in the water. The times of the datasets from the OS75 are shown in Table 4-3.

Table 4-3. ADCP record times (UTC) for the 75 kHz ADCP during the WHOTS-14 cruise.

WHOTS-14	OS75nb	OS75bb
File beginning time	25-Jul-2017 22:06:18	25-Jul-2017 22:06:18
File ending time	03-Aug-2017 18:03:04	03-Aug-2017 17:53:02

V. Moored Instrument Observations

A. MicroCAT/SeaCAT data processing procedures

Each moored MicroCAT and SeaCAT temperature, conductivity and pressure (when installed) was calibrated at Sea-Bird prior to their deployment and after their recovery on the dates shown in Table 5-1. The internally-recorded data from each instrument were downloaded on board the ship after the mooring recovery, and the nominally-calibrated data were plotted for a visual assessment of the data quality. The data processing included checking the internal clock data against external event times, pressure sensor drift correction, temperature sensor stability, and conductivity calibration against CTD data from casts conducted near the mooring during HOT and WHOTS cruises. The detailed processing procedures are described in this section.

Table 5-1. WHOTS-13 MicroCAT temperature sensor calibration dates, and sensor drift during deployments.

Nominal deployment depth (m)	Sea-Bird Serial number	Pre-deployment calibration	Post-recovery calibration	Temperature sensors annual drift during WHOTS-13 (mili°C)
1.5	1306	19-Dec-2015	19-Apr-2018	-0.21
1.5	1727	19-Dec-2015	19-Apr-2018	0.11
7	6892	15-Oct-2015	12-Sep-2017	0.68
15	3382	15-Oct-2015	07-Sep-2017	0.36
25	4663	15-Oct-2015	07-Sep-2017	0.69
35	3633	29-Sep-2015	07-Sep-2017	0.26
40	3381	29-Sep-2015	07-Sep-2017	-0.11
45	3668	01-Oct-2015	21-Sep-2017	0.51
50	3619	25-Sep-2015	12-Sep-2017	0.46
55	3620	16-Oct-2015	10-Sep-2017	1.01
65	3621	15-Oct-2015	10-Sep-2017	0.89
75	3632	21-Nov-2015	10-Sep-2017	1.06
85	4699	14-Oct-2015	07-Sep-2017	-0.02
95	3791	15-Oct-2015	07-Sep-2017	0.81
105	2769	15-Oct-2015	07-Sep-2017	0.98
120	4700	14-Oct-2015	07-Sep-2017	0.54
135	2965	17-Nov-2015	07-Sep-2017	0.53

155	4701	12-Oct-2015	10-Sep-2017	0.53
4657	12246	29-May-2014	20-Apr-2018	-0.02
4657	12247	25-May-2014	20-Apr-2018	-0.20

1. Internal Clock Check and Missing Samples

Before the WHOTS-13 mooring deployment and after its recovery (before the data logging was stopped), the MicroCATs temperature sensors were placed in contact with an ice pack to create a spike in the data, to check for any problems with their internal clocks, and for possible missing samples (Table 3-2). The cold spike was detected by a sudden decrease in temperature. For all the instruments, the clock time of this event matched correctly the time of the spike (within the sampling interval of each instrument). No missing samples were detected for any of the instruments.

2. Pressure Drift Correction and Pressure Variability

Some of the MicroCATs used in the moorings were outfitted with pressure sensors (Table 3-1). Biases were detected in the pressure sensors by comparing the on-deck pressure readings (which should be zero for standard atmospheric pressure at sea level of 1029 mbar) before deployment and after recovery. Table 5-2 shows the magnitude of the bias for each of the sensors before and after deployment. To correct for this offset, a linear fit between the initial and final on-deck pressure offset as a function of time was obtained, and subtracted from each sensor. Figure 5-1 shows the linearly corrected pressures measured by the MicroCATs during the WHOTS-13 deployment. For all the sensors, the mean difference from the nominal instrument pressure (based on the deployed depth) was less than 1.5 dbar. The standard deviation of the pressure for the duration of the record was also less than 1 dbar for all sensors, with the deeper sensors showing a slightly larger standard deviation. The sensors below 7 m seem to have been about 1 m shallower than their nominal depth. The range of variability for all sensors was about ± 3 dbar.

The causes of pressure variability can be several, including density variations in the water column above the instrument; horizontal dynamic pressure (not only due to the currents, but also due to the motion of the mooring); mooring position, etc. (see WHOTS Data Report 1, Santiago-Mandujano et al., 2007).

Table 5-2. Pressure bias of MicroCATs with pressure sensor.

Deployment	Depth (m)	Sea-Bird Serial #	Bias before deployment (dbar)	Bias after recovery (dbar)
WHOTS-13	7	SBE 37-6892	0.045	0.01
WHOTS-13	45	SBE 37-3668	0.03	-0.01
WHOTS-13	85	SBE 37-4699	0.015	0.00

WHOTS-13	105	SBE 37-2769	0.03	0.02
WHOTS-13	120	SBE 37-4700	0.05	-0.45
WHOTS-13	135	SBE 37-2965	0.08	-0.40
WHOTS-13	155	SBE 37-4701	-0.015	-0.02

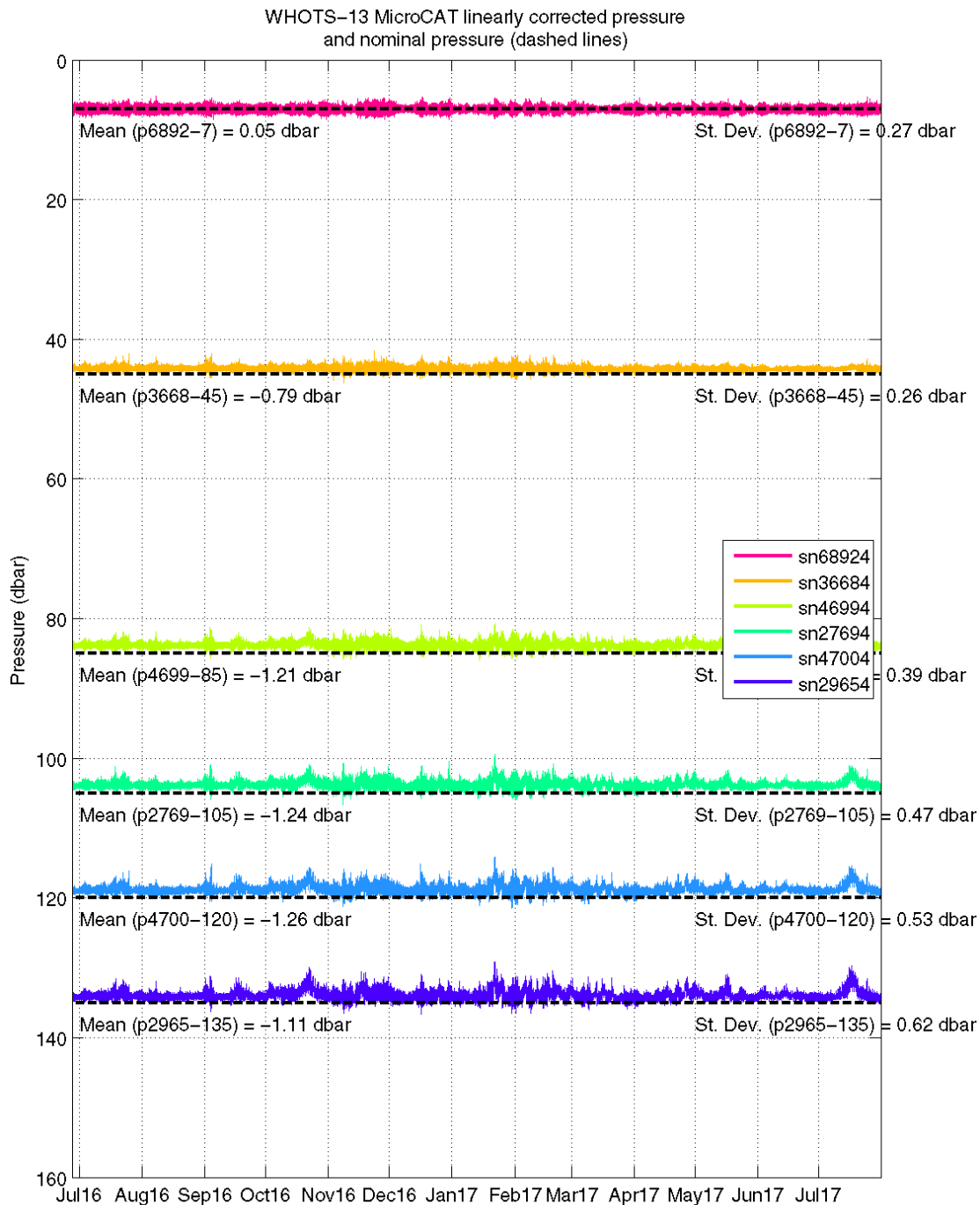


Figure 5-1. Linearly corrected pressures from MicroCATs during WHOTS-13 deployment. The horizontal dashed line is the sensor's nominal pressure, based on deployed depth.

3. Temperature Sensor Stability

The MicroCAT and SeaCAT temperature sensors were calibrated at Sea-Bird before and after each deployment, and their annual drift evaluations are shown in Table 5-1. These values turned out to be insignificant (not higher than 1.2 milli °C) for all sensors. Comparisons between the MicroCAT and CTD data from casts conducted near the mooring during HOT cruises confirmed that the temperature drift of the rest of the moored instruments was insignificant. The two MicroCATs (SN 12246 and SN 12247) deployed near the bottom were drift corrected. Figure 5-7 (upper panel) shows the temperature differences between both instruments before and after the correction. After the correction the temperature differences were in the ± 1.5 milli°C range.

Temperature comparisons between one of the WHOTS-13 near-surface MicroCATs (SN 1306) and the four SBE-56 surface temperature sensors in the buoy hull (Table 3-2) are shown in Figure 5-2. All of the SBE-56 instruments returned full records. None of the instruments show any obvious bias when compared to the Microcat measurements.

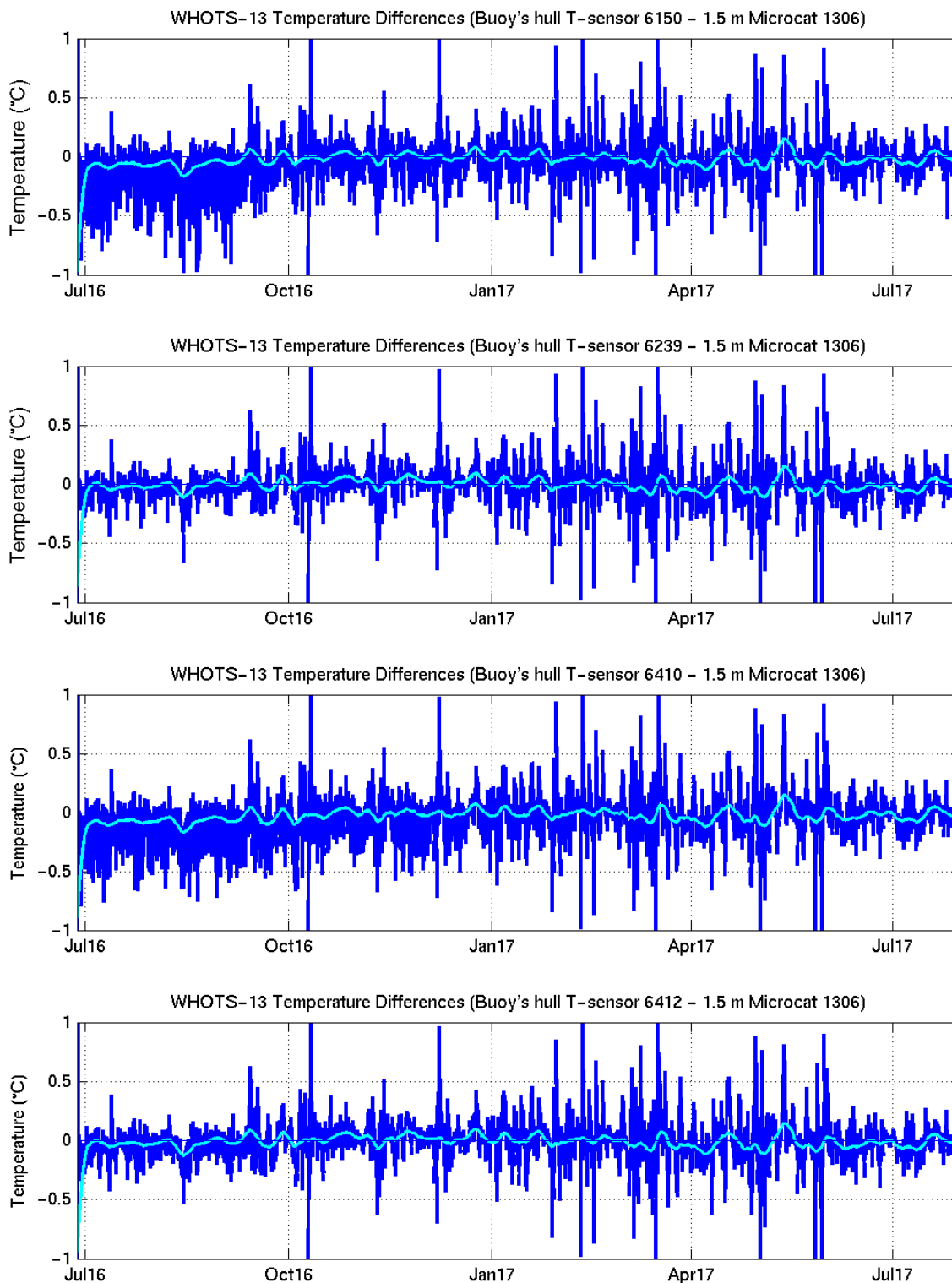


Figure 5-2. Temperature difference between MicroCAT SN 1306 at 1.5 m, and near-surface temperature sensors SN 6150 (top panel), 6239 (second panel), 6410 (third panel), and 6412 (bottom panel), during the WHOTS-13 deployment. The light blue line is a 24-hour running mean of the differences.

In addition to the temperature sensors in the Sea-Bird and the SBE-56 instruments, there were additional temperature sensors in the VMCMs (at 10 and 30 m), and in the ADCPs (at 47.5 m and 125 m). In order to evaluate the quality of the temperatures from these sensors, comparisons with the temperatures from adjacent MicroCATs were conducted.

Comparisons with VMCM and ADCP temperature sensors

Figure 5-3 shows the difference between the 10-m VMCM and the 7-m MicroCAT temperatures during WHOTS-13 (upper panel), and between the VMCM and the 15-m MicroCAT (middle panel). An offset of 0.018 °C is apparent in these plots, and will be added to the VMCM data. (The offset was the mean difference between the VMCM and the 15-m MicroCAT temperatures). The lower panel shows the temperature fluctuations in the differences between the 7 and 15-m MicroCATs, which seem to be around zero.

Temperature differences between the 30-m VMCM and the temperatures from adjacent MicroCATs at 25 and 35-m during WHOTS-13 are shown in Figure 5-4. For comparison, the differences between the MicroCATs temperatures are also shown in the lower panel. These plots indicate that there was an offset of 0.03 °C in the 30-m VMCM with respect to the adjacent MicroCATs (top and middle plots). This offset will be added to the VMCM data.

Temperature differences between the 47.5-m ADCP and the temperatures from adjacent MicroCATs at 45 and 50-m during WHOTS-13 are shown in Figure 5-5. For comparison, the differences between the MicroCATs temperatures are also shown in the lower panel. These plots indicate that there was no offset in the 47.5-m ADCP with respect to the adjacent MicroCATs (top and middle plots).

Temperature differences between the 125-m ADCP and the temperatures from adjacent MicroCATs at 120 and 135-m during WHOTS-13 are shown in Figure 5-6. For comparison, the differences between the MicroCATs temperatures are also shown in the lower panel. It is difficult to assess the quality of the ADCP temperature from these comparisons, as these sensors were located at the top of the thermocline, where we expect to find large temperature differences between adjacent sensors. However, an indication of the quality of the ADCP temperatures is given in the upper panel plot, which shows temperatures fluctuating closely around zero.

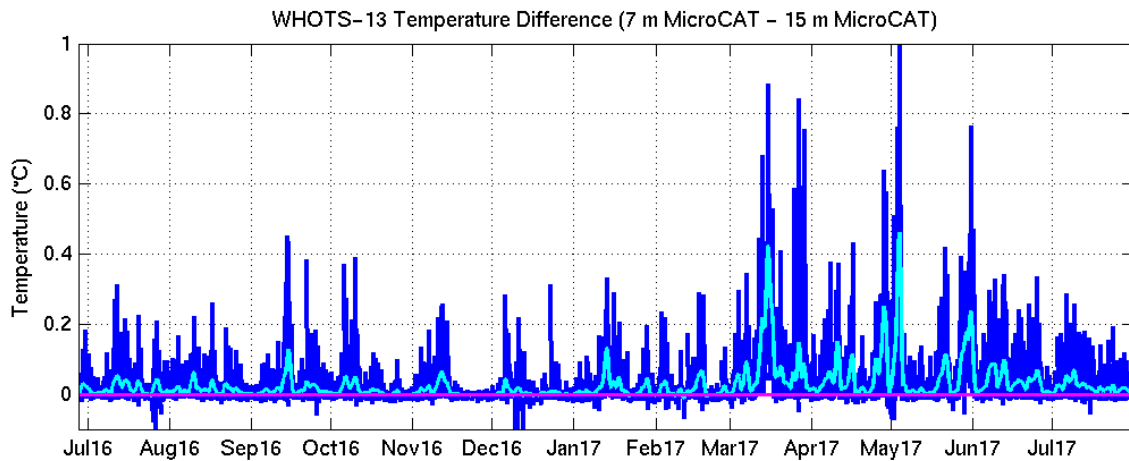
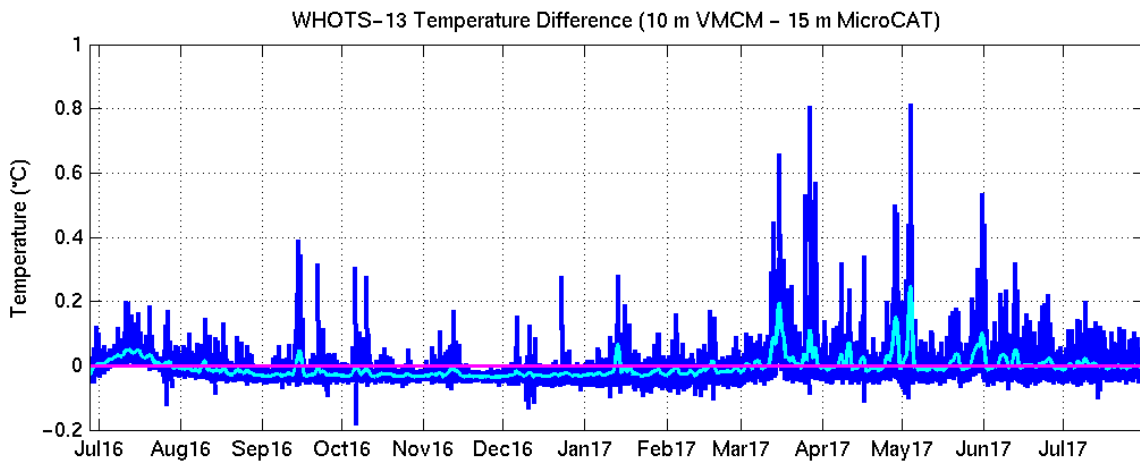
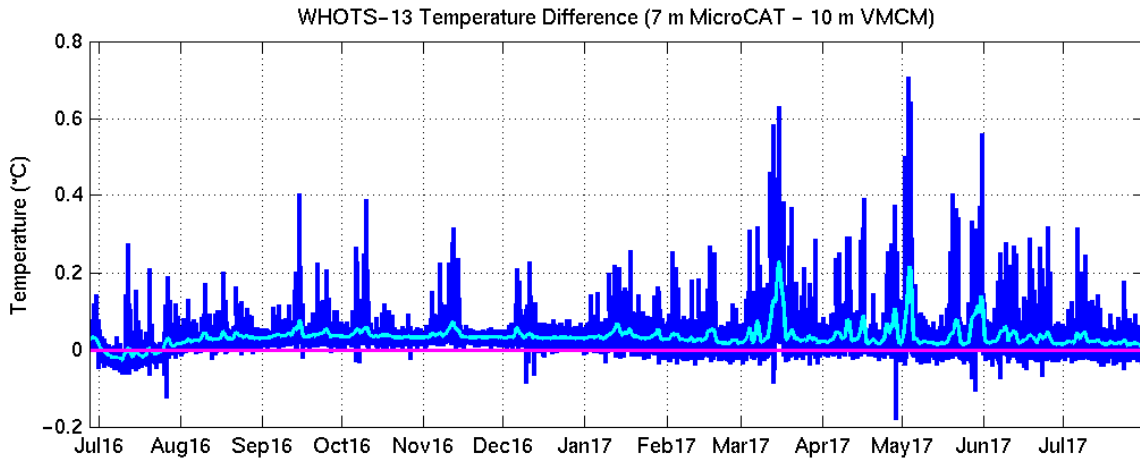


Figure 5-3. Temperature difference between the 7-m MicroCAT and the 10-m VMCM (upper panel); between the 15-m MicroCAT and the 10-m VMCM (middle panel); and between the 7-m and the 15-m MicroCATs (lower panel) during the WHOTS-13 deployment. The light blue line is a 24-hour running mean of the differences.

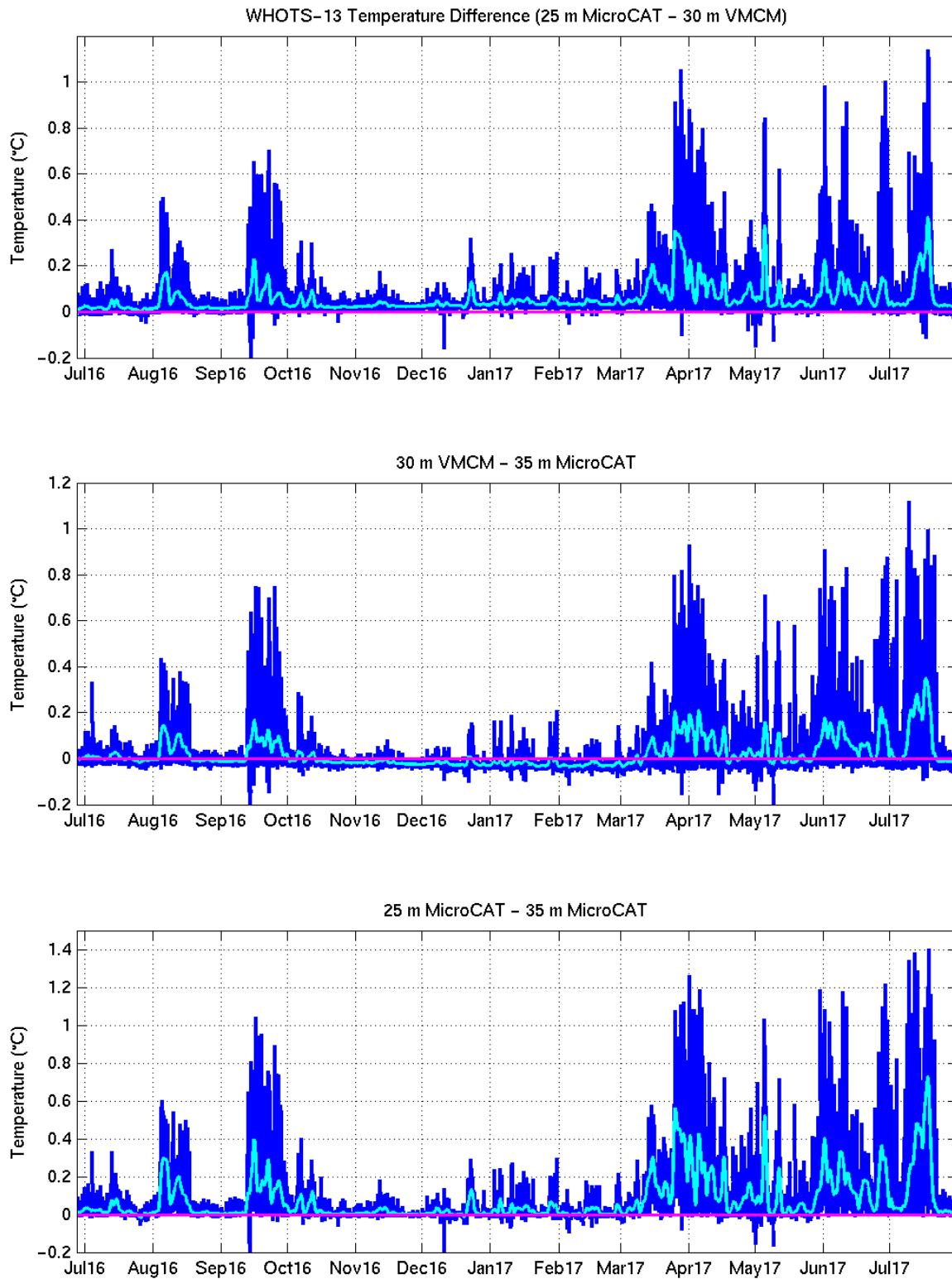


Figure 5-4. Temperature difference between the 25-m MicroCAT and the 30-m VMCM (upper panel); between the 35-m MicroCAT and the 30-m VMCM (middle panel); and between the 25-m and the 35-m MicroCATs (lower panel) during the WHOTS-13 deployment. The light blue line is a 24-hour running mean of the differences.

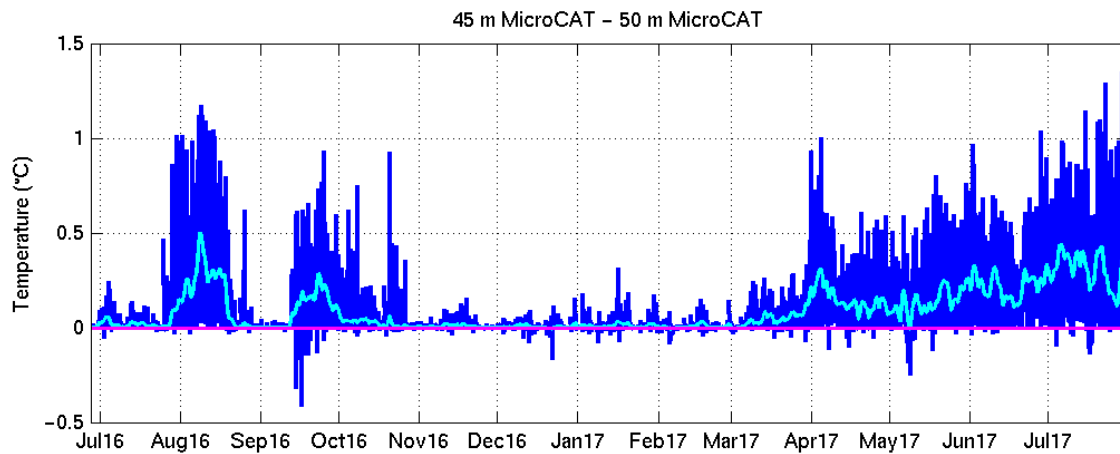
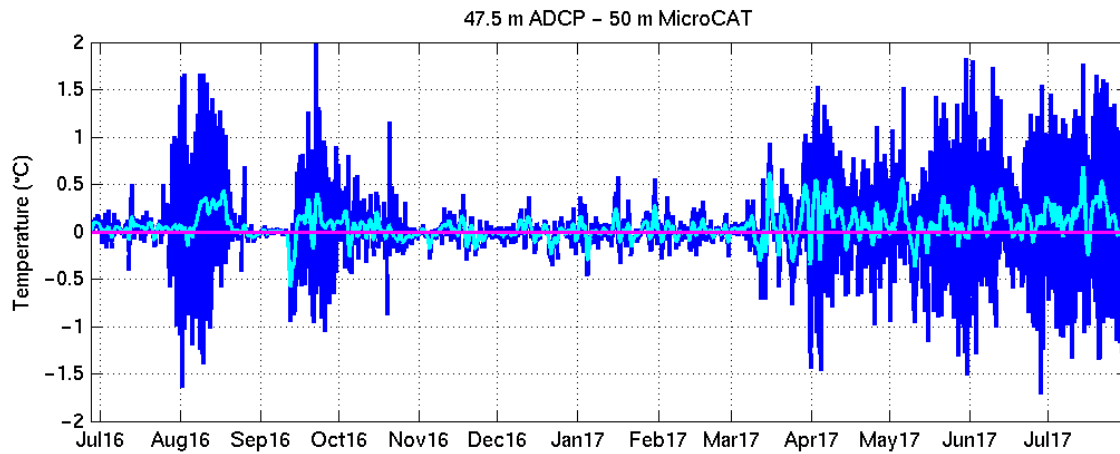
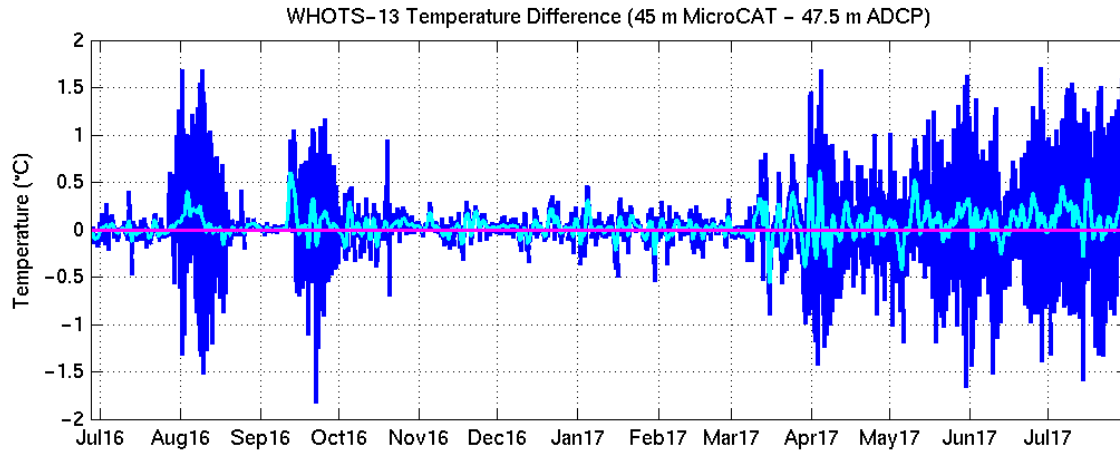


Figure 5-5. Temperature difference between the 45-m MicroCAT and the 47.5-m ADCP (upper panel); between the 50-m MicroCAT and the 47.5-m ADCP (middle panel); and between the 45-m and the 50-m MicroCATs (lower panel) during the WHOTS-13 deployment. The light blue line is a 24-hour running mean of the differences.

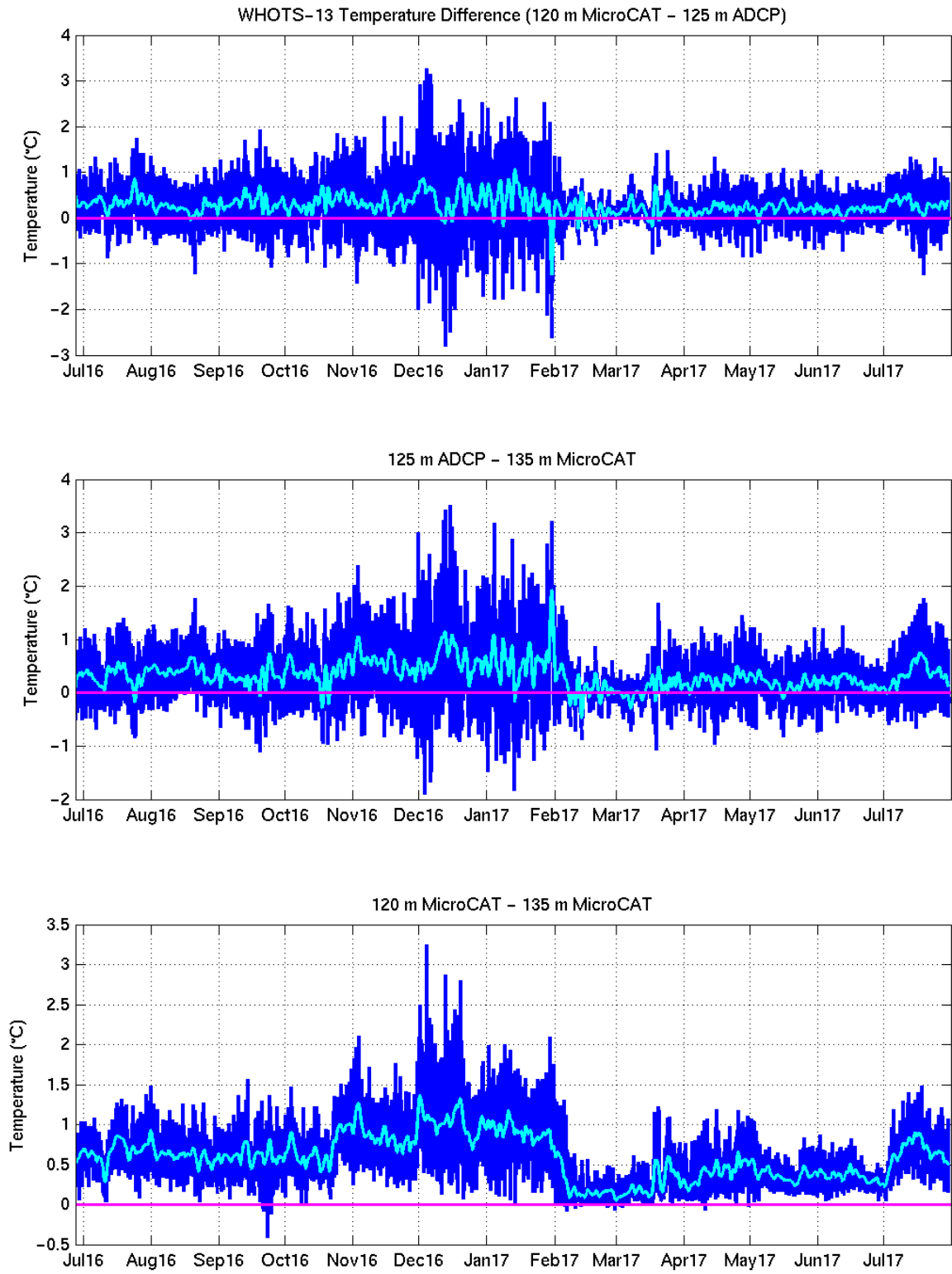


Figure 5-6. Temperature difference between the 120-m MicroCAT and the 125-m ADCP (upper panel); between the 135-m MicroCAT and the 125-m ADCP (middle panel); and between the 120-m and the 135-m MicroCATs (lower panel) during the WHOTS-13 deployment. The light blue line is a 24-hour running mean of the differences.

4. Conductivity Calibration

The results of the Sea-Bird post-recovery conductivity calibrations indicated that some of the MicroCAT and SeaCAT conductivity sensors experienced relatively large offsets from their pre-deployment calibration. These were qualitatively confirmed by comparing the mooring data against CTD data from casts conducted between 200 m and 5 km from the mooring during HOT cruises. The causes of the conductivity offsets are not clear, and there may have been multiple causes (see Freitag et. al, (1999) for a similar experience with conductivity cells during COARE). For some instruments the offset was negative, caused perhaps by biofouling of the conductivity cell while for others the offset was positive, caused possibly by scouring of the inside of the conductivity cell (possible by the continuous up and down motion of the instrument in an abundant field of diatoms). A visual inspection of the instruments after recovery did not show any obvious signs of biofouling, and there were no cell scourings reported in the post-recovery inspections at Sea-Bird.

Corrections of the MicroCATs conductivity data were conducted by comparing them against CTD data from profiles and yo-yo casts conducted near the mooring during HOT cruises, and during deployment/recovery cruises. Casts conducted between 200 and 1000 m from the mooring were given extra weight in the correction, as compared to those conducted between 1 and 5 km away. Casts more than 5 km away from the mooring were not used. Given that the CTD casts are conducted at least 200 m from the mooring, the alignment between CTD and MicroCAT data was done in density rather than in depth. For cases in which the alignment in density was not possible due to large conductivity offsets (causing unrealistic mooring density values), alignment in temperature space was done. A cubic least-squares fit (LSF) to the CTD-MicroCAT/SeaCAT differences against time was applied as a first approximation, and the corresponding correction was applied.

Some of the sensors had large offsets and/or obvious variability that could not be explained by a cubic least squares fit (see below). For these sensors, a stepwise correction was applied matching the data to the available CTD cast data, and then using the differences between consecutive sensors to determine when the sensor started to drift. For instance, during periods of weak stratification the conductivity difference between neighboring sensors A, B, and C could reach near-zero values, in particular for instruments near the surface, which are the ones most prone to suffer conductivity offsets. A sudden conductivity offset observed during this period between sensors A and B, but not between sensors A and C could indicate the beginning of an offset for sensor B.

Given that the deepest instruments on the mooring are less likely to be affected by biofouling and consequent sudden conductivity drift, the deep instruments served as a good reference to find any possible malfunction in the shallower ones. Therefore the deepest instruments' conductivity was corrected first, and the correction was continued sequentially upwards toward the shallower ones.

As a quality control to the conductivity corrections, the buoyancy frequency between neighboring instruments was calculated using finite differences. Over- or under-corrected conductivities yielded instabilities in the water column (negative buoyancy frequency) that were easy to detect and were obviously not real when lasting for several days. Based on this, the conductivity correction of the corresponding sensors was revised.

Another characteristic of the offsets in the conductivity sensors is that their development is not always linear in time, and their behavior can be highly variable (see WHOTS Data Report 1, Santiago-Mandujano et al., 2007).

Corrections of the deep MicroCATs conductivity data were conducted following similar procedures as for the shallow instruments. Both instruments were deployed at the same depth (4657 m). Comparisons with near-bottom CTD data showed that both instruments had a large drift early in the deployment (see Figure 5-7). After correction, the salinity differences between both instruments were in the ± 0.002 g/kg range.

The corrections applied to each of the conductivity sensors during WHOTS-13 can be seen in Figure 5-8. All the instruments had a positive drift of less than 0.02 Siemens/m for the duration of the deployment, except for one of the instruments near the surface (SN 1727), which drifted about 0.06 S/m near the end of the deployment; and the instrument at 40 m, which drifted nearly 0.03 S/m during the deployment.

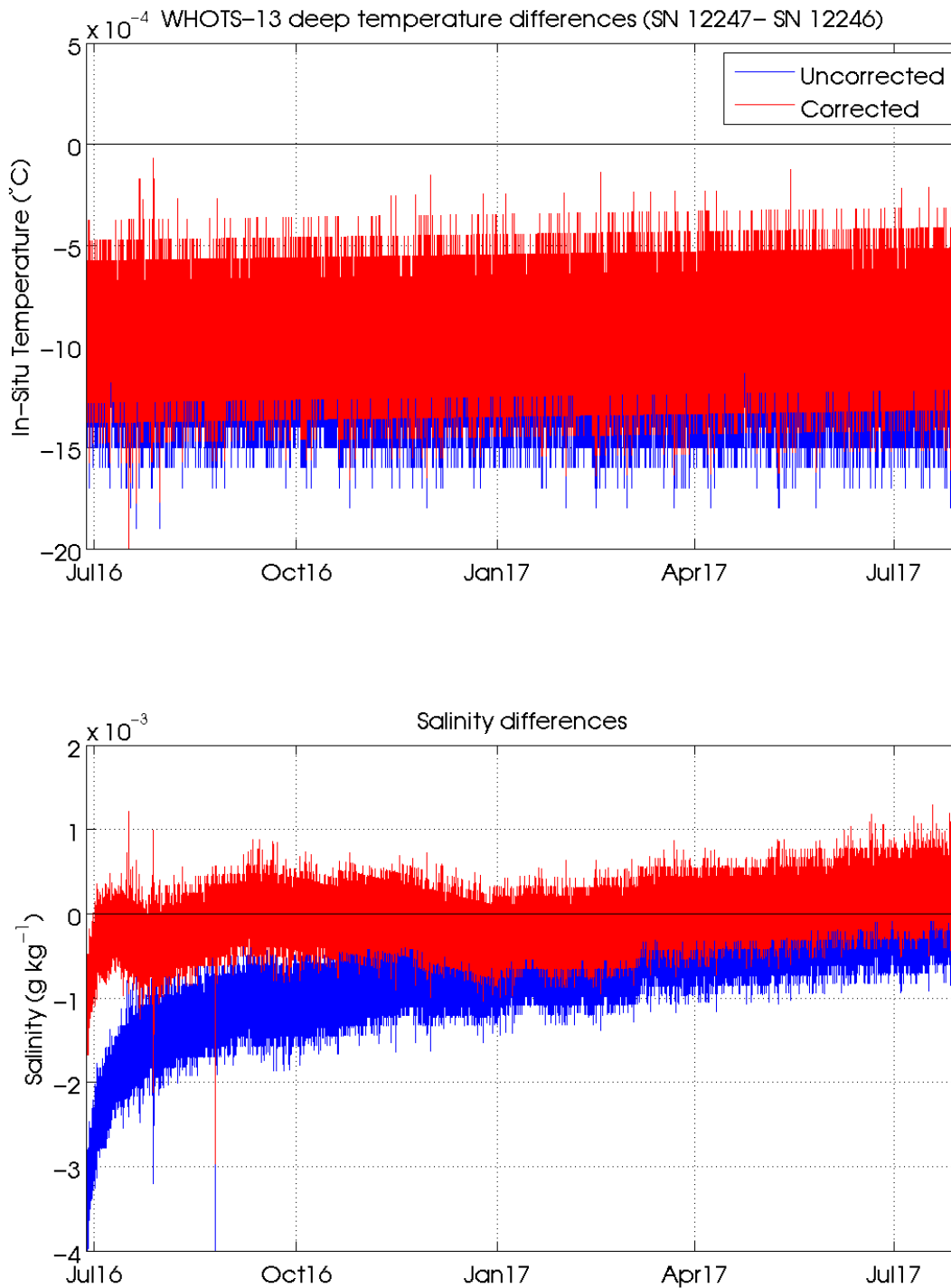


Figure 5-7. Temperature differences (top panel), and salinity differences (bottom panel) between MicroCATs #12246 and #12247 during WHOTS-13. The blue (red) lines are the differences before (after) correcting the data following procedures indicated in the text.

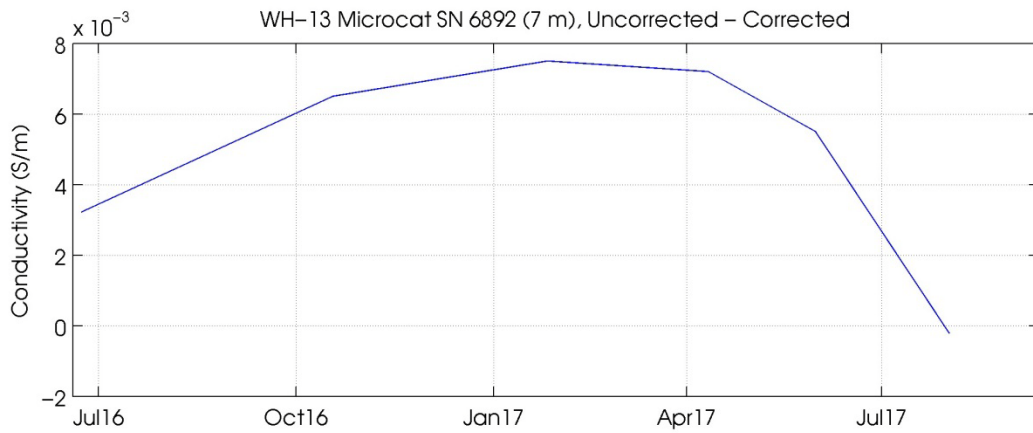
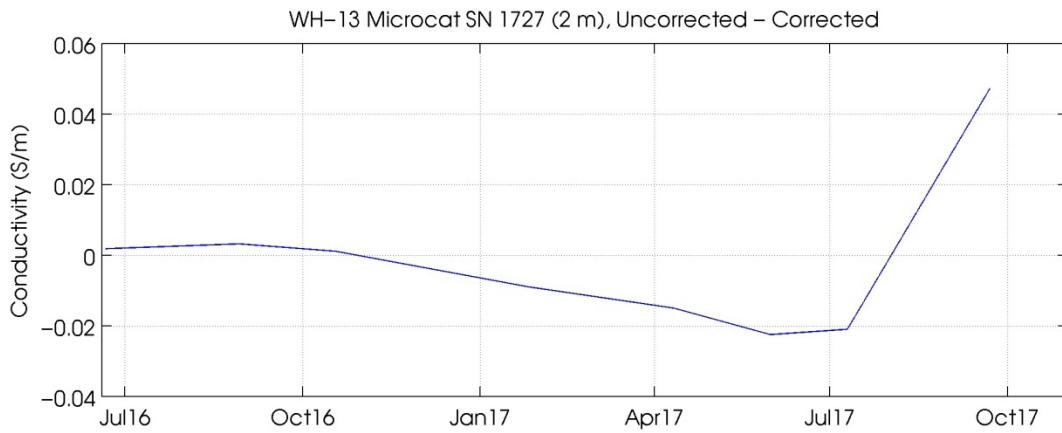
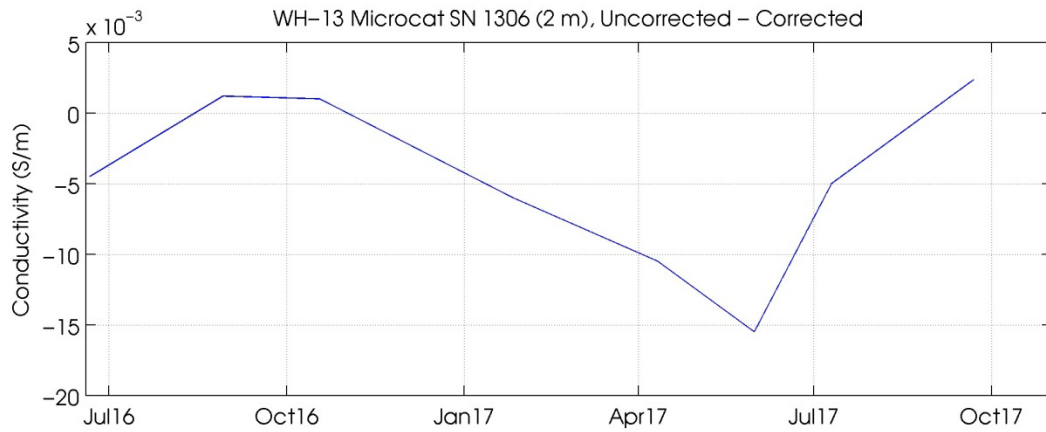


Figure 5-8. Conductivity sensor corrections for MicroCATs during WHOTS-13

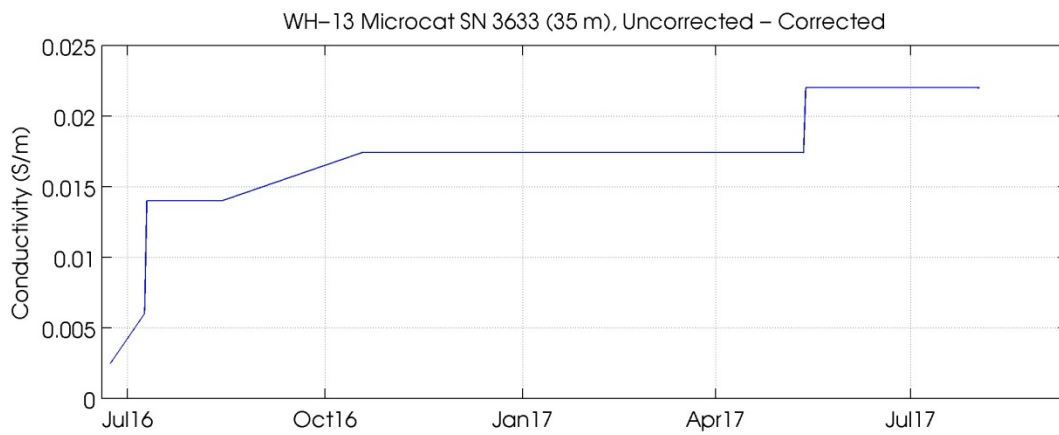
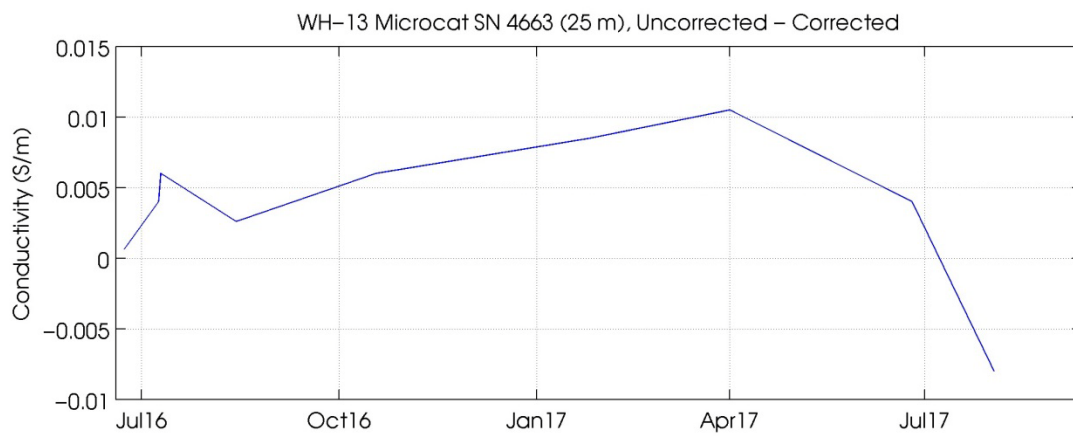
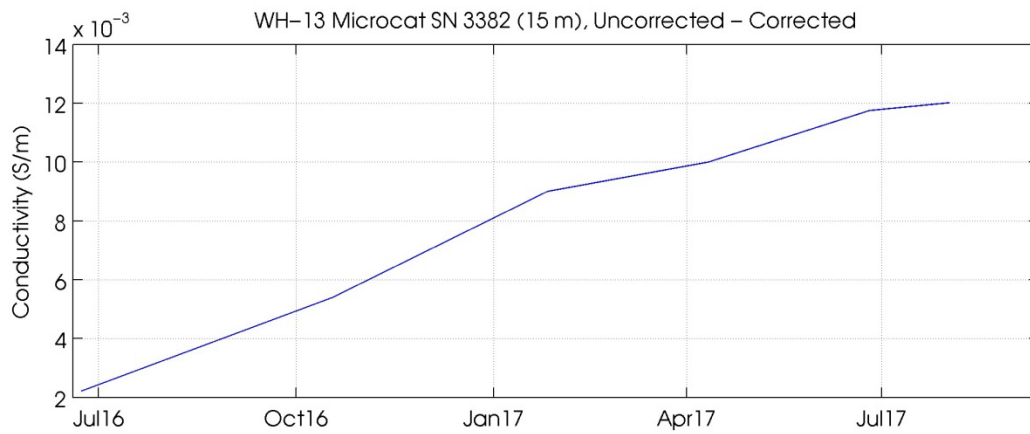


Figure 5-8. (Contd.)

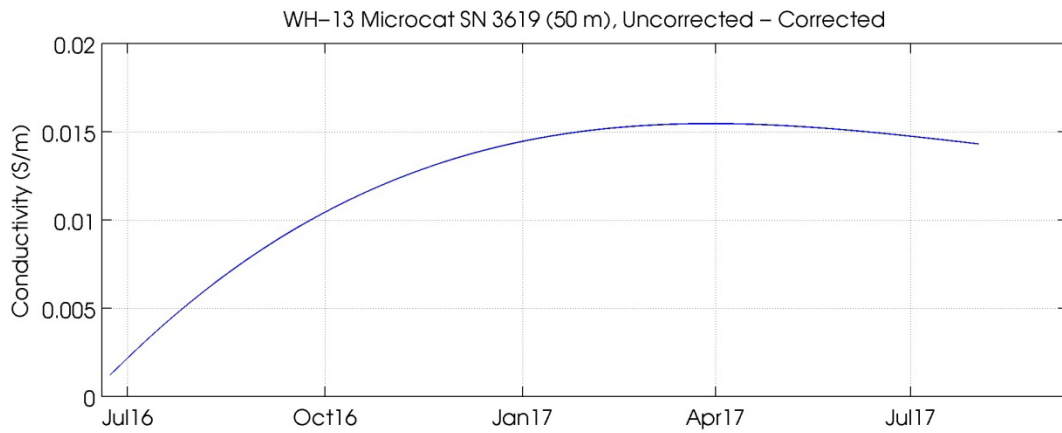
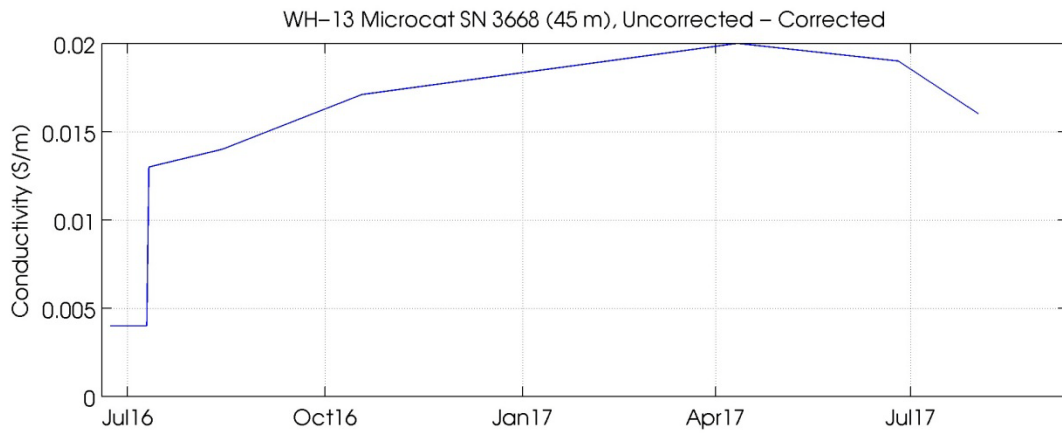
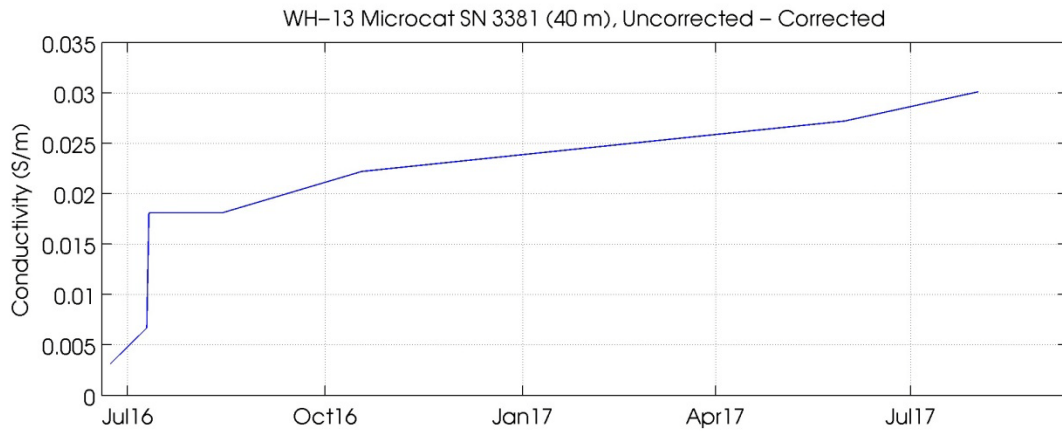


Figure 5-8. (Contd.)

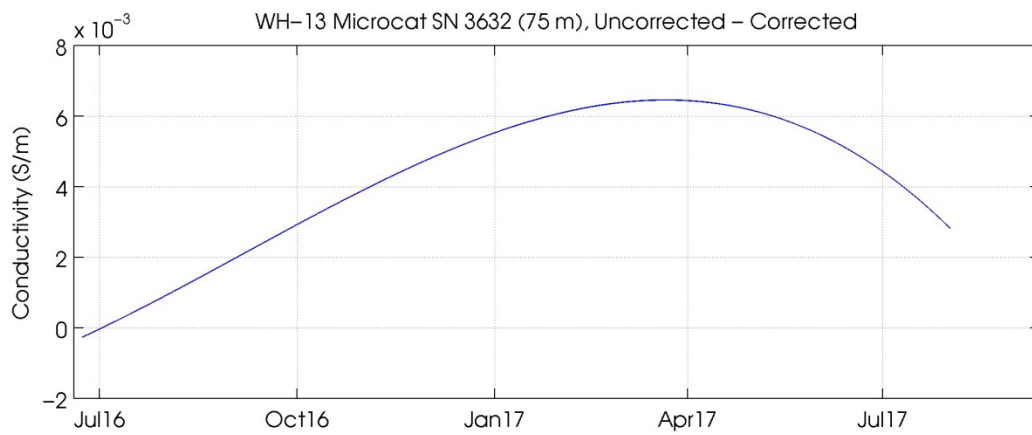
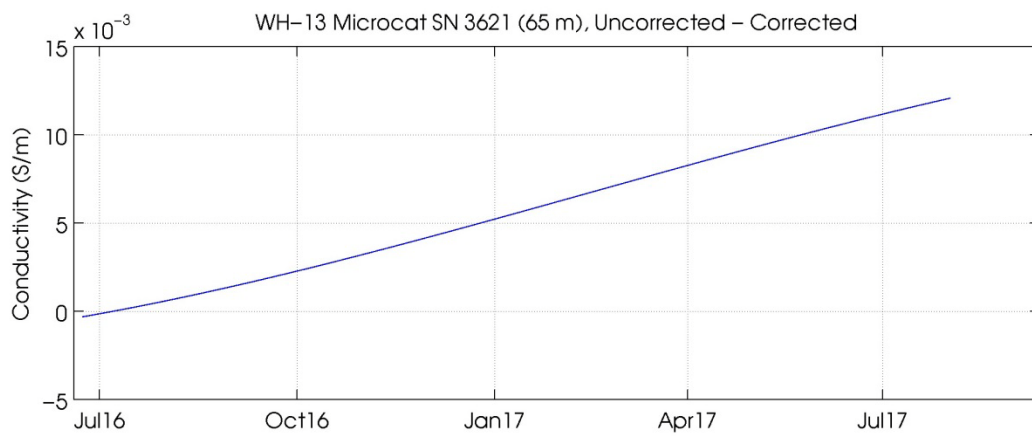
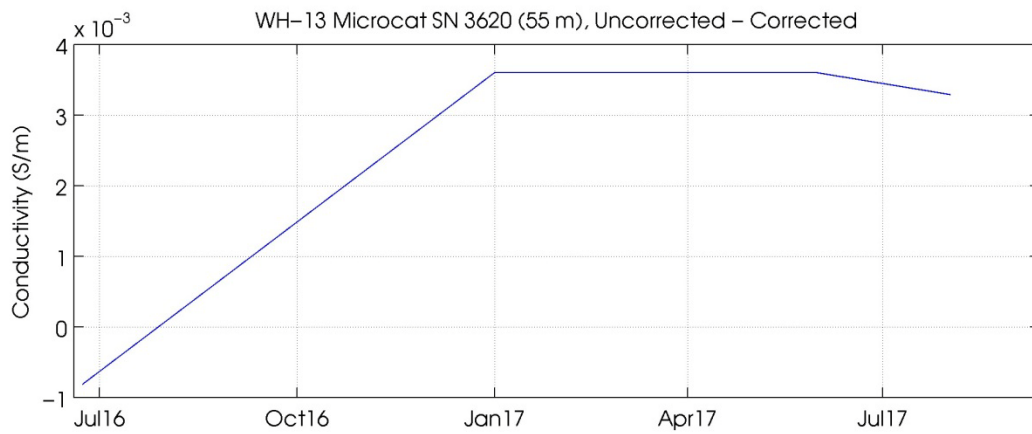


Figure 5-8. (Contd.)

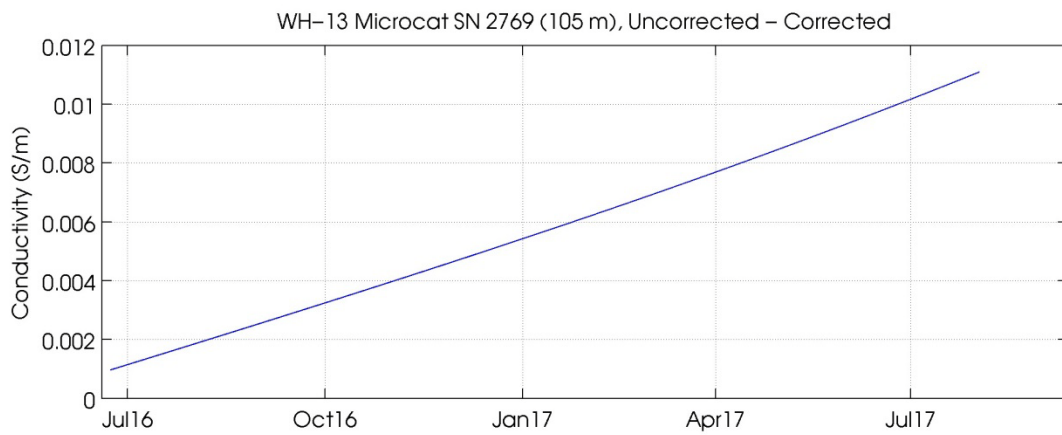
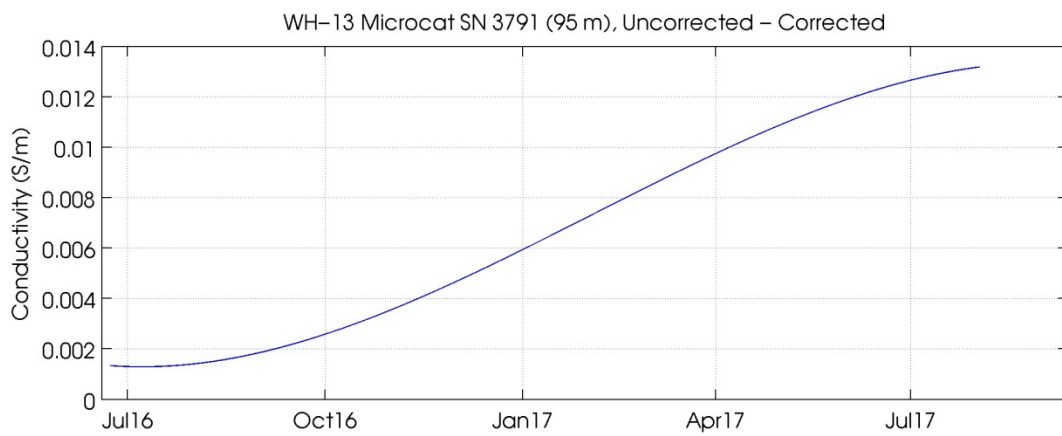
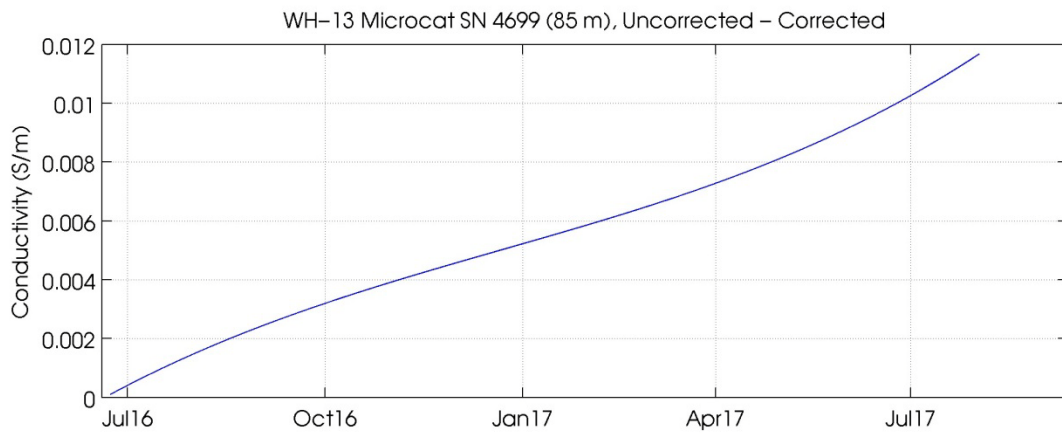


Figure 5-8. (Contd.)

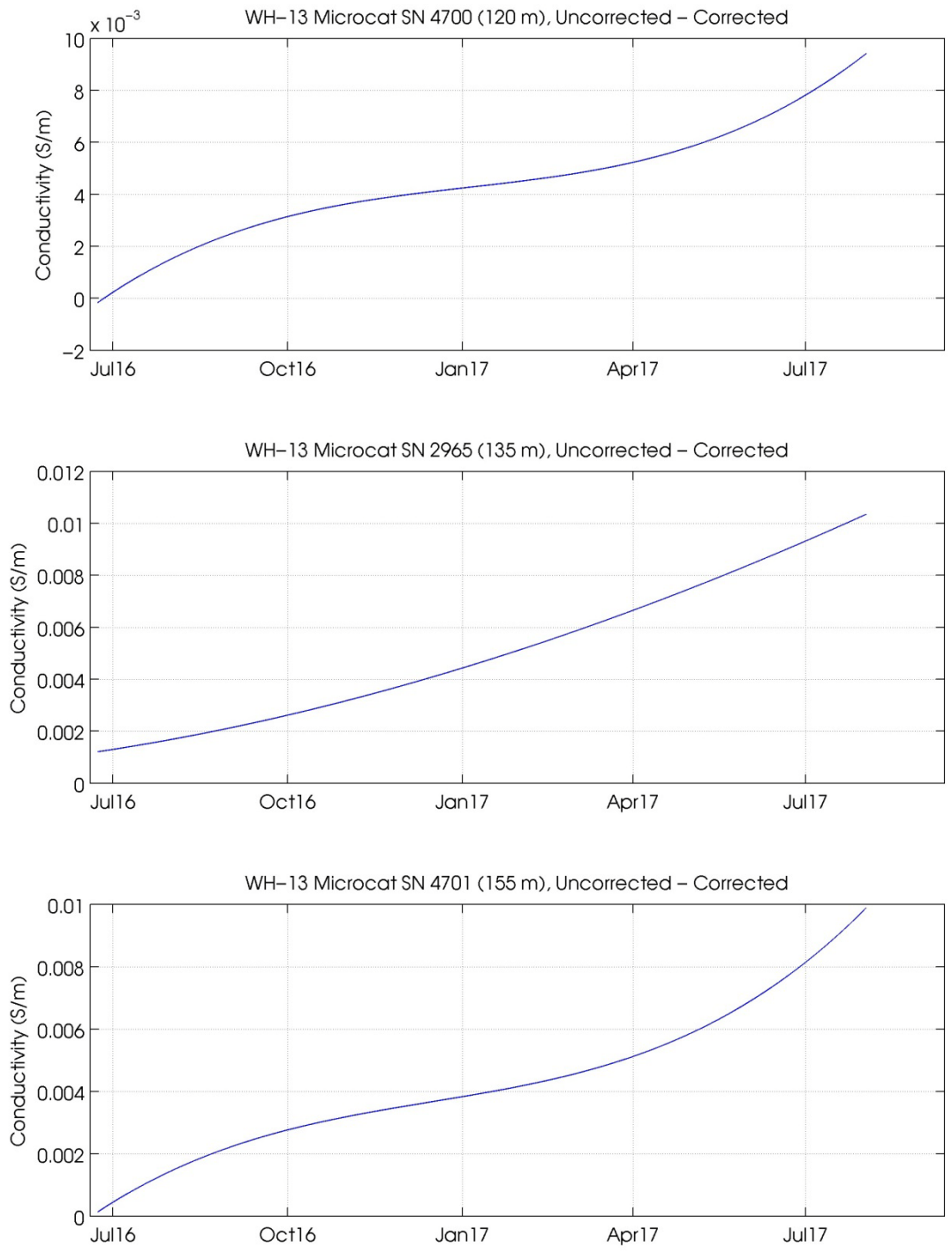


Figure 5-8. (Contd.)

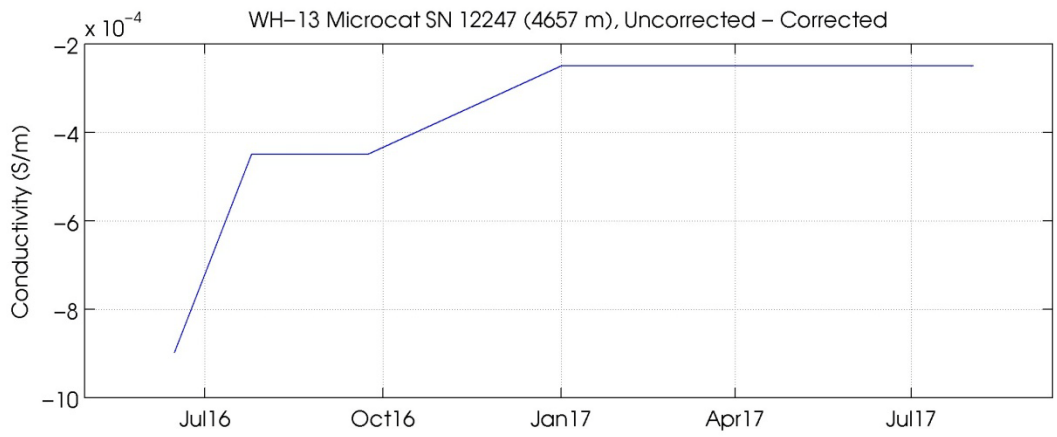
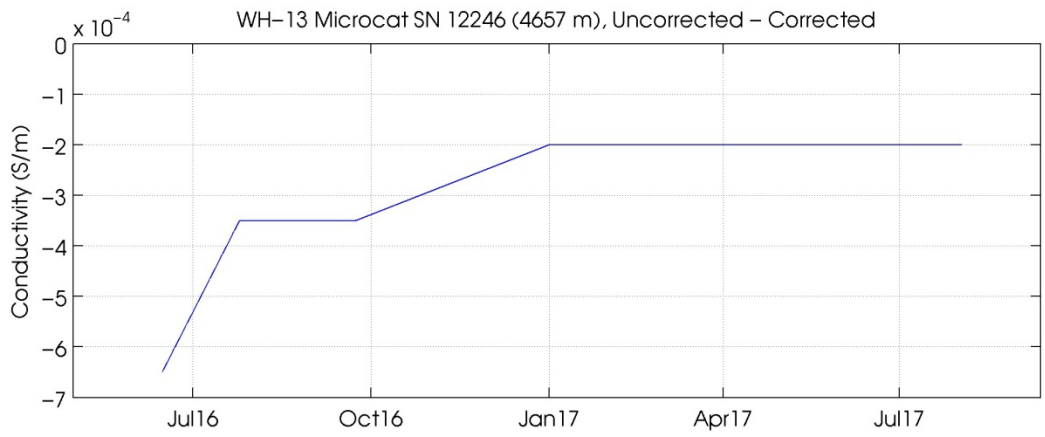


Figure 5-8. (Contd.)

B. Acoustic Doppler Current Profiler

Two TRDI broadband Workhorse Sentinel ADCP's were deployed on the WHOTS-13 mooring. A 600 kHz ADCP was deployed at 47.5 m depth in the upward-looking configuration, and a 300 kHz ADCP was deployed at 125 m, also in the upward-looking configuration. The instruments were installed in aluminum frames along with an external battery module to provide sufficient power for the intended period of deployment. The four ADCP beams were angled at 20° from the vertical line of the instrument. The ADCP was set to profile across 30 range cells of 4 m with the first bin centered 6.2 m from the transducer. The maximum range of the instrument was just short of 125 m. The specifications of the instrument are shown in Table 5-3.

Table 5-3. Specifications of the ADCP's used for the WHOTS-13 mooring.

Instrument	Description
ADCP	<i>TRDI Workhorse Sentinel, 300KHz</i> Model: WHS300-I-UG186; Serial Number: 7637
	<i>TRDI Workhorse Sentinel, 600KHz</i> Model: WHS600-I; Serial Number: 13917
Battery module	<i>300 kHz</i> Model: WH-EXT-BATTERY; Serial Numbers: 49496, 49491, 49475
	<i>600 kHz</i> Model: WH-EXT-BCL; Serial Numbers: 49485, 49474, 49481

1. Compass Calibrations

Pre-Deployment

Prior to the WHOTS-13 deployment a field calibration of the internal ADCP compass was performed at the soccer field of the University of Hawai'i at Manoa on May 24th 2015 for both the 300 kHz and the 600 kHz instruments. Each instrument was mounted in the deployment cage along with the external battery module and was located away from potential sources of magnetic field disturbances. The ADCP was mounted to a turntable, which was aligned with magnetic north using a surveyor's compass. Using the built-in RDI calibration procedure, the instrument was tilted in one direction between 10 and 20 degrees and then rotated through 360 degrees at less than 5 ° per second. The ADCP was then tilted in a different direction and a second rotation made. Based on the results from the first two rotations, calibration parameters are temporarily loaded and the instrument, tilted in a third direction is rotated once more to check the calibration. Results from each pre-deployment field calibration are shown in Table 5-4 (Figures 5-9 and 5-10).

Table 5-4. Results from the WHOTS-13 pre-deployment ADCP compass field calibration procedure.

300 kHz (SN 7637)	Single Cycle Error (°)	Double Cycle Error (°)	Largest Double + Single Cycle Error (°)	RMS of 3 rd Order and Higher + Random Error (°)	Over all Error (°)	Pitch Mean and Standard Deviation (°)	Roll Mean and Standard Deviation (°)
Before Calibration	4.87	0.41	5.28	0.17	4.94	0.09 ± 0.59	-1.40 ± 0.60
After Calibration	0.66	0.02	0.68	0.26	0.66	0.51 ± 0.60	16.97 ± 0.68

600 kHz (SN 13917)	Single Cycle Error (°)	Double Cycle Error (°)	Largest Double + Single Cycle Error (°)	RMS of 3 rd Order and Higher + Random Error (°)	Over all Error (°)	Pitch Mean and Standard Deviation (°)	Roll Mean and Standard Deviation (°)
Before Calibration	3.05	0.18	3.23	0.14	3.06	-0.41 ± 0.62	0.76 ± 0.72
After Calibration	0.14	0.37	0.51	0.24	0.47	-0.06 ± 0.64	17.75 ± 0.67

Post-Deployment

After the WHOTS-13 mooring was recovered, the performance of the ADCP compass was tested at the soccer field of the University of Hawai'i at Manoa on September 8th 2017 with an identical compass calibration procedure as during the pre-deployment calibration. Results from the WHOTS-13 post-deployment ADCP compass field calibration procedure are listed in Table 5-5 (Figures 5-9 and 5-10).

Table 5-5. Results from the WHOTS-13 post-deployment ADCP compass field calibration procedure.

300 kHz (SN 7637)	Single Cycle Error (°)	Double Cycle Error (°)	Largest Double + Single Cycle Error (°)	RMS of 3 rd Order and Higher + Random Error (°)	Over all Error (°)	Pitch Mean and Standard Deviation (°)	Roll Mean and Standard Deviation (°)
After Calibration	1.25	0.19	1.45	0.23	1.28	0.80 ± 0.88	-0.00 ± 0.68

600 kHz (SN 13917)	Single Cycle Error (°)	Double Cycle Error (°)	Largest Double + Single Cycle Error (°)	RMS of 3 rd Order and Higher + Random Error (°)	Over all Error (°)	Pitch Mean and Standard Deviation (°)	Roll Mean and Standard Deviation (°)
After Calibration	1.91	0.29	2.20	0.24	1.93	-0.35 ± 0.83	1.98 ± 0.89

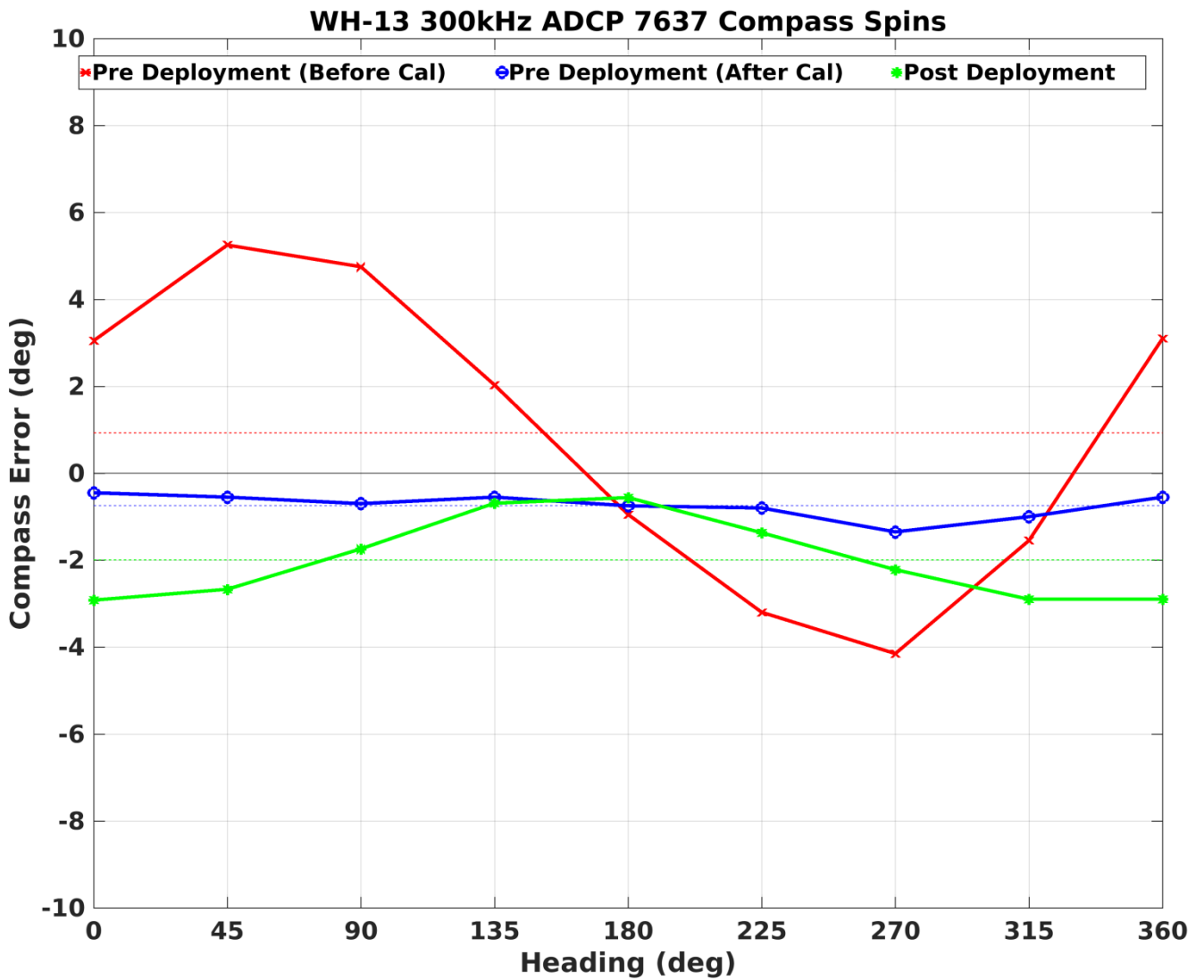


Figure 5-9. Results of the pre- and post-deployment compass calibrations, conducted on May 24th 2015, on ADCP SN 7637 at the University of Hawai'i at Manoa.

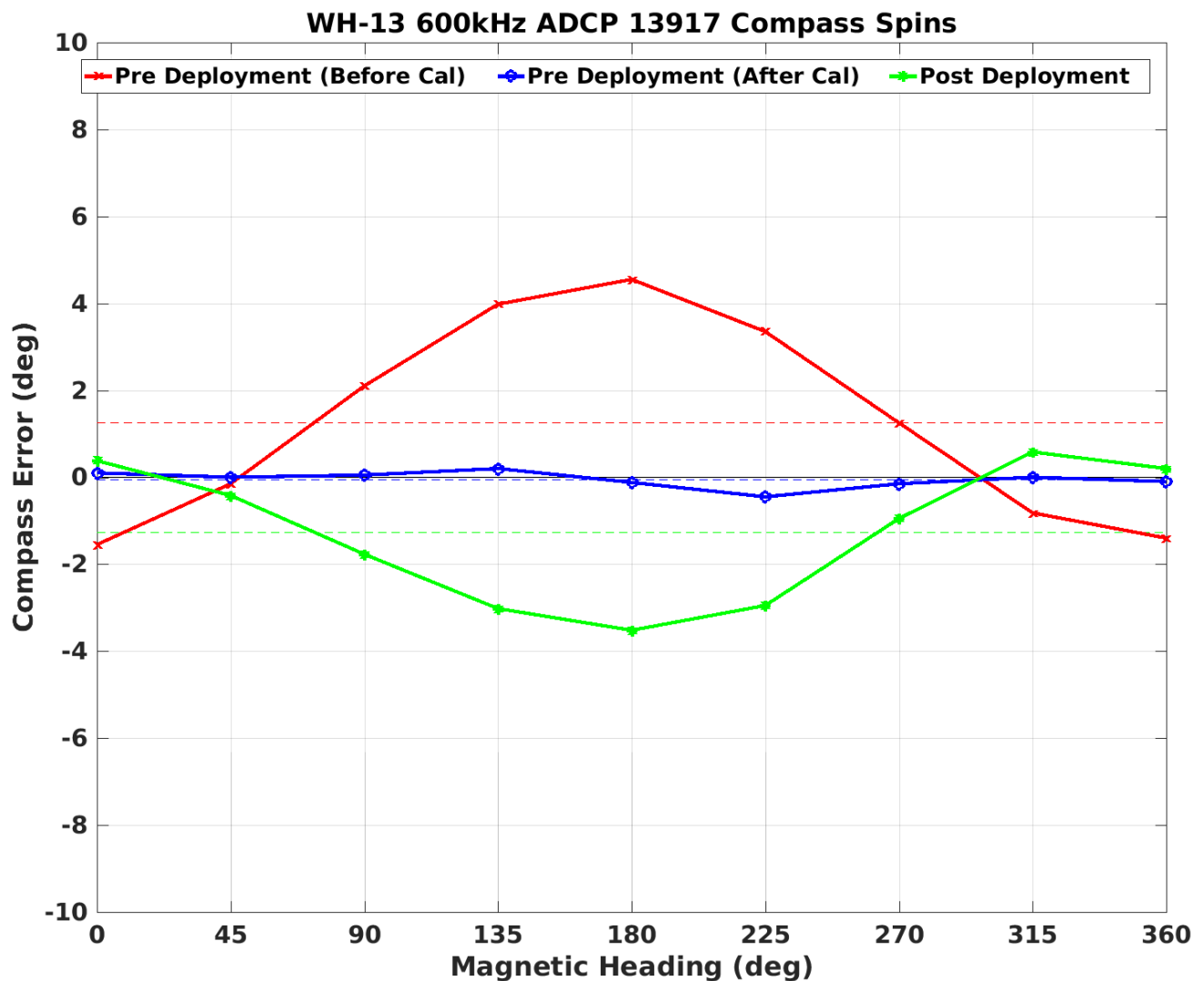


Figure 5-10. Results of the pre- and post-deployment calibrations, conducted on September 8th 2017, on ADCP SN 13917 at the University of Hawai'i at Manoa.

2. ADCP Configurations

Individual configurations for the two ADCP's on the WHOTS-13 mooring are detailed in Appendices 1 and 2. The salient differences for each of the ADCP's are summarized below.

300 kHz (125m)

The ADCP, set to a beam frequency of 300 kHz, was configured in a burst sampling mode consisting of 40 pings per ensemble in order to resolve low-frequency wave orbital motions. The interval between each ping was 4 seconds so the ensemble length was 160 seconds. The interval between ensembles was 10 minutes. Data were recorded in earth coordinates with a heading bias correction of 9.65° E due to magnetic declination. False targets, usually fish, were screened by setting the threshold maximum to 70 counts. Velocity data were rejected if the difference in echo intensity among the four beams exceeded this threshold.

600 kHz (47.5m)

The ADCP, set to a beam frequency of 600 kHz, was configured in a burst sampling mode consisting of 80 pings per ensemble. The interval between each ping was 2 seconds so the ensemble length was also 160 seconds. The interval between ensembles was 10 minutes. Data were recorded in earth coordinates with a heading bias correction of 9.65° E due to magnetic declination. The threshold maximum was also set to 70 counts. Velocity data were rejected if the difference in echo intensity among the four beams exceeded this threshold.

3. ADCP data processing procedures

Binary files output from the ADCP were read and converted to MATLAB™ binary files using scripts developed by Eric Firing’s ADCP lab (<http://current.soest.hawaii.edu>). The beginning of the raw data files were truncated to a time after the mooring anchor was released in order to allow time for the anchor to reach the seabed and for the mooring motions that follow the impact of the anchor on the sea floor to dissipate. The pitch, roll, and ADCP temperature were examined in order to pick reasonable times that ensured good data quality but without unnecessarily discarding too much data (see Figure 5-11 and Figure 5-12). Truncation at the end of the data files were chosen to be the ensemble prior to the time that the acoustic release signal was sent to avoid contamination due to the ascent of the instrument. The times of the first ensemble from the raw data, deployment and recovery time, along with the times of the truncated records of both deployments are shown in Table 5-6.

Table 5-6. ADCP record times (UTC) during WHOTS-13 deployment.

	300 kHz	600 kHz
Raw file beginning and end times	23-Jun-2016 00:00:00 02-Aug-2017 02:10:00	23-Jun-2016 00:00:00 02-Aug-2017 02:30:00
Deployment and recovery times	26-Jun-2016 19:54:00 in water 27-Jun-2016 08:48:00 anchor over 31-Jul-2017 16:38:00 release triggered 01-Aug-2017 00:37:00 on deck	26-Jun-2016 19:37:22 in water 27-Jun-2016 08:48:00 anchor over 31-Jul-2017 16:38:00 release triggered 01-Aug-2017 00:51:00 on deck
Processed data beginning and end times	27-Jun-2016 08:47 31-Jul-2017 16:38	27-Jun-2016 08:47 31-Jul-2017 16:38

ADCP Clock Drift

Upon recovery, the ADCP clocks were compared with the ship's time server and the difference between the two was recorded. It was found that for 300 kHz (SN 4891) ADCP the clock on the instrument was fast by 7 minutes, 29 seconds. The clock on the 600 kHz (SN 1825) was fast by 2 minutes, 29 seconds. Past deployments of the ADCP's suggest a 9 minute difference isn't unusual. Since the drift represents just one ensemble out of a total of over 58,000, no corrections were made. However this drift may be significant if the data are used for time dependent analysis such as tidal or spectrum analysis, a drift correction needs to be applied in those cases.

Heading Bias

As mentioned in the ADCP configuration section, the data were recorded in earth coordinates. A heading bias, the angle between magnetic north and true north, can be included in the setup to obtain output data in true earth coordinates. Magnetic variation was obtained from the National Geophysical Data Center 'Geomag' calculator. (<http://www.ngdc.noaa.gov/seg/geomag>). For a yearlong deployment a constant value is acceptable because the change in declination is small, approximately $-0.02^{\circ} \text{ year}^{-1}$ at the WHOTS location. A heading bias of 9.65° was entered in the setup of the WHOTS-13 ADCP's.

Speed of sound

Due to the constant of proportionality between the Doppler shift and water speed, the speed of sound needs only be measured at the transducer head (Firing, 1991). The sound speed used by the ADCP is calculated using a constant value of salinity (35) and the temperature recorded by the transducer temperature sensor of the ADCP. Using CTD profiles close to the mooring during HOT cruises, HOT-285 to HOT-294, and from the WHOTS deployment/recovery cruises, the mean salinity at 125 dbar was 35.16 while the mean salinity at 47.5 dbar was 34.94. Mean ADCP temperature at 125 dbar was 22.70°C and 25.46°C at 47.5 dbar (Figure 5-13). The maximum associated mean sound velocity difference is less than 0.4 m s^{-1} which represents a change of less than 0.03%, so no correction was made.

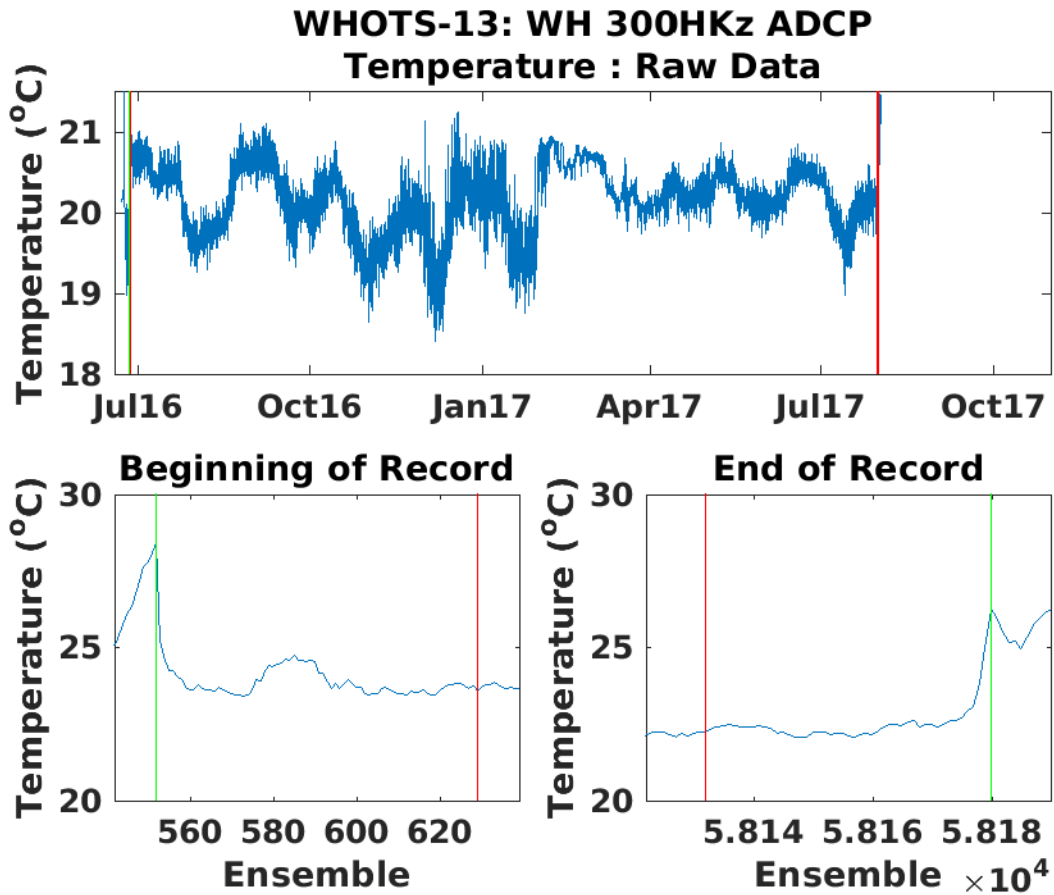


Figure 5-11. Temperature record from the 300 kHz ADCP during WHOTS-13 mooring (top panel). The bottom panel shows the beginning and end of the record with the green vertical line representing the in-water time during deployment and out-of-water time for recovery. The red line represents the anchor release and acoustic release trigger for deployment and recovery respectively.

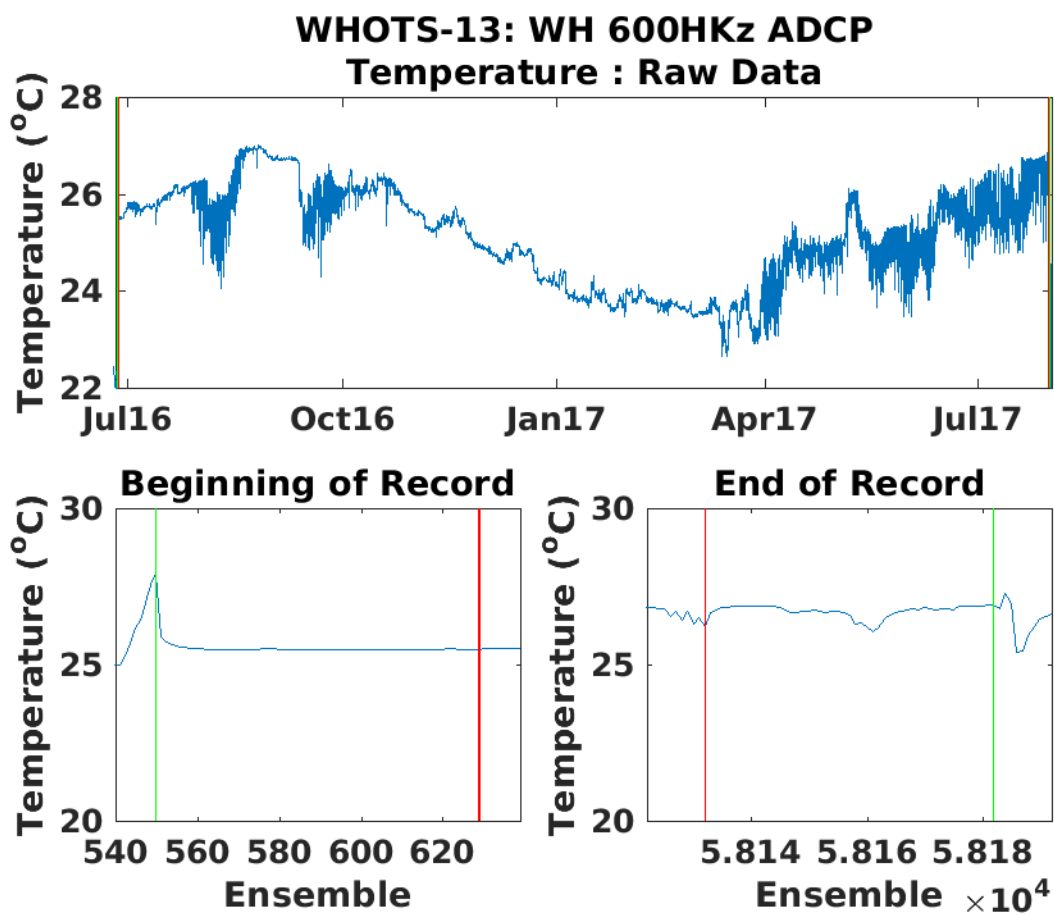


Figure 5-72. Same as Figure 5-11, but for the 600 kHz ADCP.

Sound Speed Profile (m/s) during WHOTS-13 Deployment 25-Jun-2016 to 03-Jul-2016 from HOT Stn 50 CTD casts and CTD casts during WHOTS-13/14 cruises

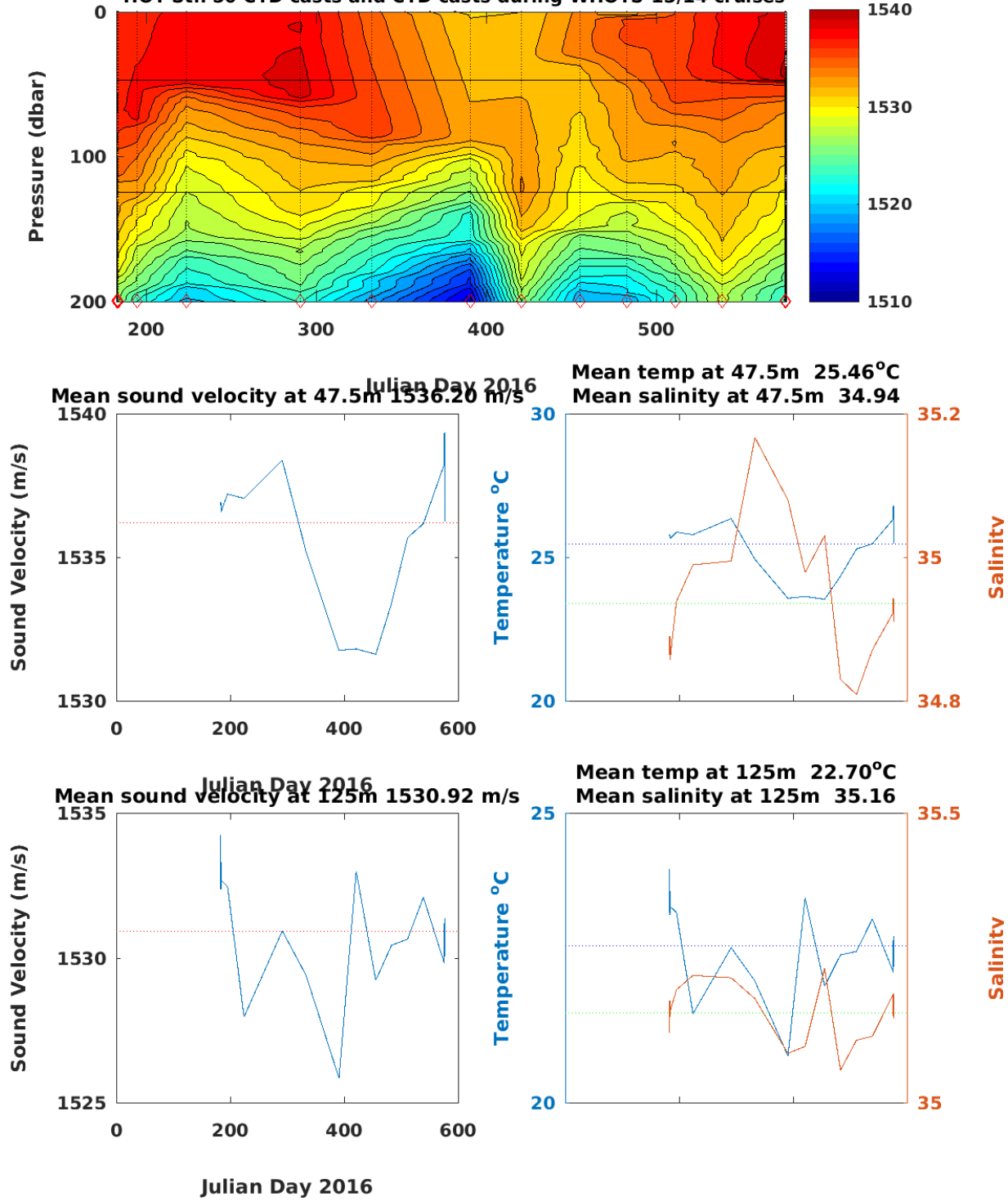


Figure 5-8. Sound speed profile (top panel) during the deployment of the WHOTS-13 mooring from 2 dbar CTD data taken during regular HOT cruises and CTD profiles taken during the WHOTS-14 deployment cruise (individual casts marked with a red diamond). The bottom left panels show the sound velocity at the depth of the ADCP's (47.5 m and 125 m), with the mean sound velocity indicated with a red line. The lower right panels show the temperature and salinity at each ADCP depth for the time series with the mean temperatures indicated with blue lines and mean salinity indicated with green lines.

Quality Control

Quality control of the ADCP data involved the thorough examination of the velocity, instrument orientation and diagnostic fields to develop the basis of the QC flagging procedures. Details of the methods used can be found in the WHOTS Data Report 1 (Santiago-Mandujano et al., 2007). The following QC procedures were applied to the WHOTS-13 deployment ADCP data.

- 1) The first bin (closest to the transducer) is sometimes corrupted due to what is known as ringing. A period of time is needed for the sound energy produced during a transmit pulse at the transducer to dissipate before the ADCP is able to properly receive the returned echoes. This “blanking interval” is used to prevent useless data from being recorded. If it is too short, signal returns can be contaminated from the lingering noise from the transducer. The blanking interval is expressed as a distance. The default value of 1.76 m was used for the 300 kHz ADCP, whereas an interval of 0.88 m was used for the 600 kHz ADCP. As a result, bin 1 was flagged and replaced with Not a Number (NaN) in the quality controlled dataset (Figure 5-14).

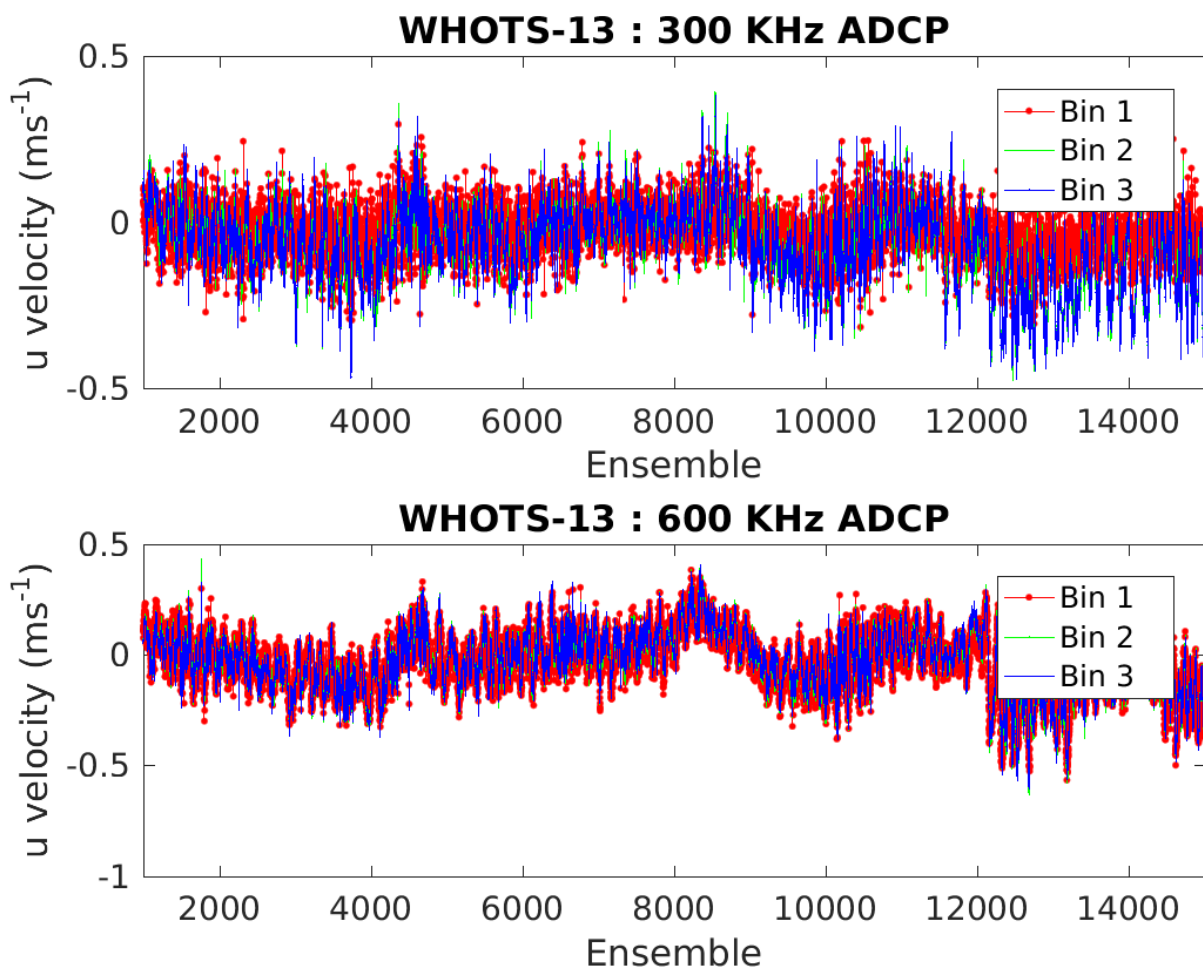


Figure 5-94. Eastward velocity component for the 300 kHz (top panel) and the 600 kHz (bottom panel) ADCPs showing the incoherence between depth bins 1 (red), 2 (green) and 3 (blue).

- 2) For an upward-looking ADCP with a beam angle of 20° within range of the sea surface, the upper 6% of the depth range is contaminated with sidelobe interference (Teledyne RD Instruments, 2011). This is a result of the much stronger signal reflection from the sea surface than from scatterers, overwhelming the sidelobe suppression of the transducer. Data quality is quantified using echo intensity, a measure of the strength of the backscattered echo for each depth cell. With distance from the transducer, echo intensity is expected to decrease. Sharp increases in echo intensity indicate

contamination from surface reflection. In practice, the majority of the data within the upper 4 bins (~14% of the vertical range) were flagged. These upper 4 bins range from about 15 m up to the sea surface.

- 3) The Janus configuration of four beams (along with instrument orientation) is used to resolve currents into their component earth-referenced velocities, providing a second estimate of the vertical velocity. The scaled difference between these estimates is defined as the error velocity and it is useful for assessing data quality. Error velocities with an absolute magnitude greater than 0.15 m s^{-1} (a value comparable to the standard deviation of observed horizontal velocities) were flagged and removed.
- 4) An indication of data quality for each ensemble is given by the “percent good” data indicator which accompanies each individual beam for each individual bin. The use of the percent good indicator is determined by the coordinate transformation mode used during the data collection. For profiles transformed into earth coordinates, the percent good field shows the percentage of pings that could be used to create the earth coordinate velocities. The percent good fields show the percentage of data that was made using 4 and 3 beam solutions in each depth cell within an ensemble, and the percentage that was rejected as a result of failing one of the criteria set during the instrument setup (see Appendix 1: WHOTS-13 300 kHz ADCP Configuration). Data were flagged when data in each depth cell within an ensemble made from 3 or 4 beam solutions was 20% or less.
- 5) Data were rejected using correlation magnitude, which is the pulse-to-pulse correlation (in ping returns) for each depth cell. Correlation magnitude represents a measure of how the shape of the received signal corresponds to the outgoing signal for each ping. For a given bin, if at least three of the beams exhibited a correlation magnitude greater than 64 counts, then the profile is able to be transformed into earth coordinates. Low correlation magnitudes may be indicative of sudden changes in particle density, or sudden changes in ADCP tilt. More research is needed at this time into relationships between ADCP tilt and correlation magnitude. If anyone beam had a correlation magnitude of 20 counts or less, that data point was flagged.
- 6) Histograms of raw vertical velocity data and partially cleaned data from the ADCP [see Figures 5-15 and 5-16 and the WHOTS Data Report 1 (Santiago-Mandujano et al., 2007)] showed vertical velocities larger than expected, some exceeding 1 m s^{-1} . Recall that the instruments’ burst sampling (4-second intervals for the 300 kHz and 2-second intervals for the 600 kHz, for 160 seconds every 10 minutes) was designed to minimize aliasing by occasional large ocean swell orbital motions (Section 3), and therefore are not the source of these large speeds in the data. These large vertical speeds are possibly fish swimming in the beams based on the histograms of the partially cleaned data; depth cells with an absolute value of vertical velocity greater than 0.3 m s^{-1} were flagged.

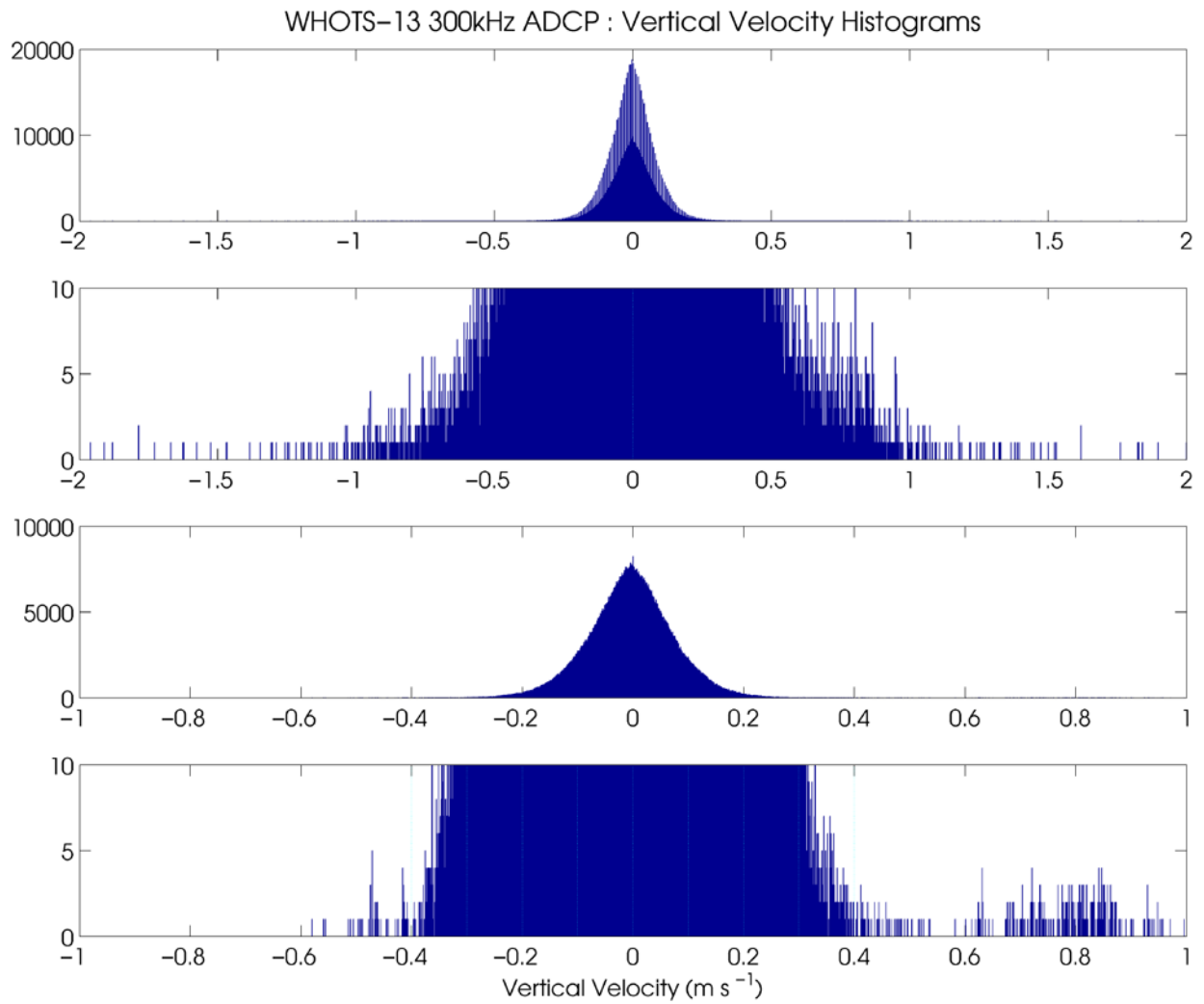


Figure 5-105. Histogram of vertical velocity of the 300 kHz ADCP for raw data (top panel) and enlarged for clarity (upper middle panel), and for partial quality controlled data (lower middle panel) and enlarged for clarity (bottom).

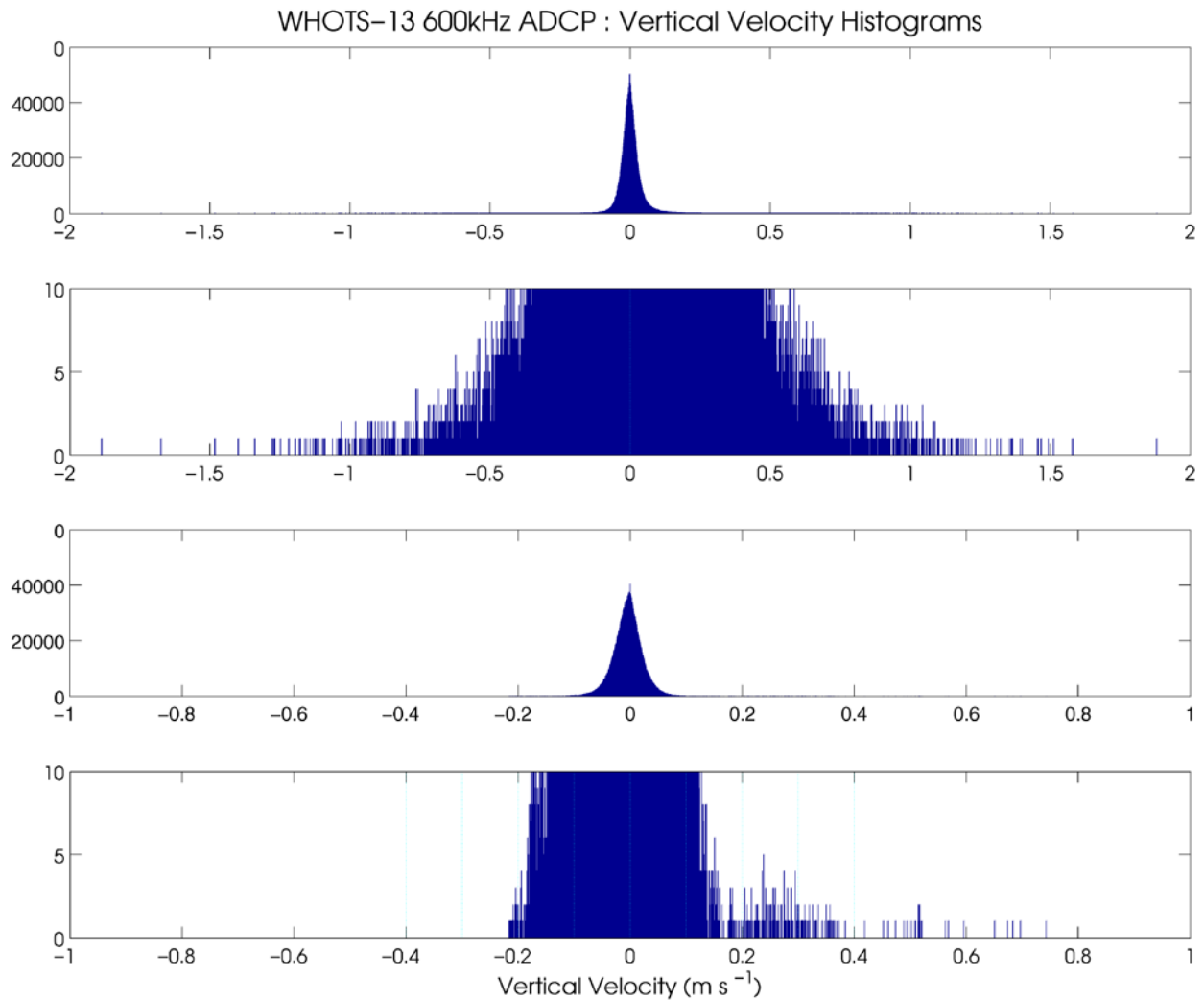


Figure 5-116. Histogram of vertical velocity of the 600 kHz ADCP for raw data (top panel) and enlarged for clarity (upper middle panel), and for partial quality controlled data (lower middle panel) and enlarged for clarity (bottom).

- 7) A quality control routine known as ‘edgers’ identifies outliers in surface bins using a five point median differencing method. The median velocity from surface bins was calculated for each ensemble, and then a five point running median of the surface bin median was calculated. This was then compared to individual velocity observations in the surface bins, and those differing by greater than 0.48 m/s were flagged.
- 8) A 5-pole low pass Butterworth filter with a cutoff frequency of 1/4 cycles/hour was used upon the length of the time-series to isolate low frequency flow for each bin

independently. The low frequency flow is then subtracted giving a time series of high frequency velocity component fluctuations for each bin. Data points were considered outliers when their values exceeded four standard deviations from the mean (for each bin) and were removed.

- 9) A median residual filter used a 7-point (70 minute) median differencing method to define velocity fluctuations. A 7-point running median is calculated for each bin independently and the result is subtracted out giving time series of fluctuations relative to the running median. Outliers greater than four standard deviations from the mean of the 7 points are flagged and removed for each bin.
- 10) Meticulous verification of all the quality control routines was performed through visual inspections of the quality controlled velocity data. Two methods were utilized; time-series of u and v components for multiple bins were evaluated as well as individual vertical profiles. The time-series methodology involved inspecting u and v components separately, five bins at a time, over 600 ensembles (100 hours). Any instance showing one bin behaving erratically from the other four bins was investigated further. If it seemed that there could be no reasonable rationale for the erratic points from the identified bin, the points were flagged [see Figure 5-14 and Figure 5-15 and the WHOTS Data Report 1 (Santiago-Mandujano et al., 2007)]. The intent of the vertical inspection of vertical profiles of the u and v components was to find entire profiles that were not aligned with neighboring profiles. Thirty u and v profiles were stacked at a time and were visually inspected for any anomalous data.

C. Vector Measuring Current Meter (VMCM)

Vector measuring current meters (VMCM) were deployed on the WHOTS-13 mooring at depths of 10 m and 30 m, serial numbers SN 16 and 75 respectively. VMCM data were processed by the WHOI/UOP group. VMCM record times are shown in Table 5-7.

The instrument at 10 m had problems with its compass, and it did not yield current direction data, the directions from the 600 kHz ADCP were used to provide data directions to this VMCM data set. The VMCM 1-minute data were sub-sampled at the 10-minute ADCP times, and directions from ADCP bin 10 (centered at 10.39 m) were used to replace the missing data of the 10-m VMCM.

Table 5-7. Record times (UTC) for the VMCMs at 10 m and 30 m during the WHOTS-13 deployment

	WHOTS-13	
	VMCM016	VMCM075
Deployment and recovery times	26-Jun-2016 18:33 01-Aug-2017 02:17	26-Jun-2016 18:19 01-Aug-2017 02:25
Processed file beginning and end times	27-Jun-2016 12:10 31-Jul-2017 16:30	27-Jun-2016 10:30 31-Jul-2017 16:38

Daily (24 hour) moving averages of quality controlled 600 kHz ADCP data are compared to VMCM data interpolated to the ADCP ensemble times in the top panels of Figure 5-17 through Figure 5-20, and the difference is shown in the middle panels. The absolute value of the mean difference plus or minus one standard deviation is shown at the top of the middle panel. Velocities are not compared if greater than 80% of the ADCP data within a 24 hour average was flagged. The absolute value of mean differences for all deployments and both velocity components varied between 3 and 4 cm/s, with standard deviations between 2.5 and 5 cm/s. The VMCM data does not appear to degrade over time for any deployment. Propeller fouling would dampen measured VMCM velocity magnitudes, but a decrease in VMCM velocity magnitude compared to ADCP velocity magnitude with time is not observed.

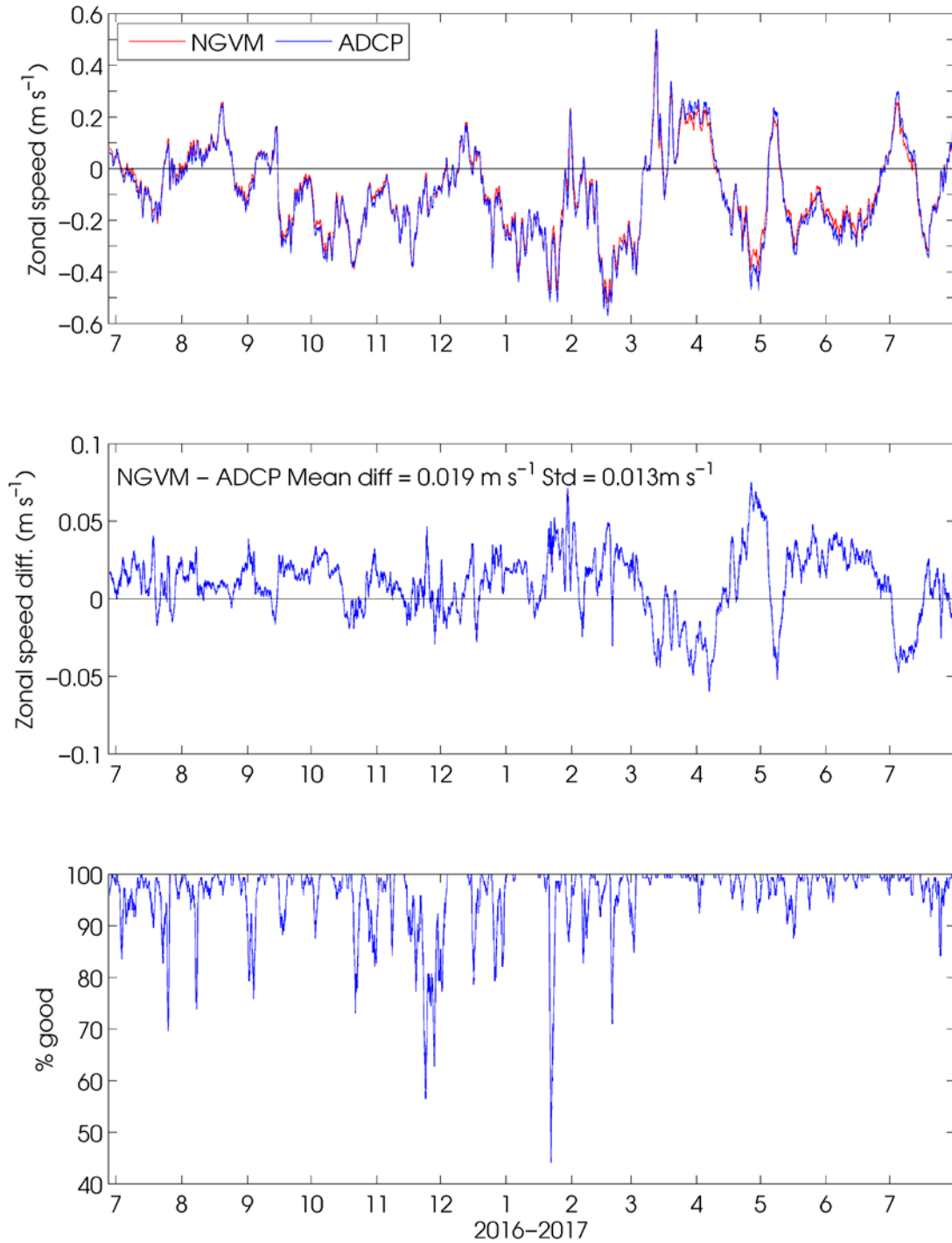


Figure 5-12. A comparison of 30 m VMCM and ADCP zonal current for WHOTS-13. The top panel shows 24 hour moving averages of VMCM zonal current at 30 m depth (red) and ADCP (blue) from the nearest depth bin to 30 m (30.22 m). The middle panel shows the current difference, and the bottom panel shows the percentage of ADCP data within the moving average not flagged by quality control methods.

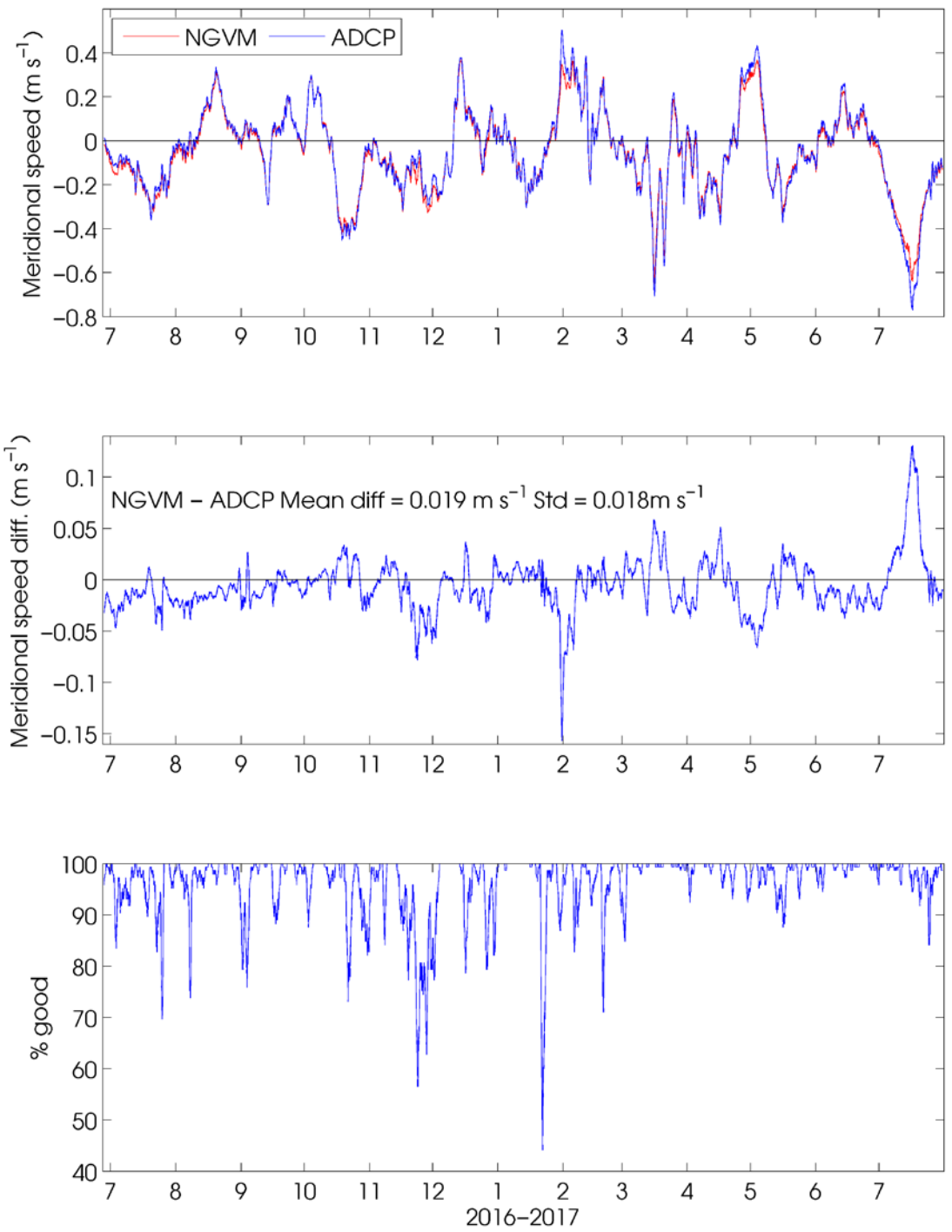


Figure 5-18. Same as in Figure 5-17 but for the meridional current component.

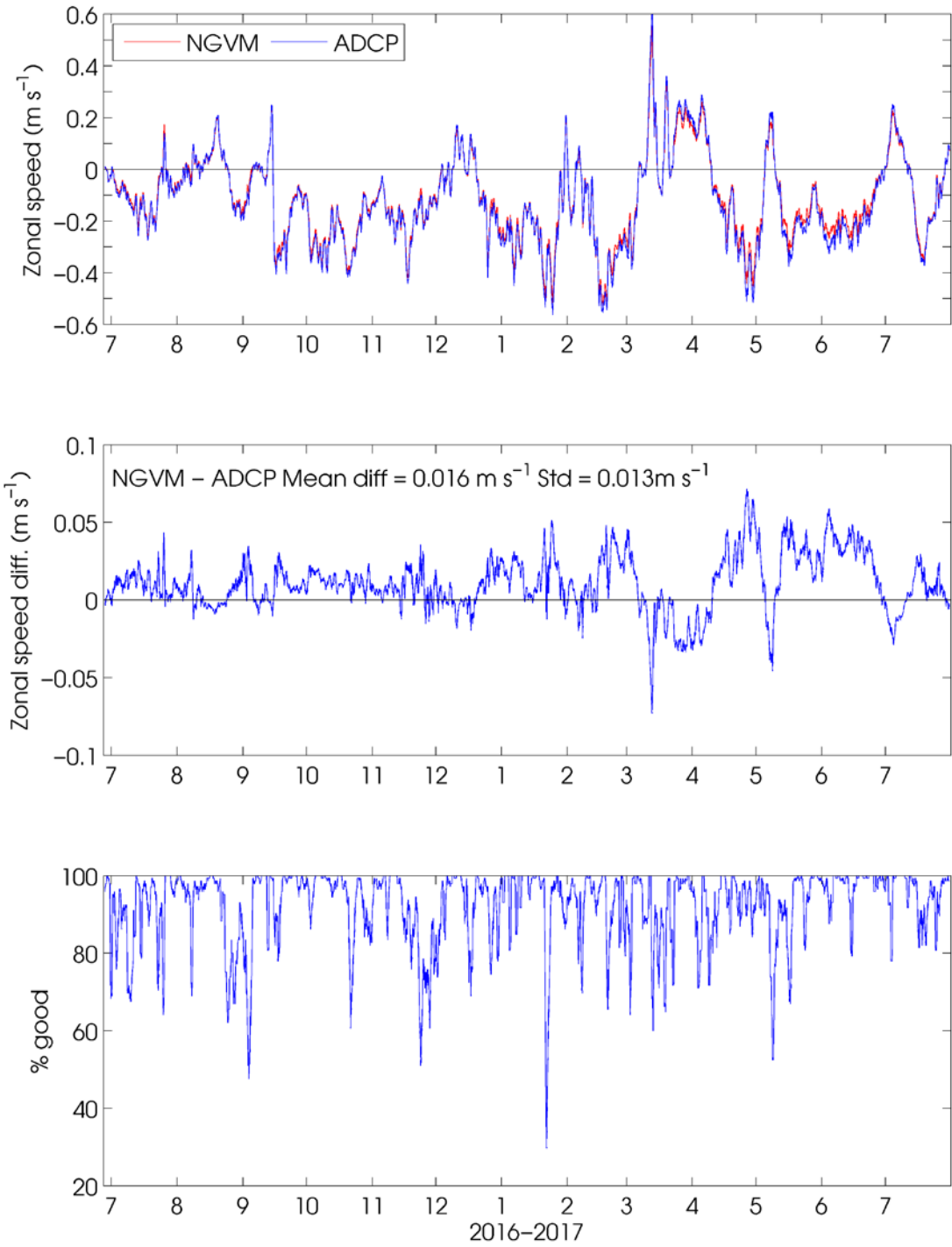


Figure 5-19. Same as in Figure 5-17 but for the 10 m VMCM.

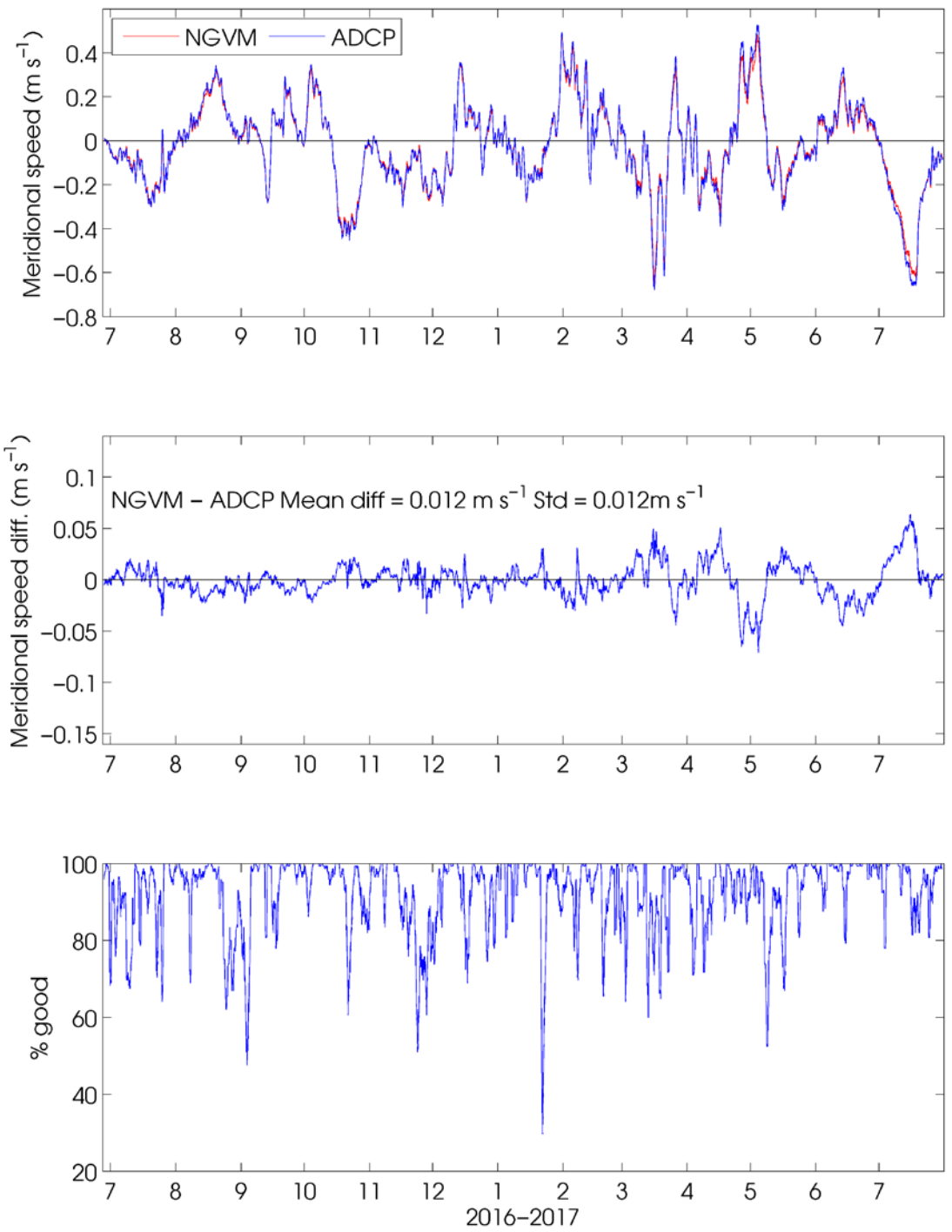


Figure 5-20. Same as in Figure 5-19 but for the meridional current component.

D. Global Positioning System Receiver and ARGOS Positions

Xeos Global Positioning System receiver (IMEI 300034013701980) and ARGOS beacon were attached to the tower top of the buoy during the WHOTS-13 deployment. Data returns from the receivers were high (Table 5-8).

Table 5-8. GPS and ARGOS record times (UTC) during WHOTS-13

WHOTS-13	Xeos GPS	ARGOS
Raw file beginning and end times	28-Jun-2016 00:23 30-Jun-2017 21:03	27-Jun-2016 09:17 01-Aug-2017 08:00

ARGOS positions were available during the WHOTS-13 deployment and they provided additional information on the buoy's motion. ARGOS data were recorded at 10 minutes intervals, although there are some small gaps at repeated times present in the records. Samples taken before mooring deployment were eliminated. Data were screened for points that were greater than 2.5 nautical miles from the surveyed anchor positions for each deployment which was considered to be the buoy watch circle radius. The velocity magnitude was calculated and positions that resulted in speeds greater than 1 m s^{-1} were removed. Data were interpolated onto a regular time grid in order to compute spectra.

For comparison, Figure 5-21 shows the ARGOS buoy's positions together with the GPS positions during the WHOTS-13 deployment. The standard deviation of the difference between these two records is about 800 m.

The ARGOS positions of the WHOTS-13 buoy for the duration of the deployment are in Figure 5-22, and shows the color-coded positions according to their data quality. The data quality is determined by its distance from the satellite track. Data of a better quality have a higher flag number: 3 is for a distance less than 150 m, 2 is for a distance between 150 and 350 m, and 1 is for a distance between 350 and 1000 m. For the duration of the deployment, the buoy had a mean position of about 1.6 km from the anchor, with a standard deviation of about 500 m.

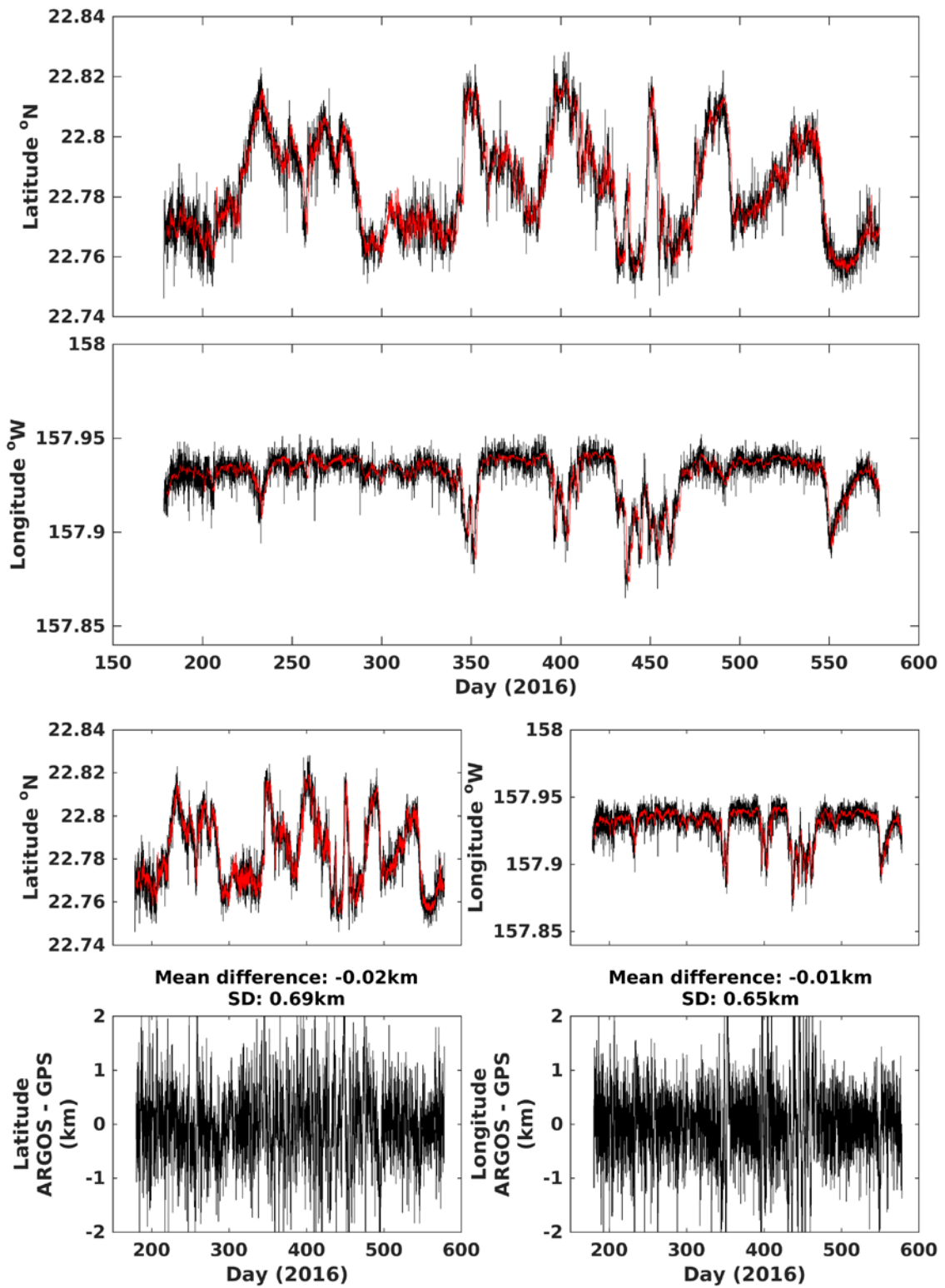


Figure 5-131. WHOTS-13 buoy position from ARGOS data (black line), and from GPS data (red line). The top and two middle panels show the latitude and longitude of the buoy. The bottom panel shows the difference between the GPS positions and the ARGOS positions interpolated to the GPS times.

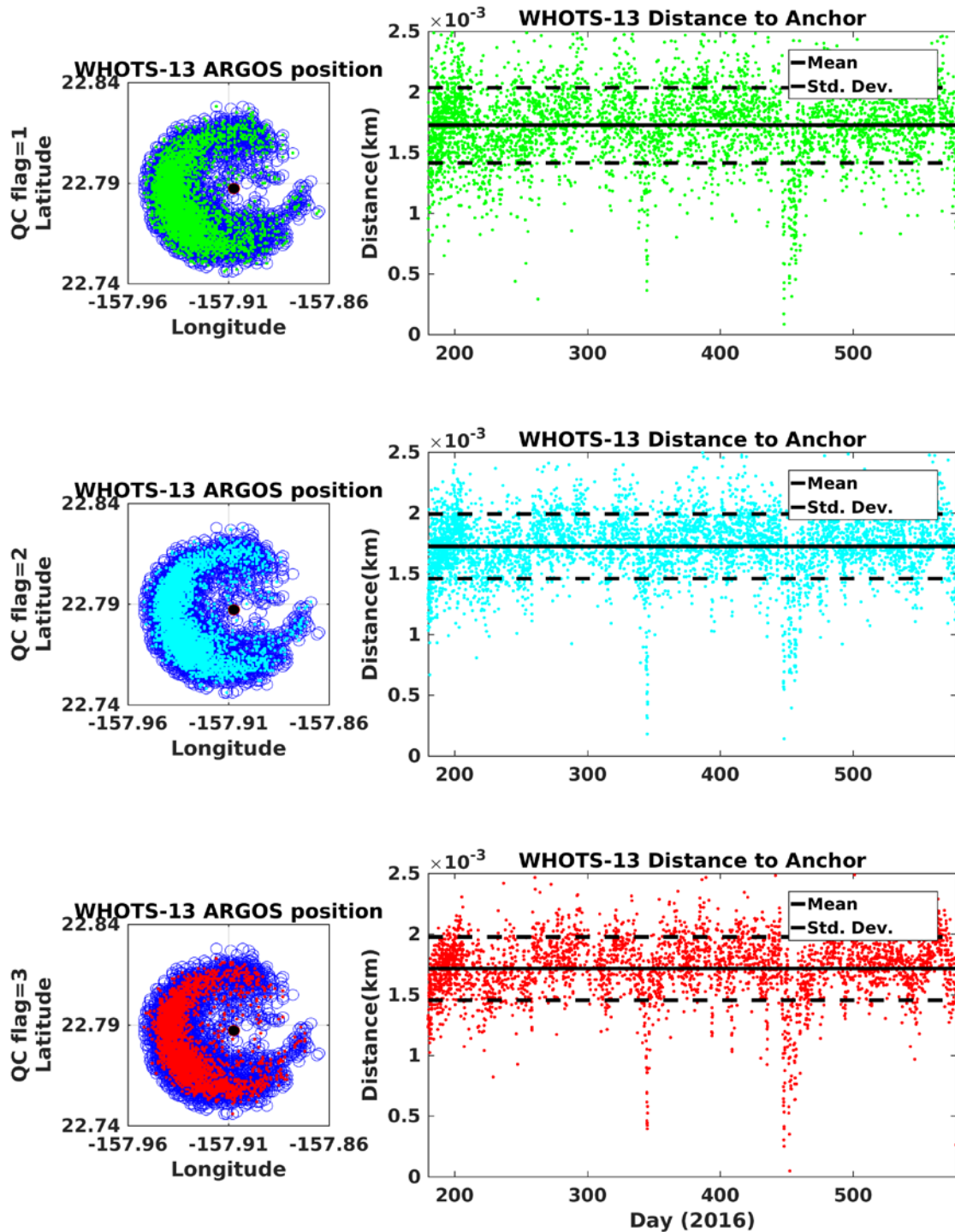


Figure 5-22. WHOTS-13 buoy ARGOS positions (circles, left panels), and distance from its anchor (dots, right panels). The data are colored according to their quality control flag, 1: green, 2: light blue, 3: red. The black circle in the center of the left side panels is the location of the mooring's anchor. The black line in the right panel plots is the mean distance between the buoy and its anchor, and the dashed line is the mean plus minus one standard deviation.

VI. Results

Conditions during the WHOTS-13 cruise (WHOTS-13 mooring deployment) were favorable. The WHOTS-13 mooring was deployed on June 26th-27th, 2016 under 10-15 kt NE winds and 2-3 m waves from NE. These conditions persisted on 28th through the 30th, with occasional higher wind gusts. Winds were 12 kt from the east on June 29th-30th during the WHOTS-12 recovery, increasing to between 15 and 18 kt on June 30th – July 2nd.

Near-surface currents were up to 1 kt westward during transit to Station ALOHA, turning NNEward upon arrival to Station ALOHA, and fluctuating the rest of the cruise. There was a nearly stationary anticyclonic eddy east of ALOHA, suggesting a possible increasing geostrophic flow towards the NW, although a combination of internal semidiurnal and diurnal tides, along with near-inertial oscillations, were more noticeable especially in vertical shear.

CTD casts conducted near the mooring (Station 50) during the cruise (Figure 6-1 through Figure 6-5) showed a broad salinity maximum between 120 and 180 dbar.

During the WHOTS-14 cruise (WHOTS-13 mooring recovery), Station ALOHA was under the influence of the eastern North Pacific high pressure system, and the associated east-northeasterly trade winds. Moisture associated with former Tropical Cyclone Fernanda, which passed north of the islands during the days before the cruise was moving westward away from the state with a drier air-mass gradually filling in from the east at the beginning of the cruise. By July 27th moisture associated with the remnants of former Tropical Cyclone Greg, passing 400 miles SE of Hilo started to bring increased humidity. Conditions during the WHOTS-14 deployment on July 27th-28th were favorable, with 11-16 kts NE winds and 1.5-2 m waves from the east.

Weather conditions were favorable during 28th through the 30th, with NE wind speeds of 10-16 kts with occasional higher gusts. Weather conditions were favorable on July 31st - August 1st during the WHOTS-13 recovery, winds were 10-17 kt from the east. CTD casts conducted near the mooring sites (Station 50 and 52, Figure 6-6 through Figure 6-11), displayed a deep mixed layer (up to 60 m) and a broad subsurface salinity maximum between 80 and ~200 dbar (see Figure 6-11).

The temperature MicroCAT records during the WHOTS-13 deployment (Figure 6-16 through Figure 6-20) show obvious seasonal variability in the upper 100 m, and a sudden drops in early August and mid-September 2016, and sudden increases in August and May 2017. Persistent high temperatures between mid-August and mid-September 2016 show a corresponding decrease in salinity in the upper 130 m (Figures 6-21 through 6-25), and in density (Figures 6-26 through 6-30). A sharp salinity drop is also seen in the upper 30 m in late July 2016, and a second drop in May 2017, reaching 55 m.

Figure 6-31 and Figure 6-32 show contours of the WHOTS-13 MicroCAT data in context with data from the previous 12 deployments. The seasonal cycle is obvious in the temperature record, with record temperatures (higher than 26 °C) in the summer of 2004, and again in the summer of 2014 and 2015. Salinities in the subsurface salinity maximum were relatively low during the first 6 years of the record, only to increase drastically after 2008 through 2015, with some episodes of lower salinity in mid-2011 and early 2012. The salinity maximum extended to near the surface in some instances in early 2010, 2011, late 2012-early 2013 and during February-March 2013. The low salinity periods in July and August-September 2016, and in May 2017 observed in the MicroCAT time-series plots (Figures 6-21 through 6-25) are apparent in Figures 6-31 and 6-32. When plotted in σ_θ coordinates (Figure 6-32), the salinity maximum seems to be centered roughly between 24 and 24.5 σ_θ .

Records from the WHOTS-13 MicroCATs (Figure 6-33) deployed near the bottom of the mooring (4657 m) detected temperature and salinity changes related to episodic ‘cold events’ apparently caused by bottom water moving between abyssal basins (Lukas et al., 2001). These events are being monitored by instruments at the ALOHA Cabled Observatory (ACO, Howe et al., 2011), a deep water observatory located at the bottom of Station ALOHA (about 6 nautical miles west from the WHOTS-13 anchor), since June 2011. Figure 6-33 shows temperature and salinity records from the WHOTS-13 MicroCATs superimposed on the ACO data. The MicroCAT data agreed with the temperature decrease and the salinity variability registered by ACO instruments during three cold events in August and December 2016, and by the end of July 2017, during the WHOTS-13 period.

Figure 6-37 through Figure 6-39 show time series of the zonal, meridional, and vertical currents recorded with the moored ADCPs during the WHOTS-13 deployment. Figure 6-34 through Figure 6-36 show contours of the ADCP current components in context with data from the previous deployments. In spite of the gaps in the data, an obvious variability is seen in the zonal and meridional currents, apparently caused by passing eddies. On top of this variability there have been periods of intermittent positive or negative zonal currents, for instance during 2007-2008. The contours of vertical current component (Figure 6-36) show a transition in the magnitude of the contours near 47 m, indicating that the 300 kHz ADCP located at 126 m moves more vertically than the 600 kHz ADCP located at 47.5 m.

A comparison between the moored ADCP data and the shipboard ADCP data obtained during the WHOTS-13 cruise is shown in Figure 6-40 and Figure 6-41 and a similar comparison during the WHOTS-14 cruise is shown in Figure 6-42 and Figure 6-43. Some of the differences seen especially in the zonal component may be due to the mooring motion, which was not removed from the data. Comparisons between the available shipboard ADCP from HOT-285 through 294 cruises and the mooring data are shown in Figure 6-44 and Figure 6-45.

The motion of the WHOTS-13 buoy was registered by the Xeos-GPS receiver, and its positions are plotted in Figure 6-45. The buoy was located west of the anchor for the majority of the deployment, except during December 2016 and February-March 2017 when it was east of it sporadically. Power spectrum of these data (Figure 6-46) shows extra energy at the inertial period (~31 hr). Combining the buoy motion with the tilt (a combination of pitch and roll) from the ADCP data (Figure 6-47), showed that the tilt increased as the buoy distance from the anchor

increased. This was expected since the inclination of the cable increases as the buoy moves away from the anchor.

A. CTD Profiling Data

Profiles of temperature, salinity and potential density (σ_θ) from the casts obtained during the WHOTS-13 deployment cruise are presented in Figure 6-1 through Figure 6-5, together with the results of bottle determination of salinity. Figure 6-6 through Figure 6-11 are the results of the CTD profiles during the WHOTS-14 cruise.

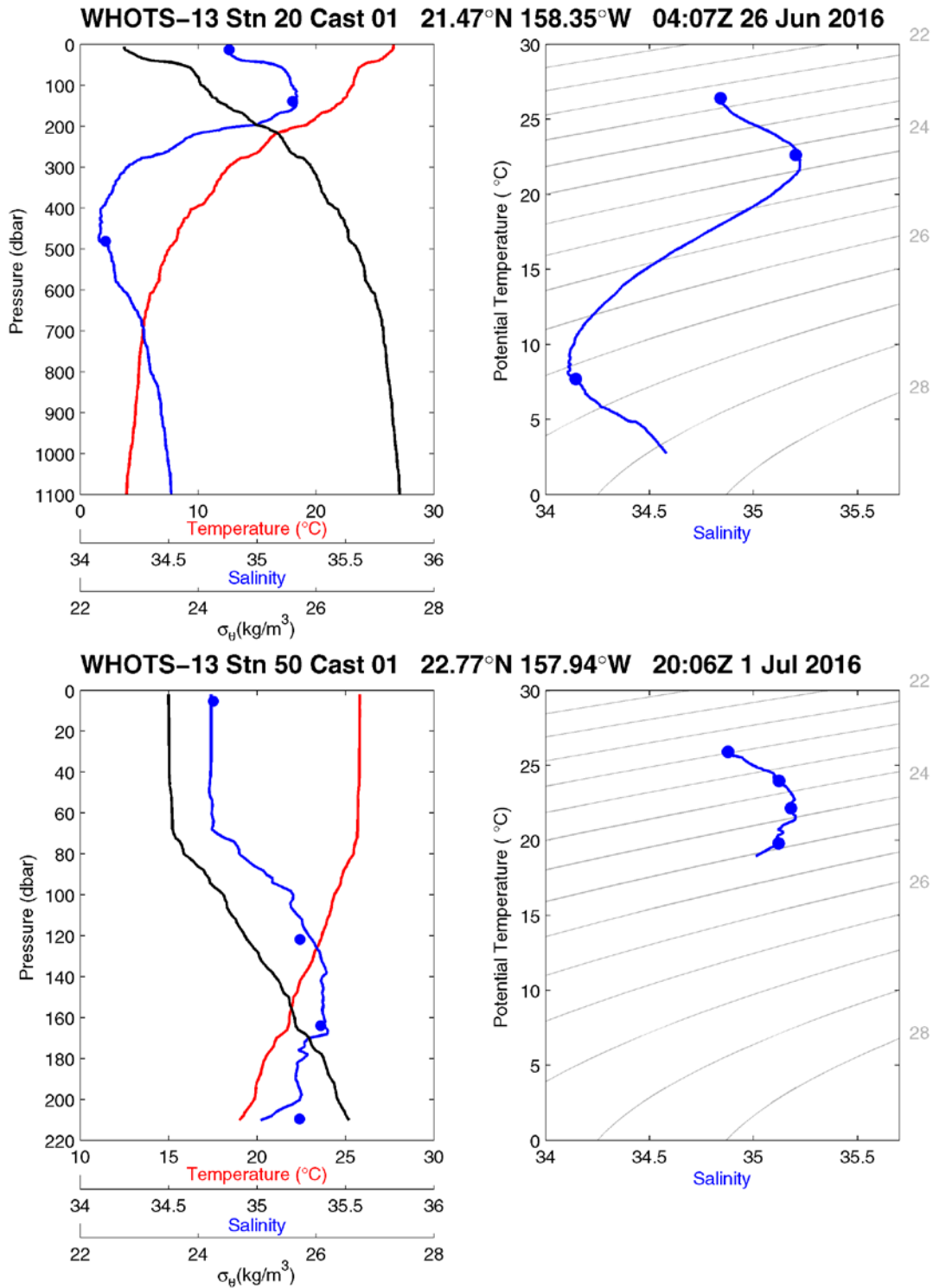


Figure 6-1. [Upper left panel] Profiles of CTD temperature, salinity, and potential density (σ_θ) as a function of pressure, including discrete bottle salinity samples (when available) for station 20 cast 1 during the WHOTS-13 cruise. [Upper right panel] Profiles of CTD salinity as a function of potential temperature, including discrete bottle salinity samples (when available) for station 20 cast 1 during the WHOTS-13 cruise. [Lower left panel] Same as in the upper left panel, but for station 50 cast 1. [Lower right panel] Same as in the upper right panel, but for station 50 cast 1.

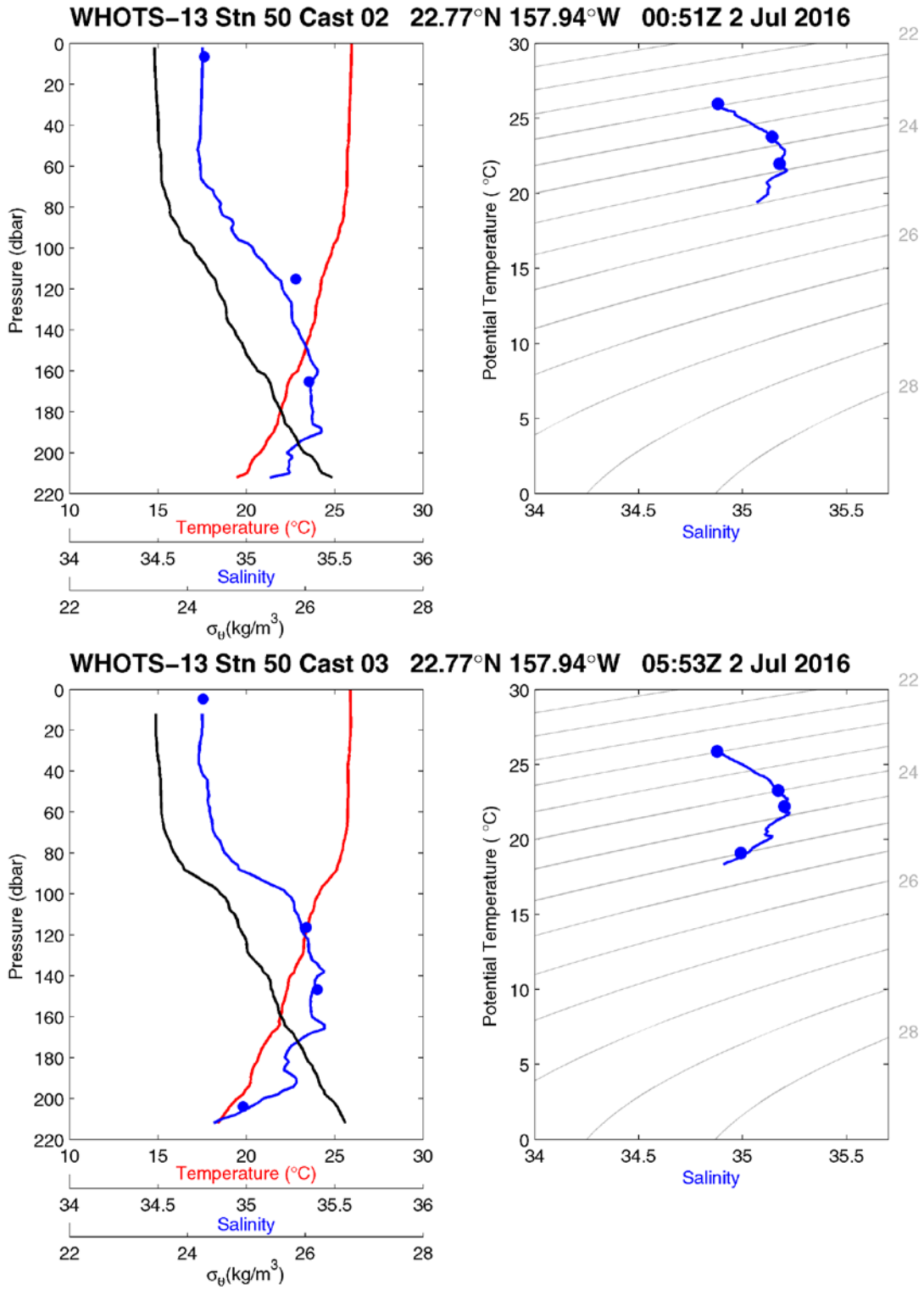


Figure 6-2. [Upper panels] Same as in Figure 6-1, but for station 50, cast 2. [Lower panels] Same as in Figure 6-1, but for station 50, cast 3.

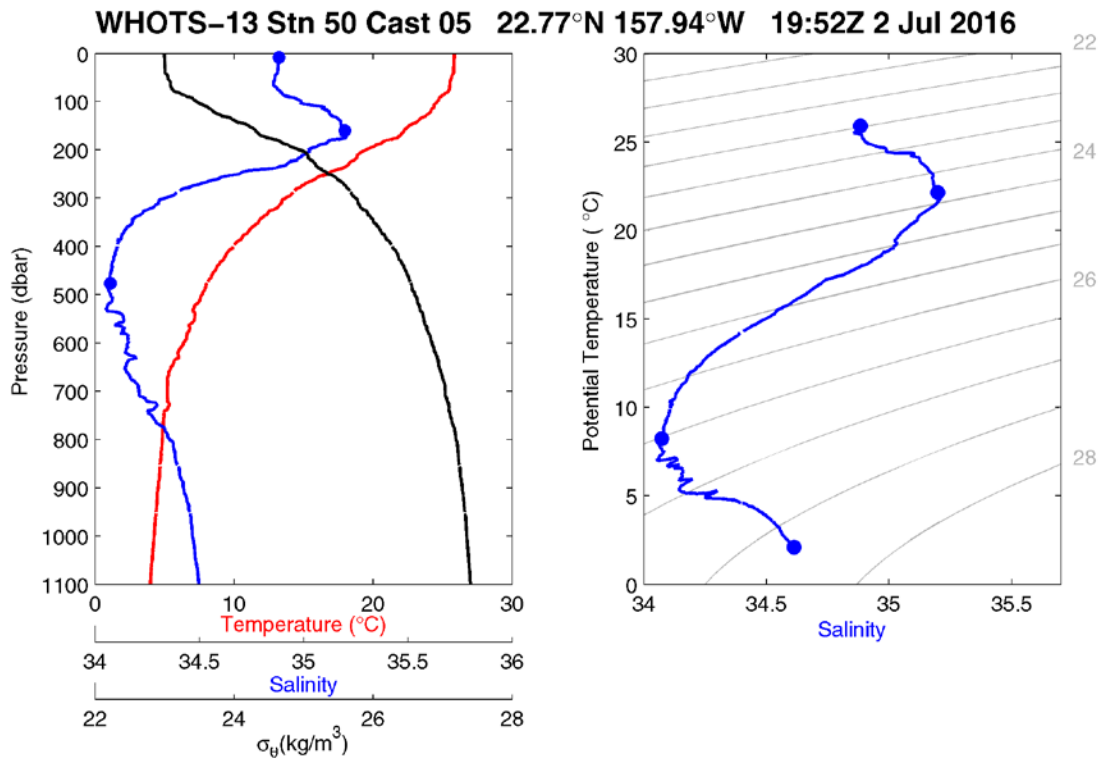
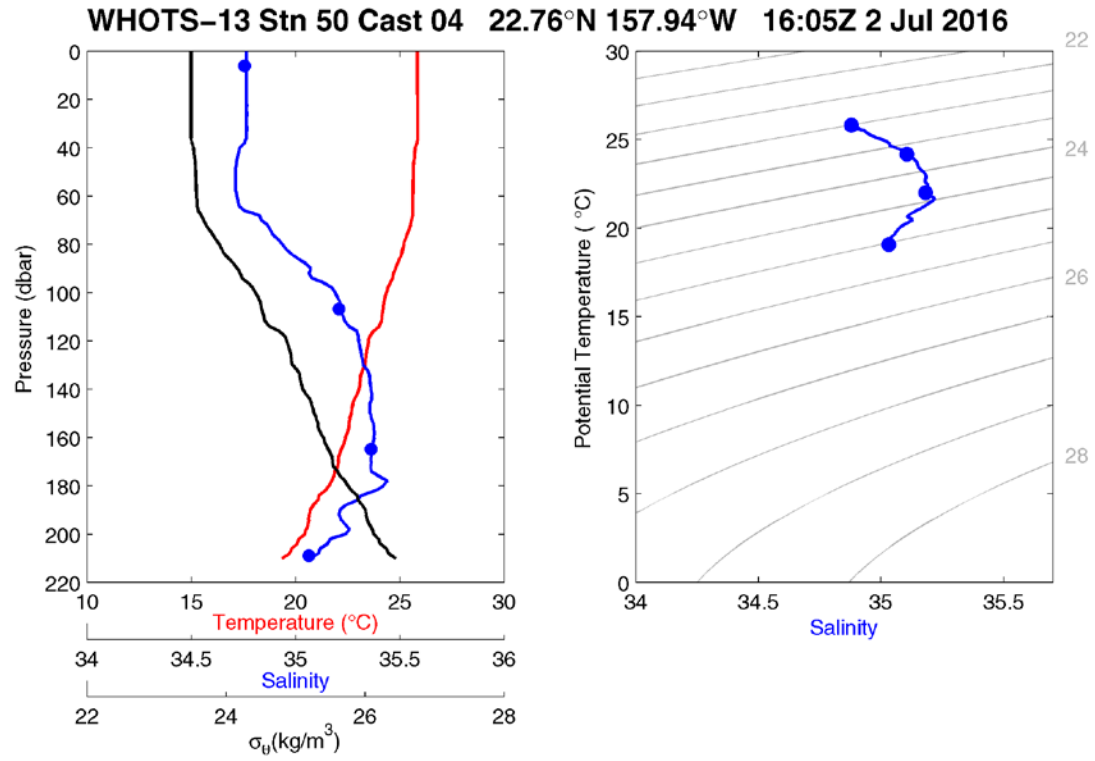


Figure 6-3. [Upper panels] Same as in Figure 6-1, but for station 50, cast 4. [Lower panels] Same as in Figure 6-1, but for station 50 cast 5.

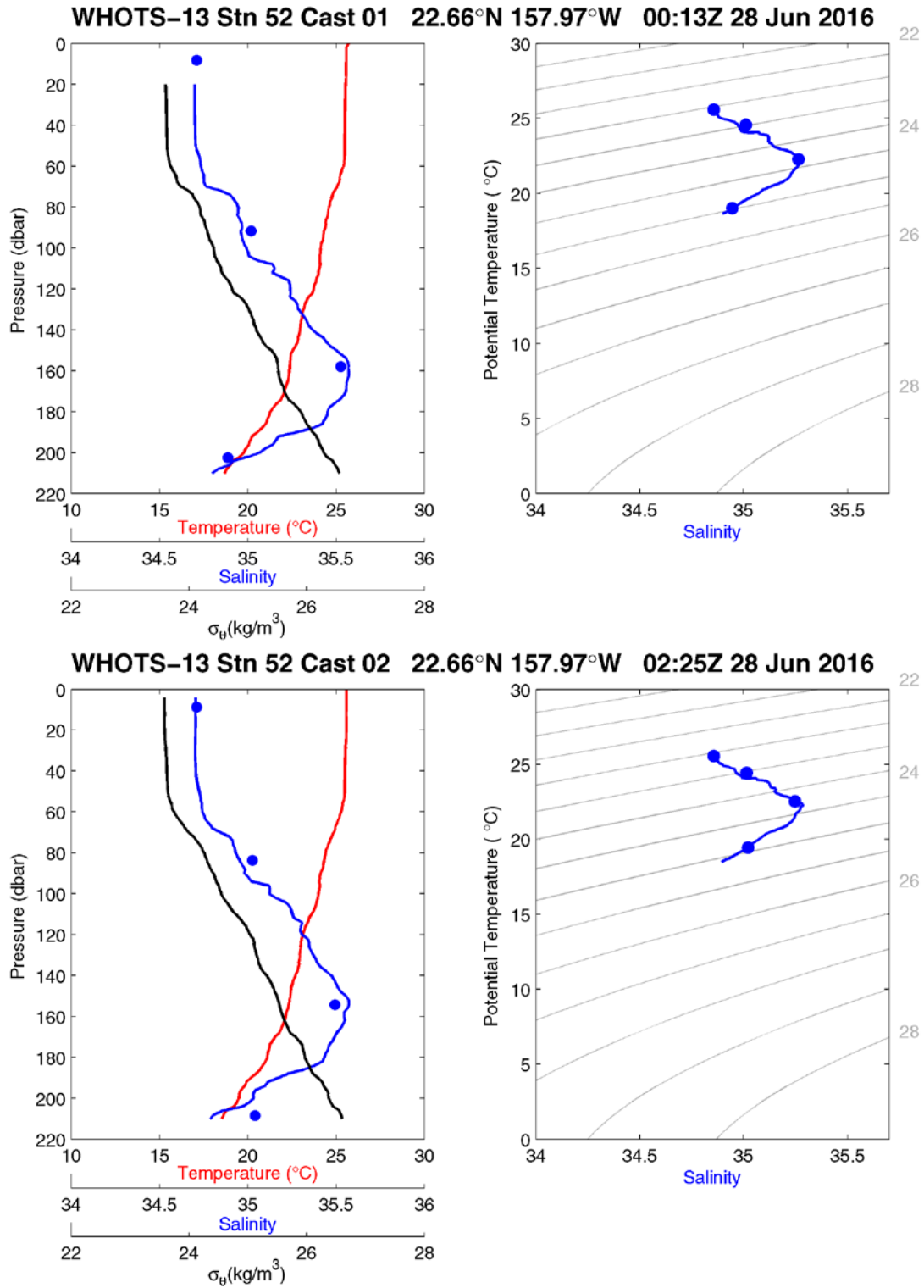


Figure 6-4 [Upper panels] Same as in Figure 6-1, but for station 52, cast 1. [Lower panels] Same as in Figure 6-1, but for station 52 cast 2.

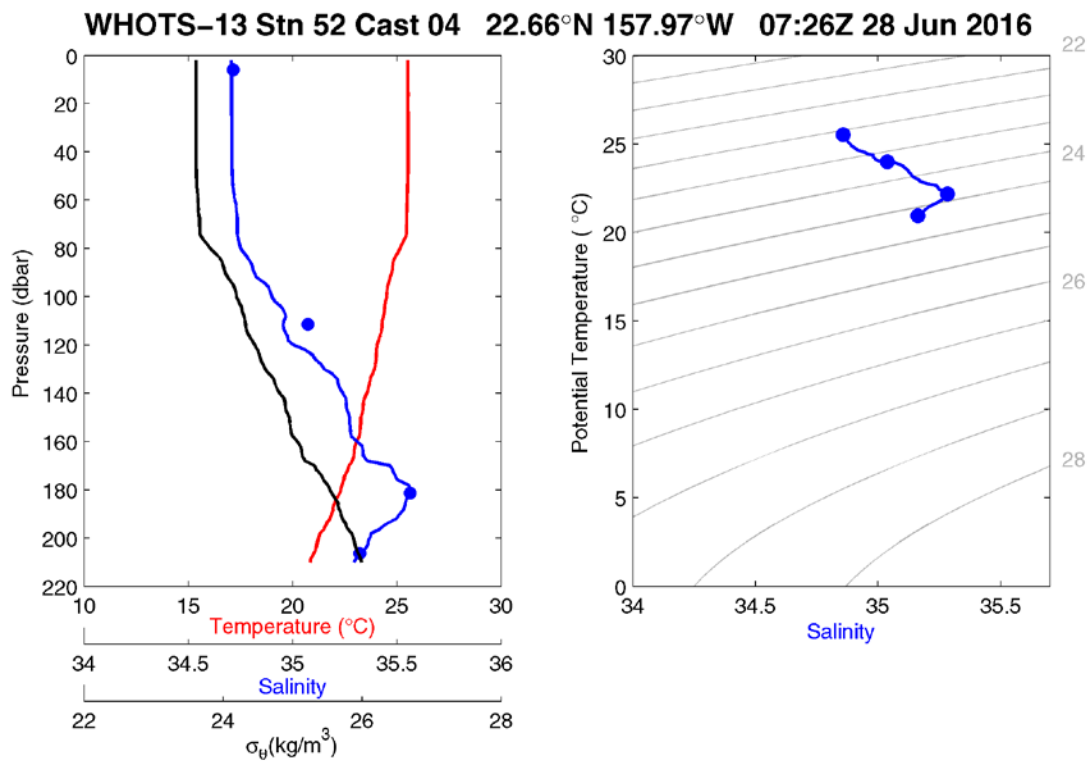
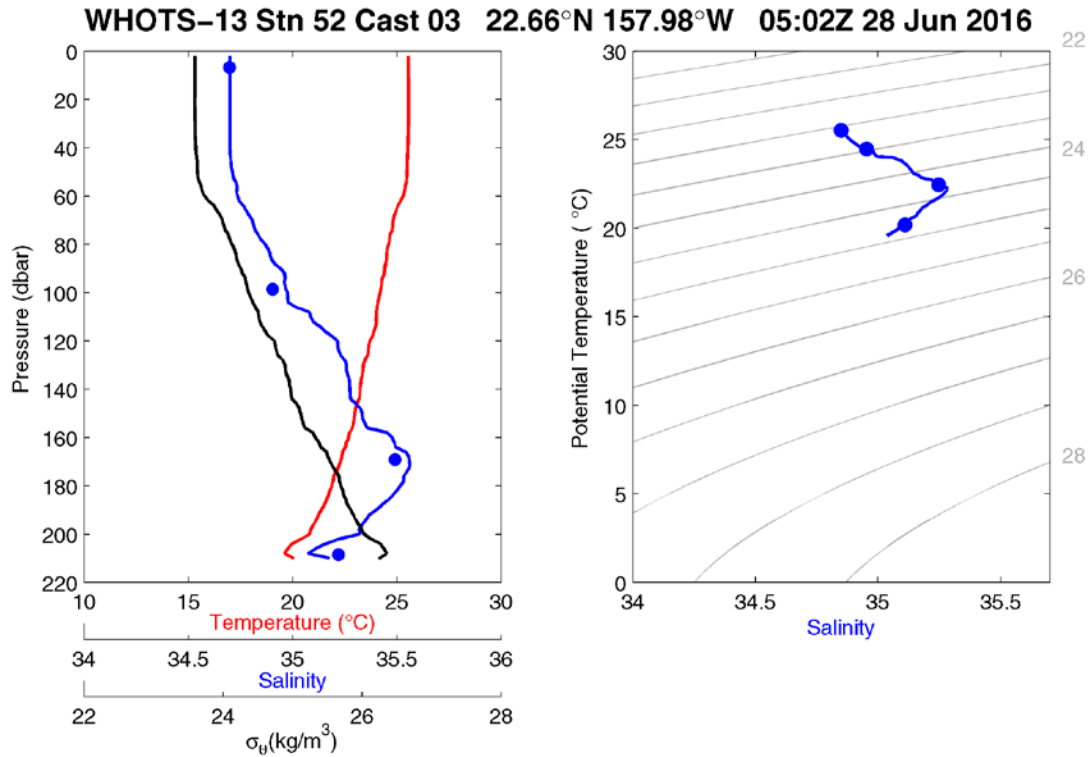


Figure 6-5. [Upper panels] Same as in Figure 6-1, but for station 52, cast 3. [Lower panels] Same as in Figure 6-1, but for station 52 cast 4.

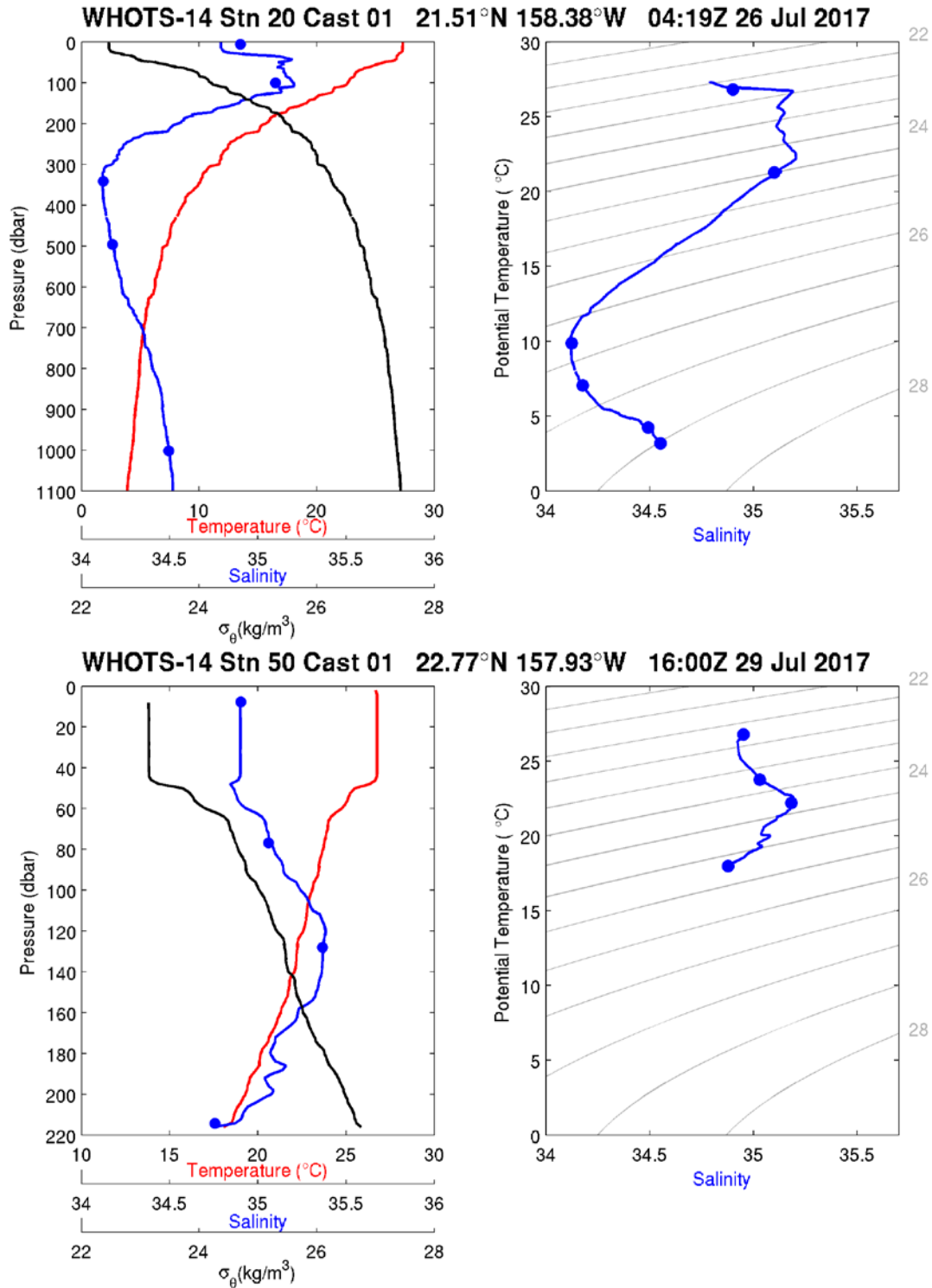


Figure 6-6. [Upper left panel] Profiles of CTD temperature, salinity, and potential density (σ_θ) as a function of pressure, including discrete bottle salinity samples (when available) for station 20 cast 1 during the WHOTS-14 cruise. [Upper right panel] Profiles of CTD salinity as a function of potential temperature, including discrete bottle salinity samples (when available) for station 20 cast 1 during the WHOTS-14 cruise. [Lower left panel] Same as in the upper left panel, but for station 50 cast 1. [Lower right panel] Same as in the upper right panel, but for station 50 cast 1.

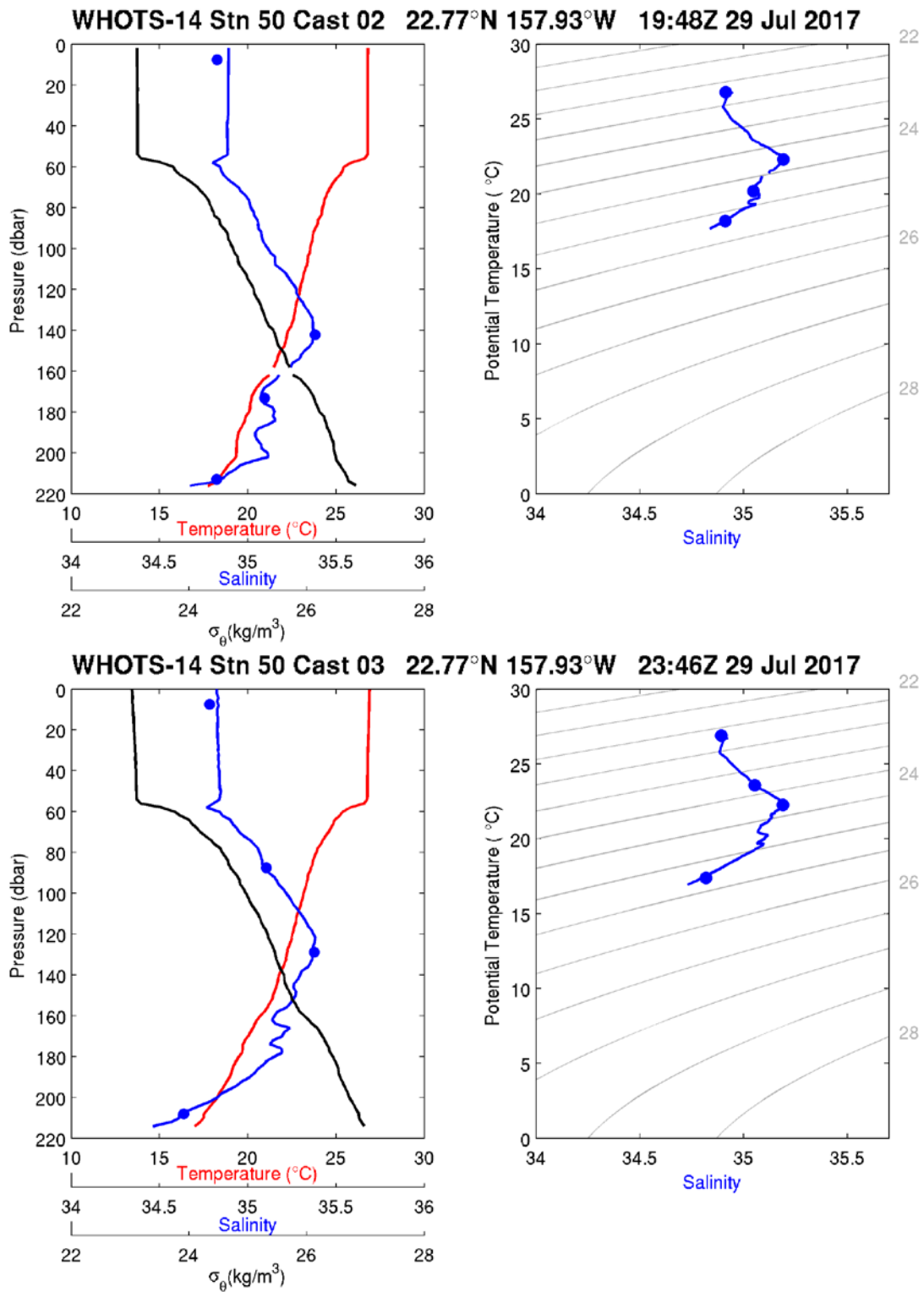


Figure 6-7. [Upper panels] Same as in Figure 6-6, but for station 50, cast 2. [Lower panels] Same as in Figure 6-6, but for station 50, cast 3.

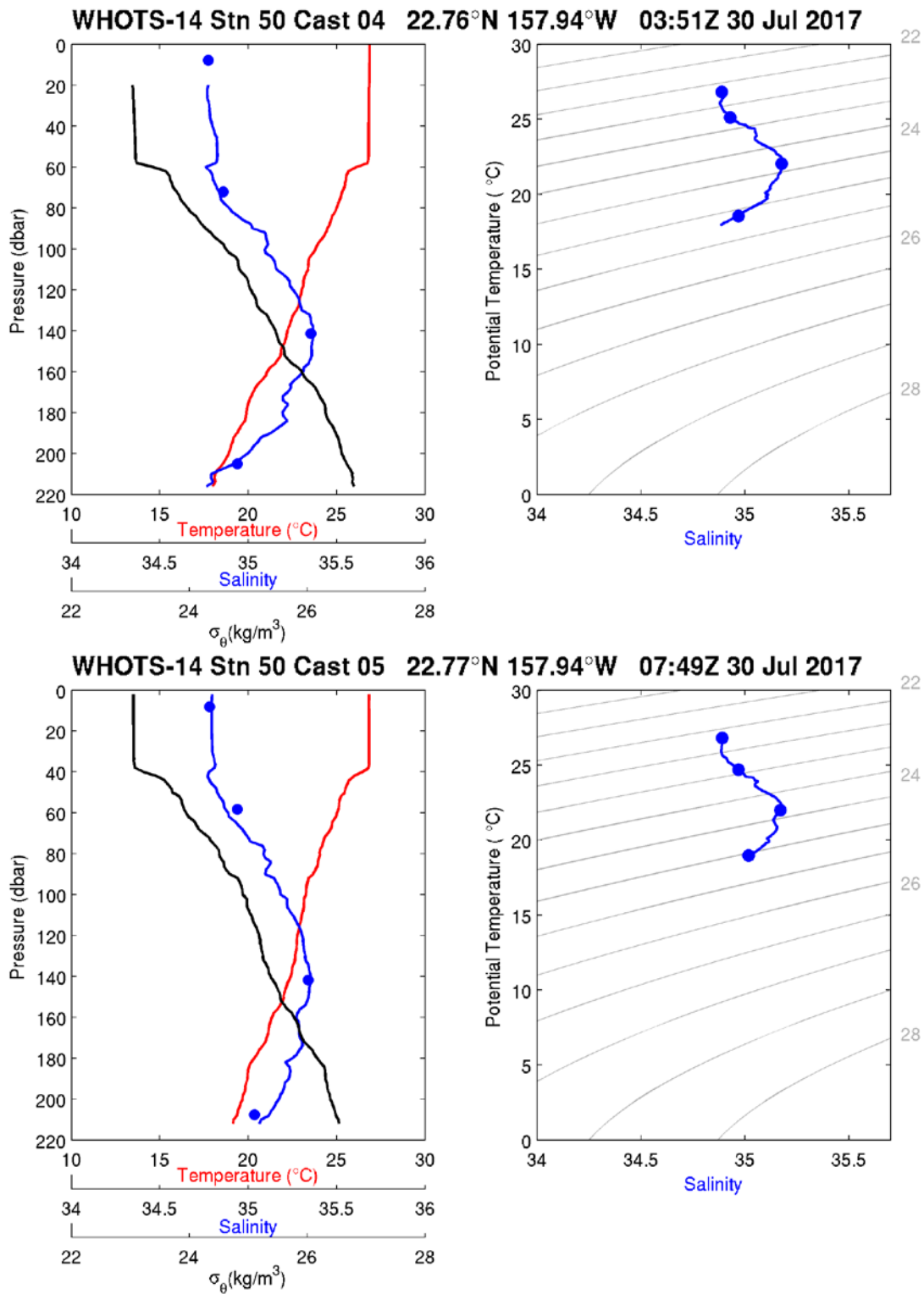


Figure 6-8. [Upper panels] Same as in Figure 6-6, but for station 50, cast 4. [Lower panels] Same as in Figure 6-6, but for station 50 cast 5.

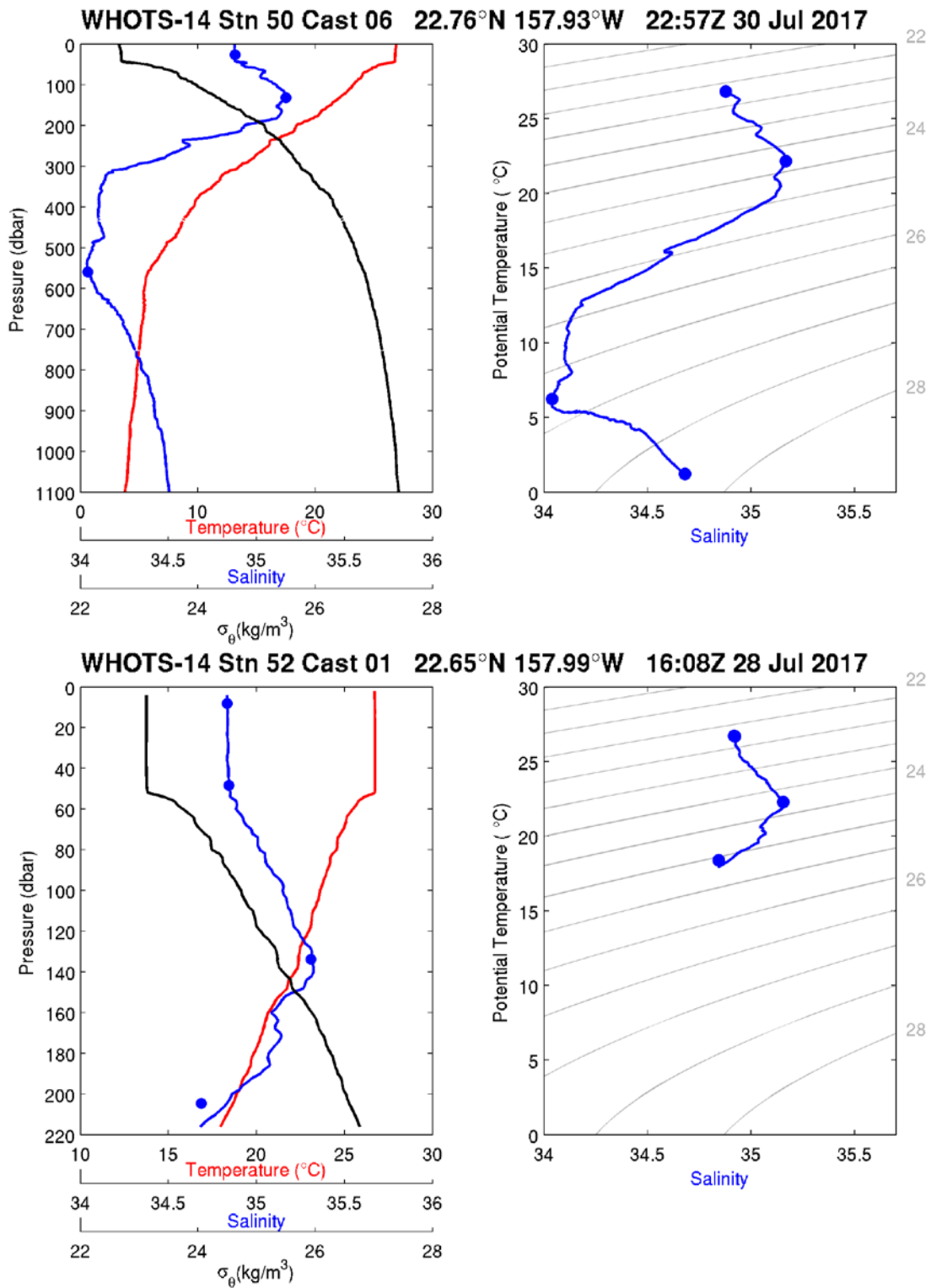


Figure 6-9. [Upper panels] Same as in Figure 6-6, but for station 50, cast 6. [Lower panels] Same as in Figure 6-6, but for station 52, cast 1.

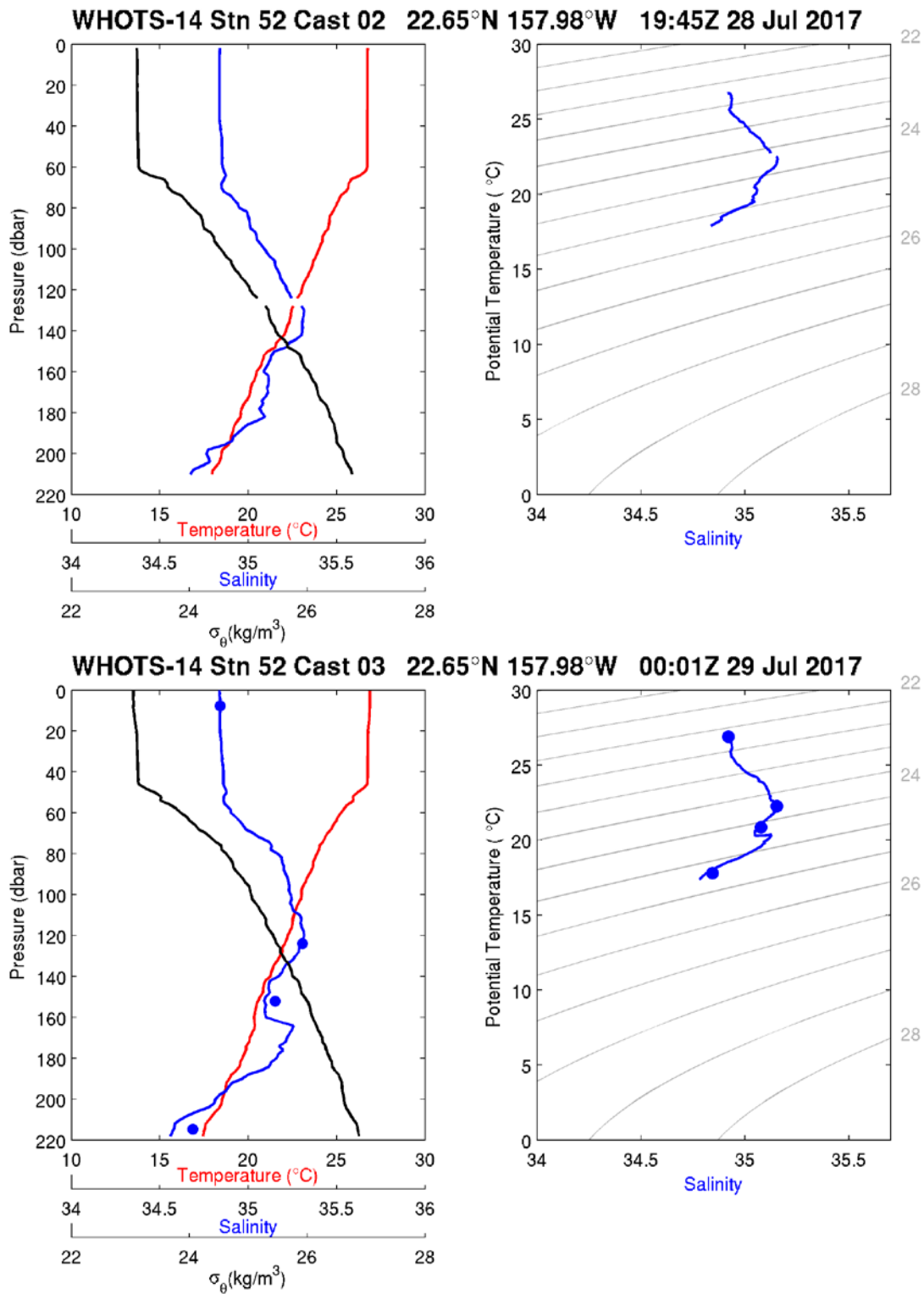


Figure 6-10. [Upper panels] Same as in Figure 6-6, but for station 52, cast 2. [Lower panels] Same as in Figure 6-6, but for station 52, cast 3.

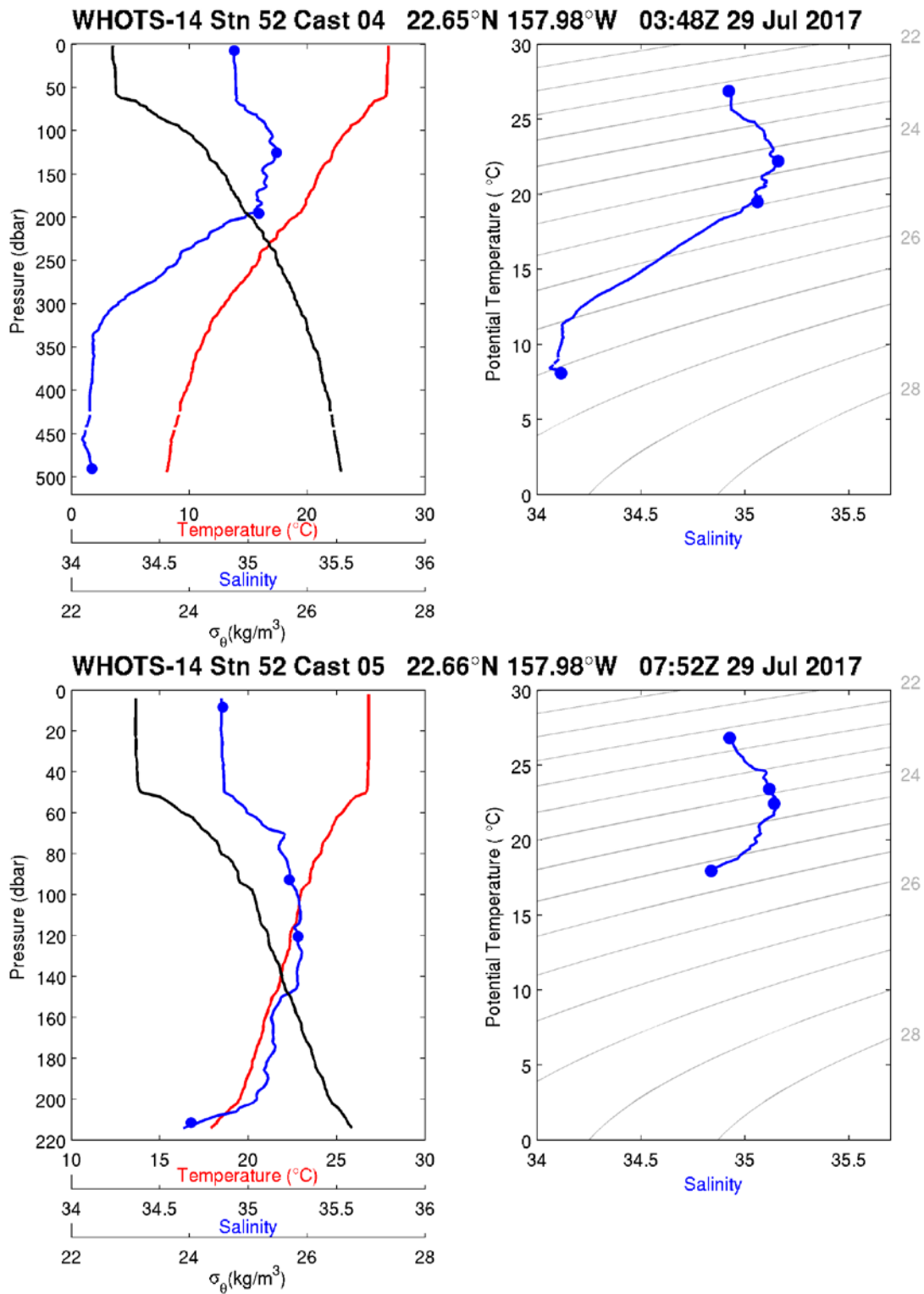


Figure 6-11. Same as in Figure 6-6, but for station 52, cast 4. [Lower panels] Same as in Figure 6-6, but for station 52, cast 5.

B. Thermosalinograph data

Underway measurements of near surface temperature and salinity from the thermosalinograph (TSG) system on board the ship *Hi'ialakai* is presented in Figure 6-12 and navigational data is presented in Figure 6-13 for the WHOTS-13 cruise. TSG and navigational data during the WHOTS-14 cruise is presented in Figures 6-14 and Figures 6-15. Only data from the SBE-21 TSG are shown, as the SBE-45 TSG data had large glitches (see Section II-A and II-B).

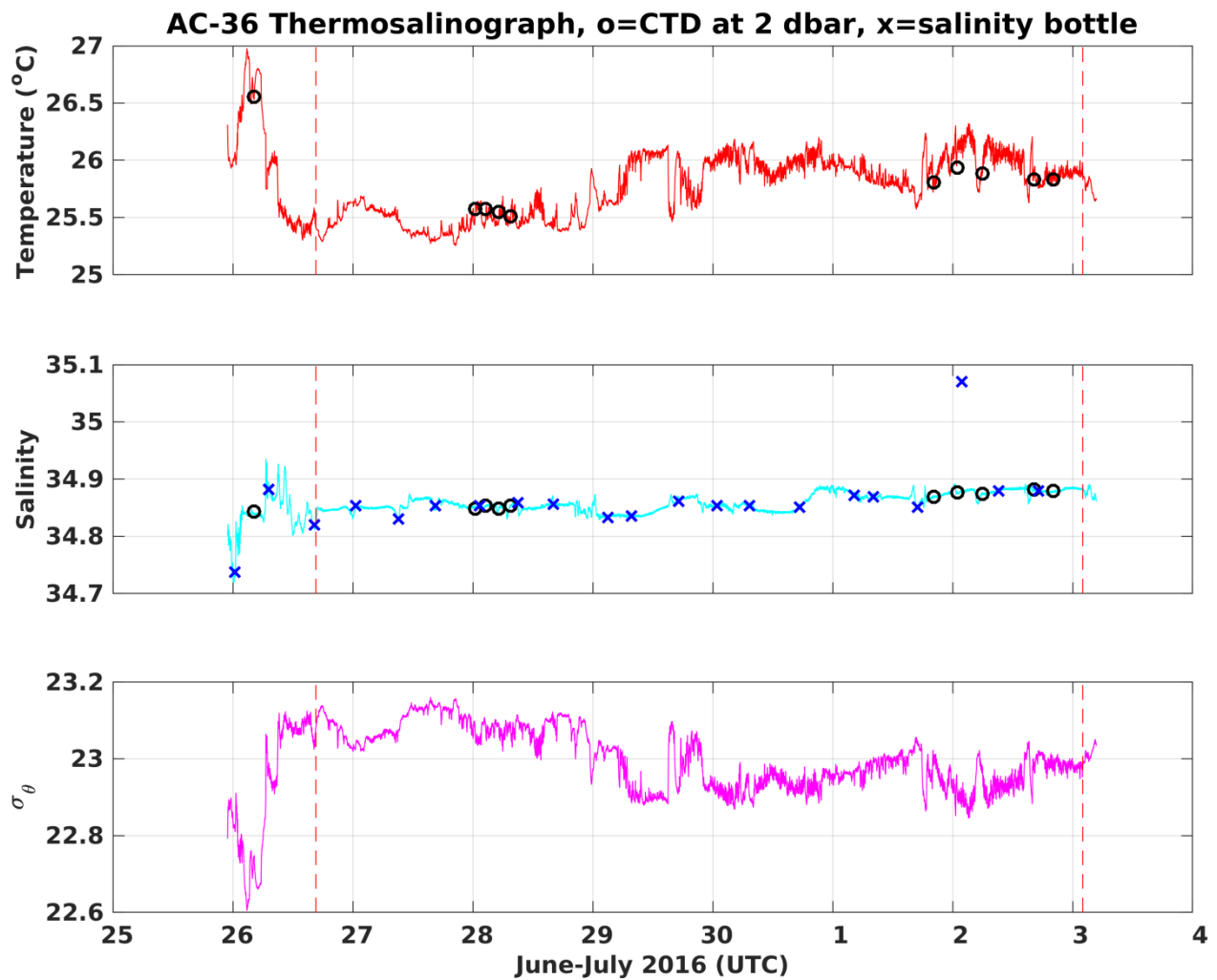


Figure 6-12. Final processed temperature (upper panel), salinity (middle panel) and potential density (σ_θ) (lower panel) data from the continuous underway system on board the R/V *Hi'ialakai* during the WHOTS-13 cruise. Temperature and salinity taken from 6-dbar CTD data (circles) and salinity bottle sample data (crosses) are

superimposed. The dashed vertical red line indicates the period of occupation of Station ALOHA and the WHOTS site.

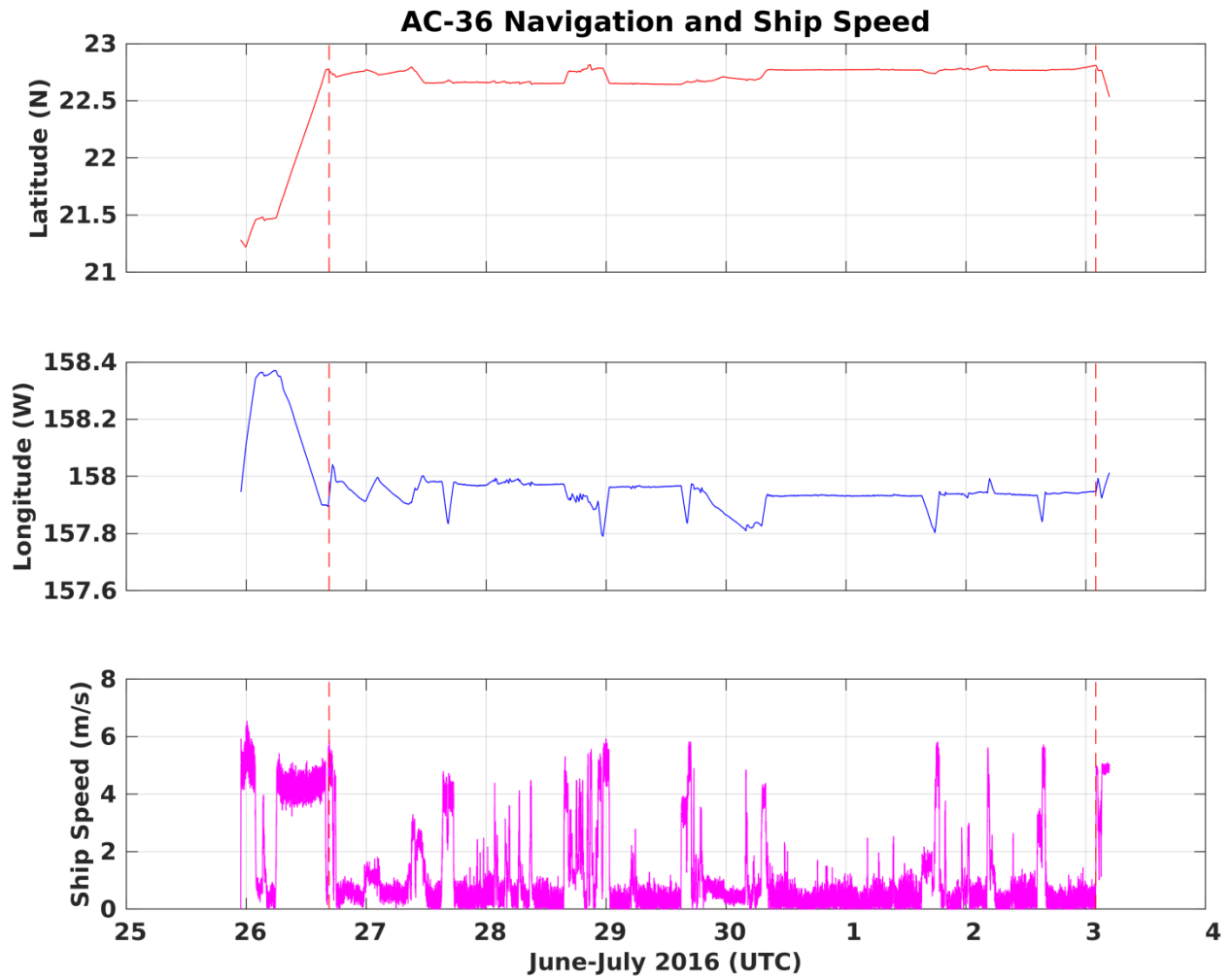


Figure 6-23. Time series of latitude (upper panel), longitude (middle panel), and ship's speed (lower panel) during the WHOTS-13 cruise.

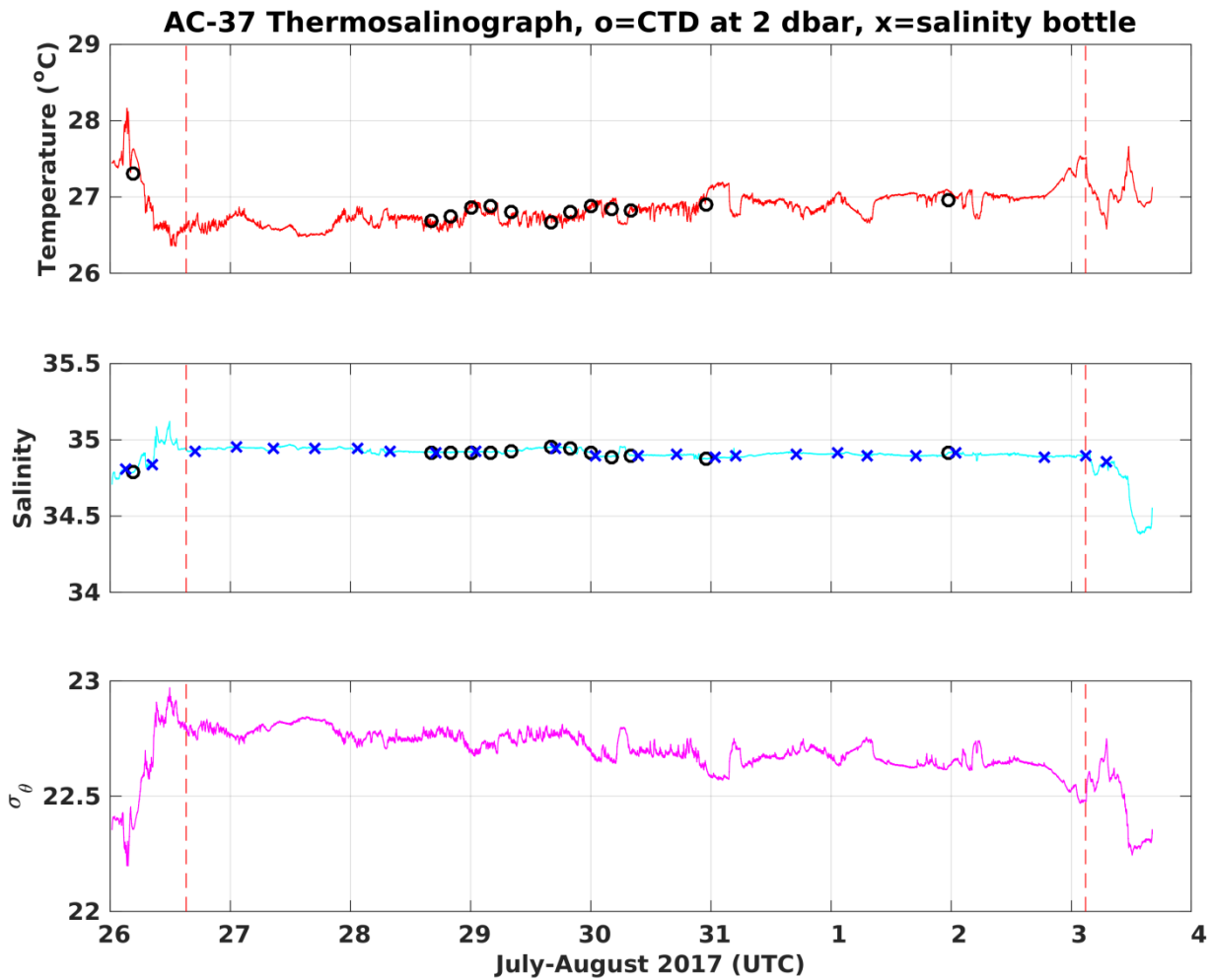


Figure 6-34. Final processed temperature (upper panel), salinity (middle panel) and potential density (σ_θ) (lower panel) data from the continuous underway system on board the R/V Hi'ialakai during the WHOTS-14 cruise. Temperature and salinity taken from 6-dbar CTD data (circles) and salinity bottle sample data (crosses) are superimposed. The dashed vertical red line indicates the period of occupation of Station ALOHA and the WHOTS site.

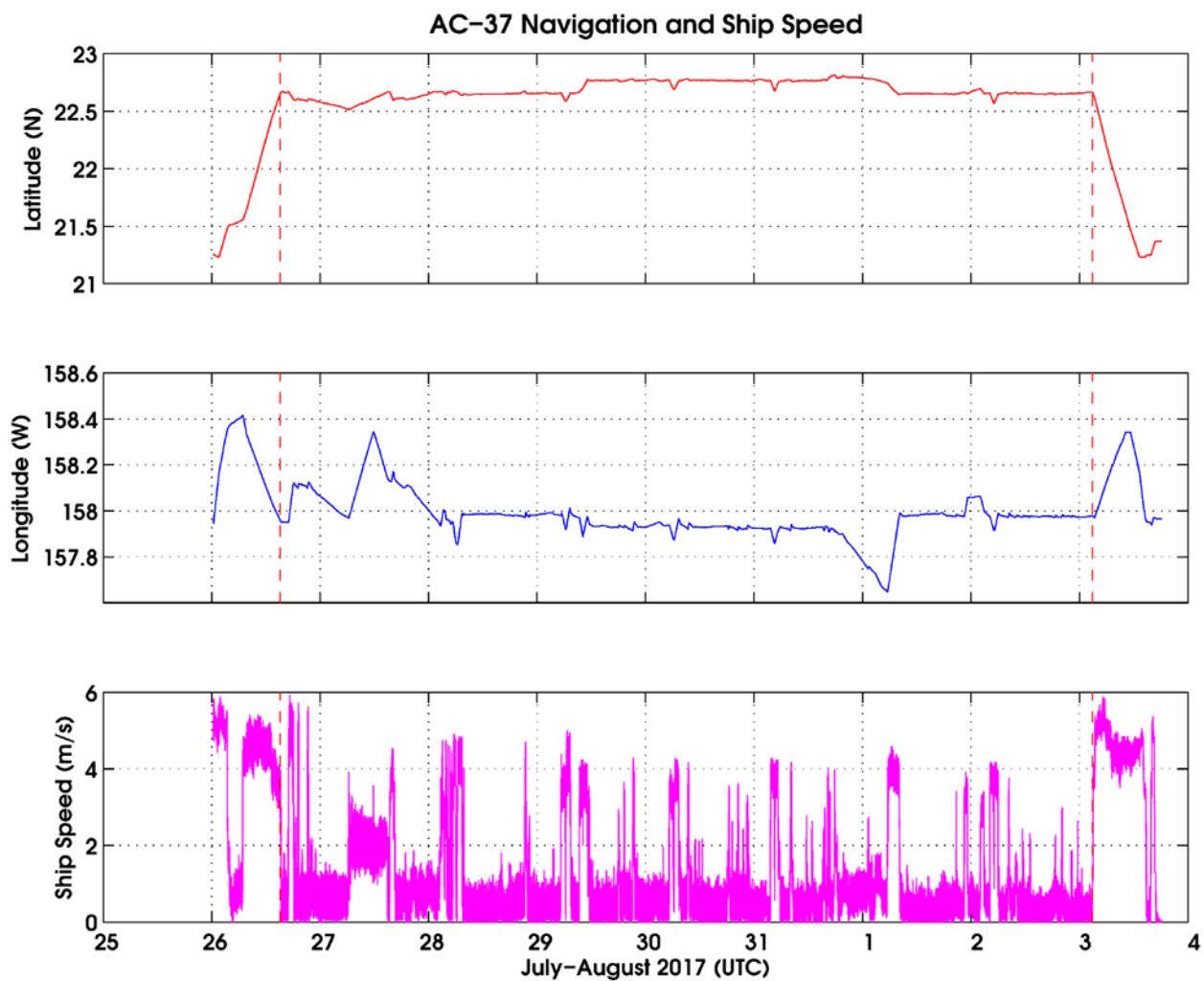


Figure 6-45. Final processed temperature (upper panel), salinity (middle panel) and potential density (σ_θ) (lower panel) data from the continuous underway system on board the R/V *Hi'ialakai* during the WHOTS-14 cruise. Temperature and salinity taken from 6-dbar CTD data (circles) and salinity bottle sample data (crosses) are superimposed. The dashed vertical red line indicates the period of occupation of Station ALOHA and the WHOTS site.

C. MicroCAT data

The temperature measured by MicroCATs during the mooring deployment for WHOTS-13 is presented in Figures 6-16 to 6-20 for each of the depths where the instruments were located. The salinity is plotted in Figures 6-21 to 6-25. The potential density (σ_θ) is plotted in Figures 6-26 to 6-30.

Contoured plots of temperature and salinity as a function of depth are presented in *Figure 6-31*; and contoured plots of potential density (σ_θ) as a function of depth, and of salinity as a function of σ_θ are in *Figure 6-32*.

The potential temperature and salinity measured by the deep MicroCATs during the mooring deployment are shown in *Figure 6-33*. Also shown in the plot are the potential temperature and salinity data obtained with a MicroCAT (SBE-37) installed in the ALOHA Cabled Observatory, about 6 nautical miles west from the WHOTS-13 anchor, the instrument is located 2 m above the bottom.

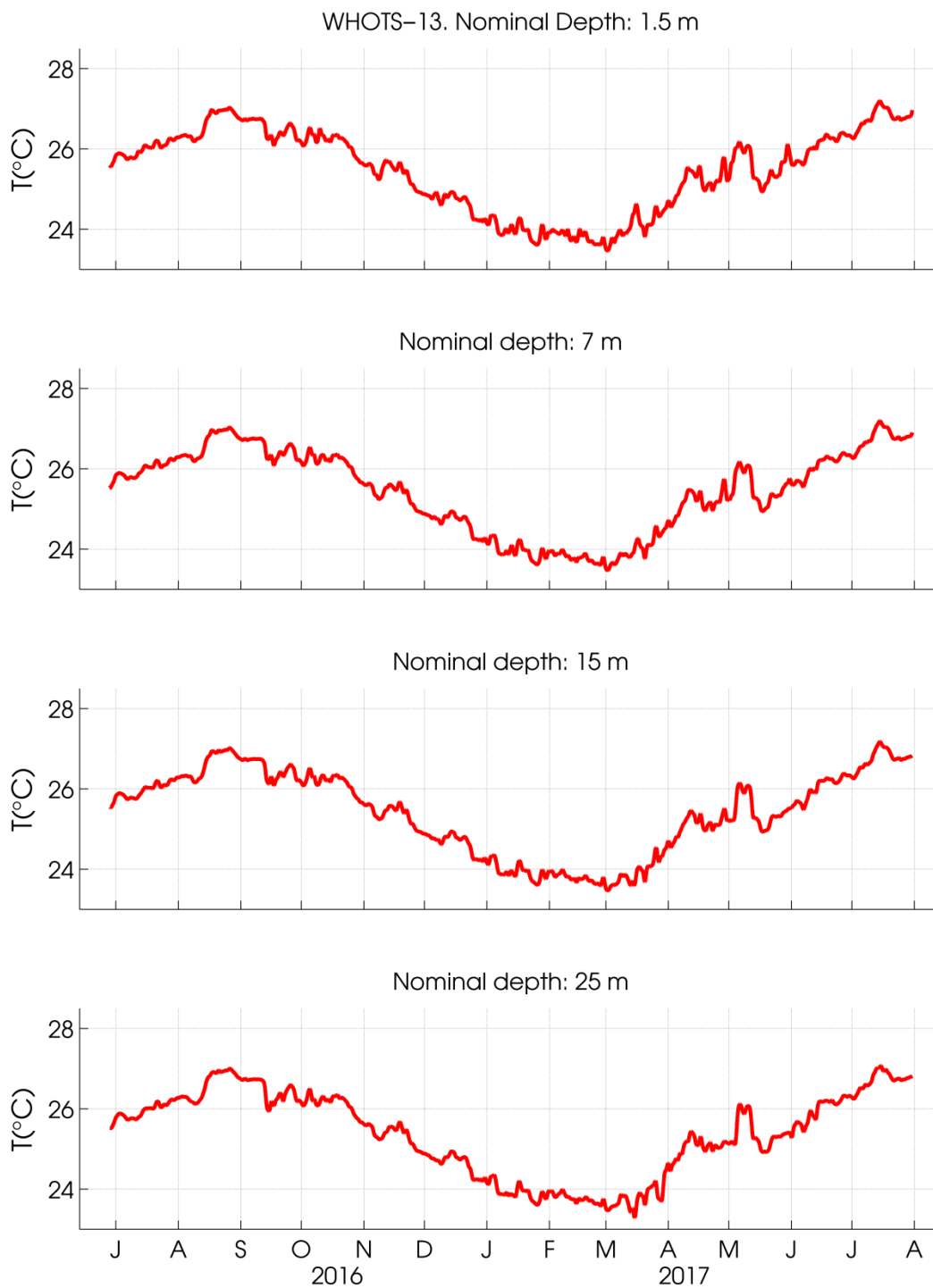


Figure 6-16. Temperatures from MicroCATs during WHOTS-13 deployment at 1.5, 7, 15, and 25 m.

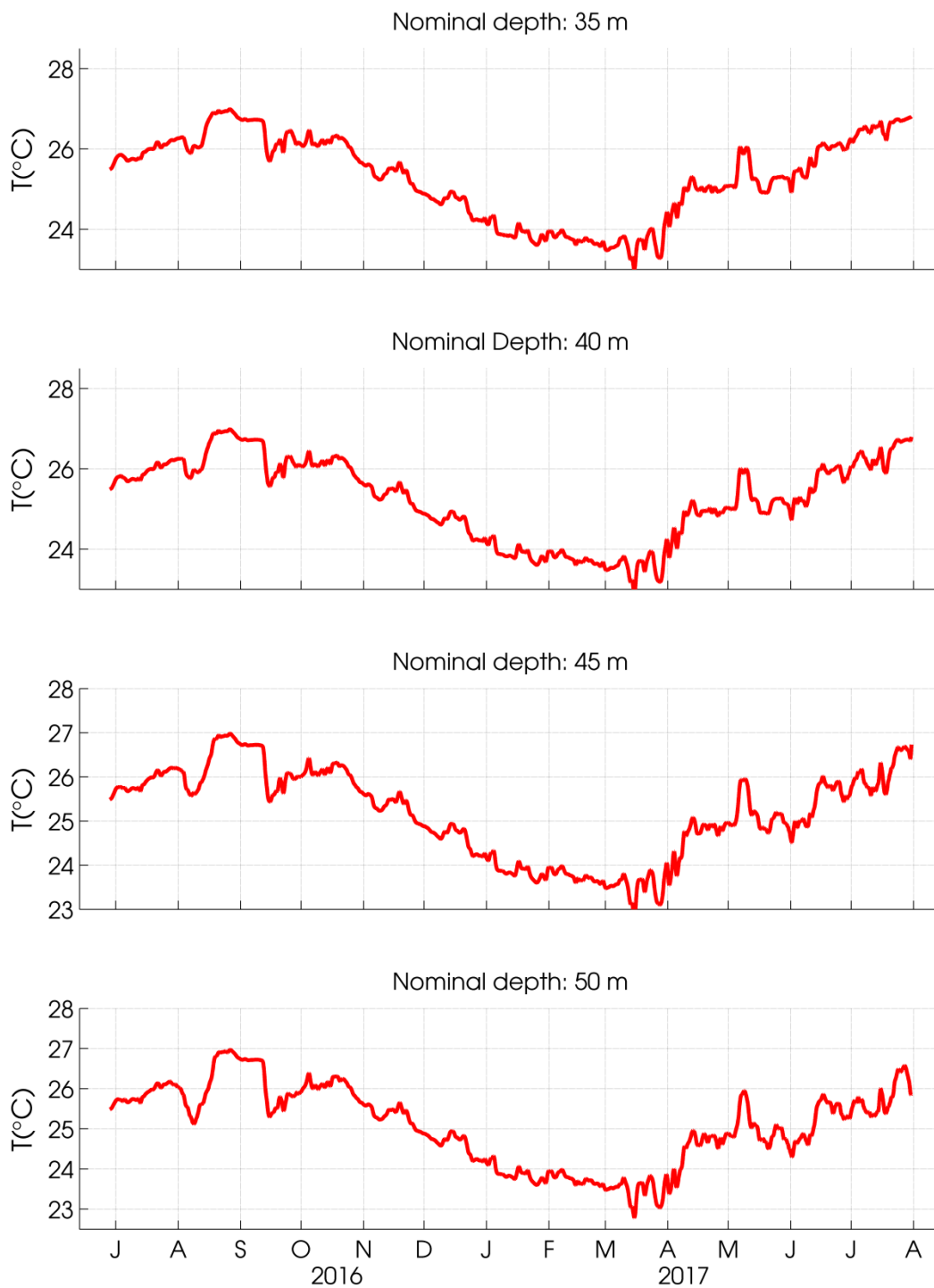


Figure 6-17. Same as in Figure 6-16, but at 35, 40, 45, and 50 m.

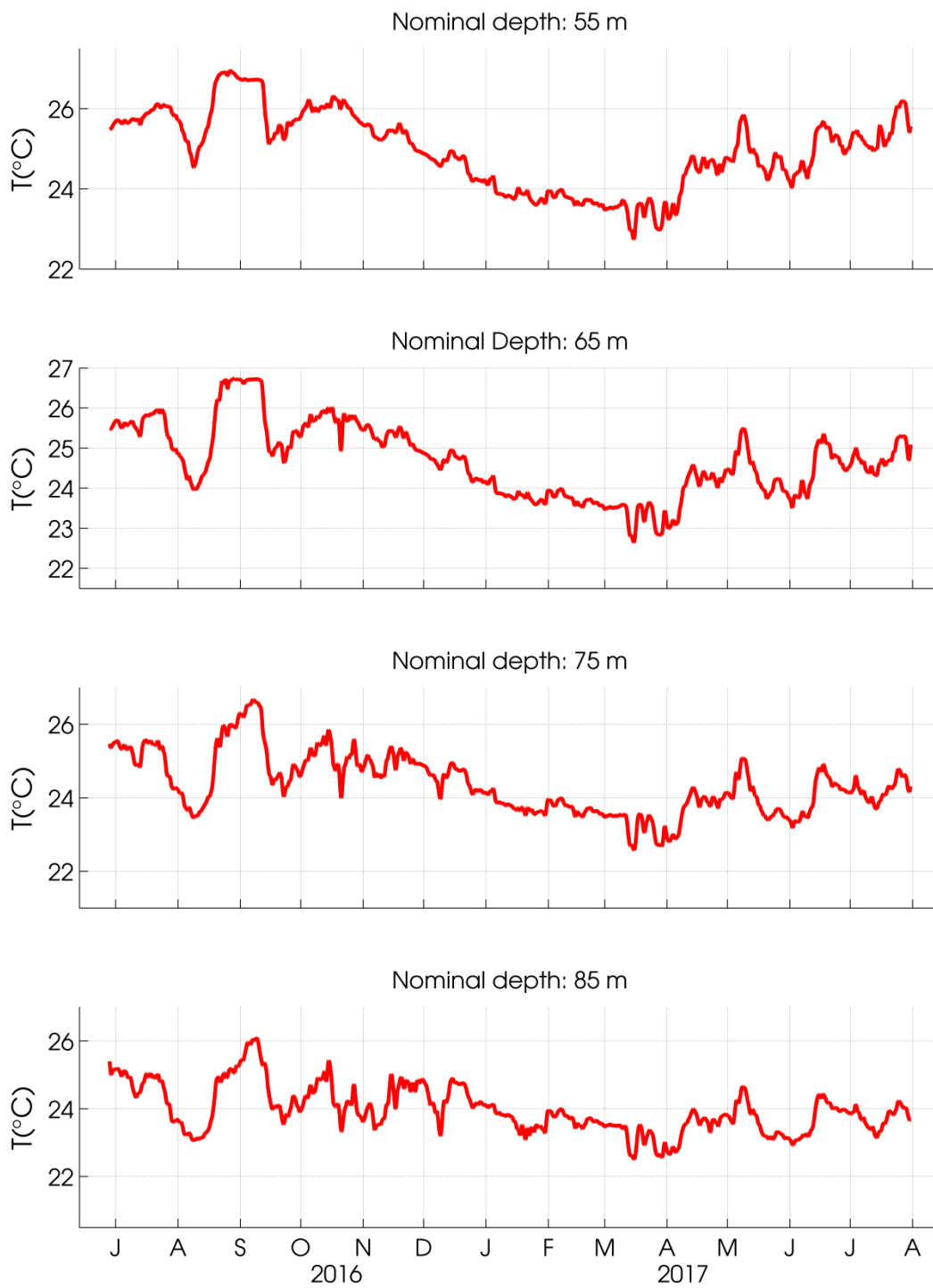


Figure 6-18. Same as in Figure 6-16, but at 55, 65, 75, and 85 m.

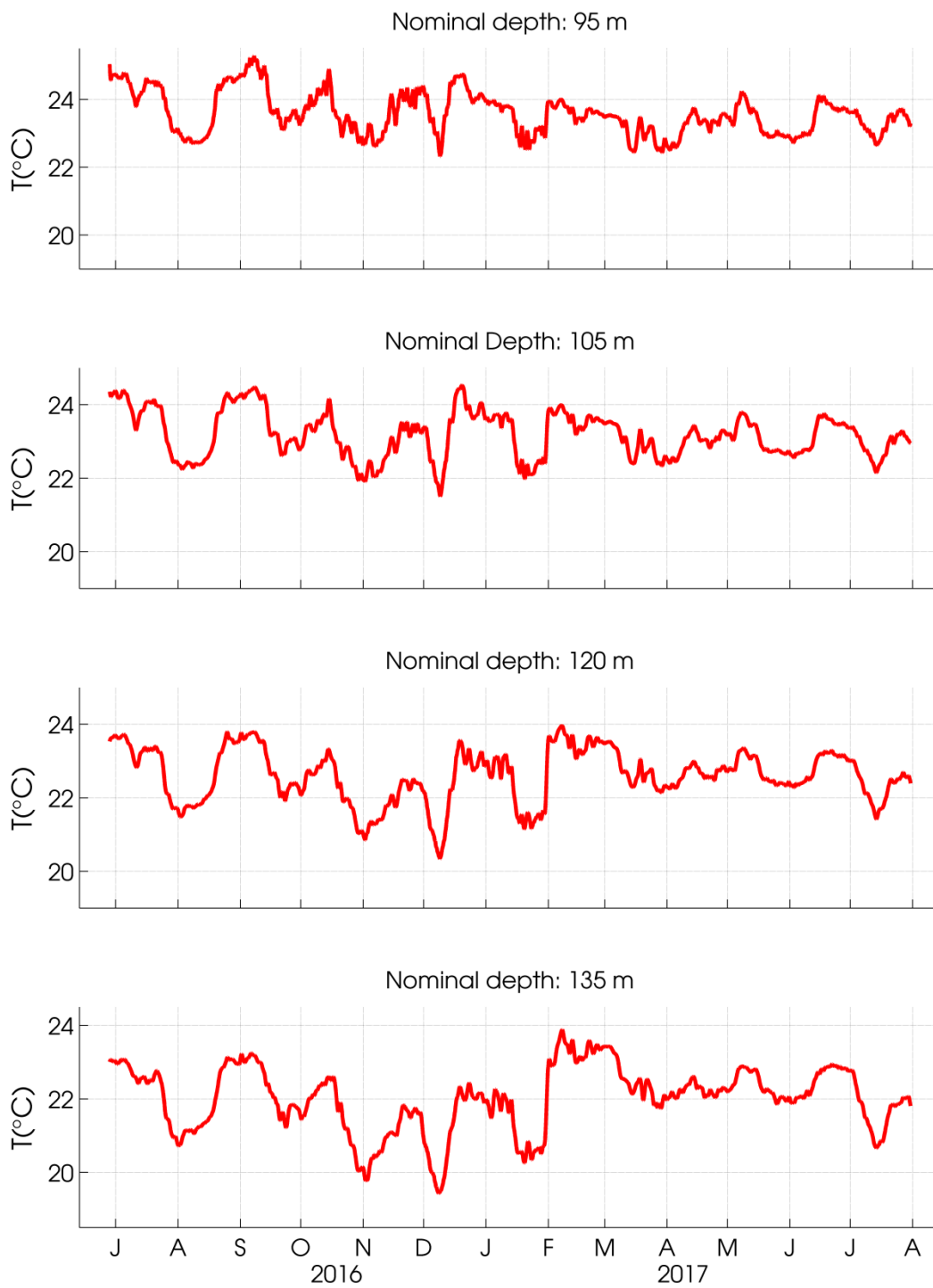


Figure 6-19. Same as in Figure 6-16, but at 95, 105, 120, and 135 m.

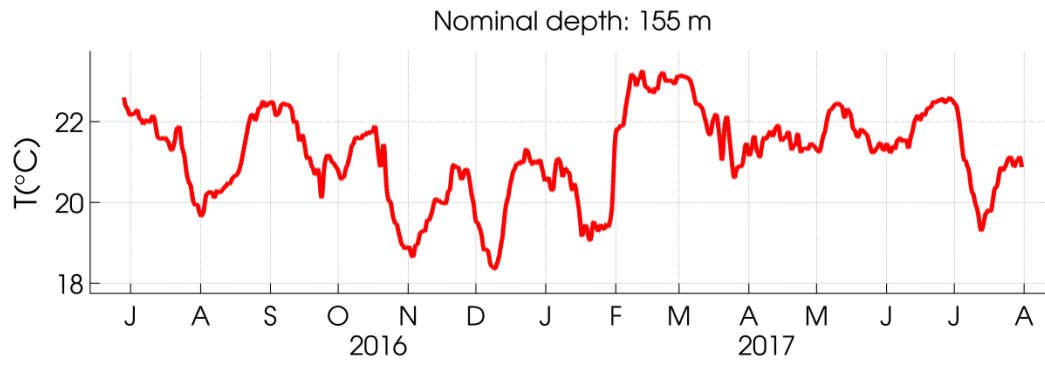


Figure 6-20. Same as in Figure 6-16, but at 155 m.

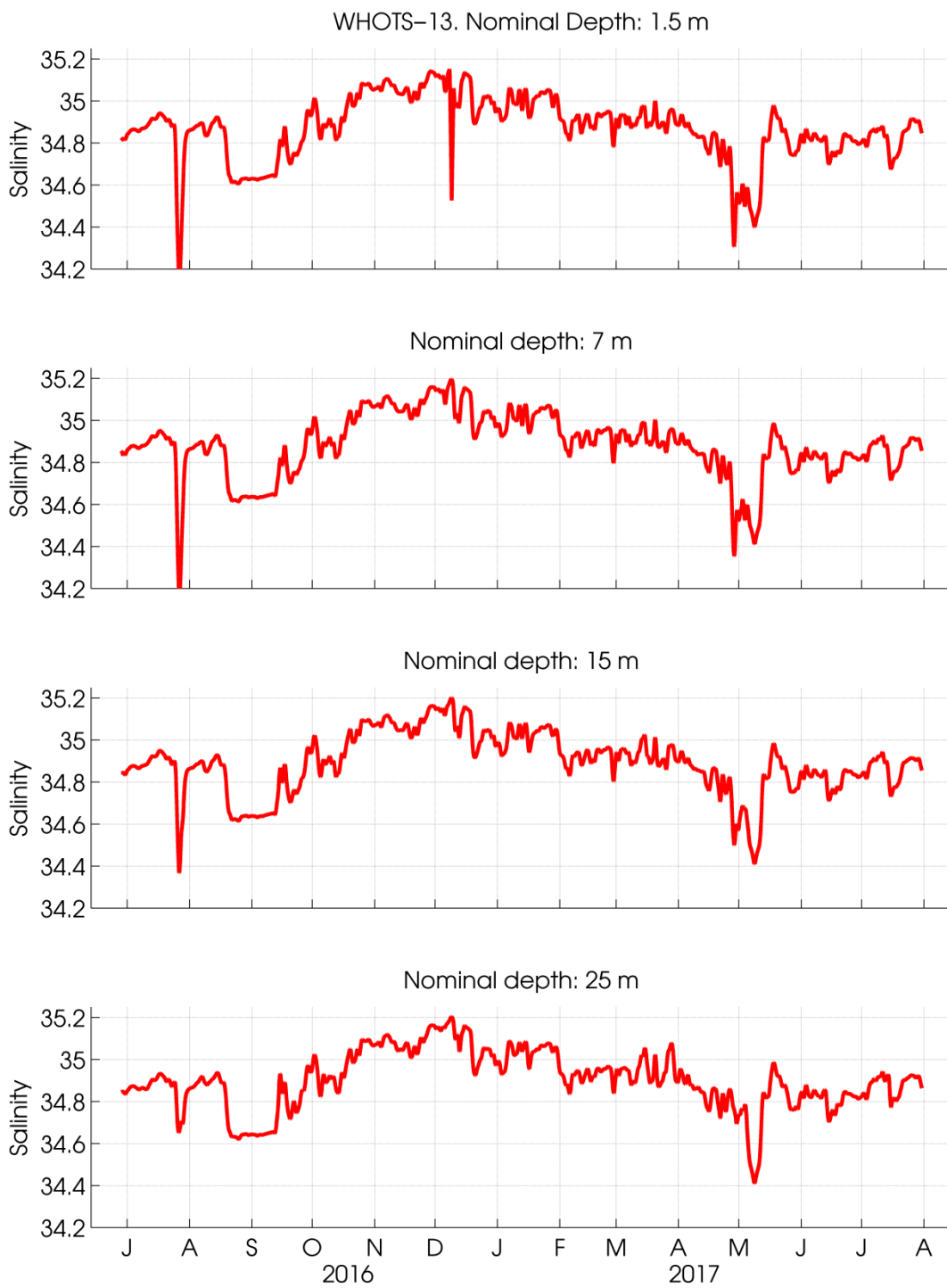


Figure 6-21. Salinities from MicroCATs during WHOTS-13 deployment at 1.5, 7, 15, and 25 m.

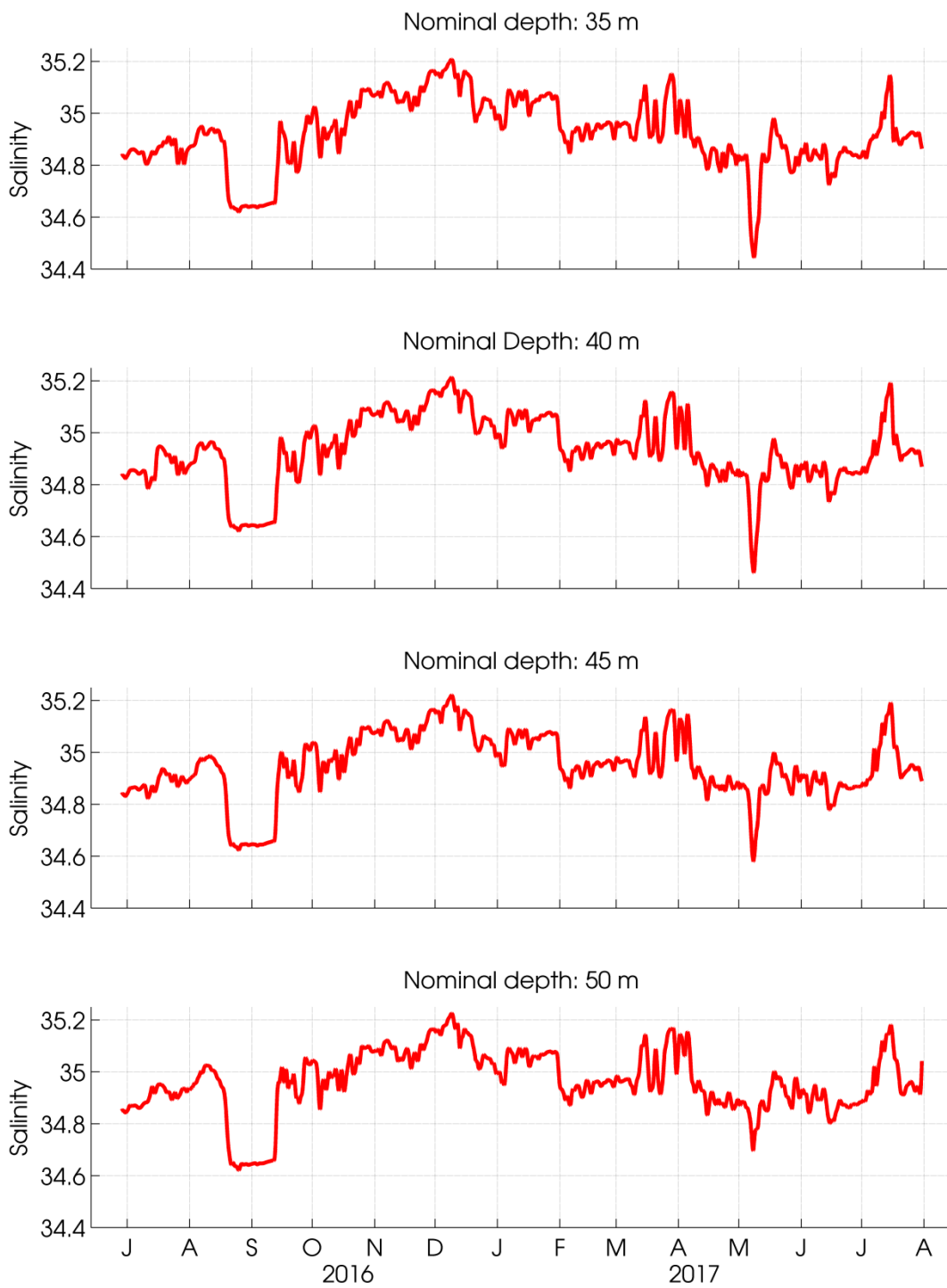


Figure 6-22. Same as in Figure 6-21, but at 35, 40, 45, and 50 m.

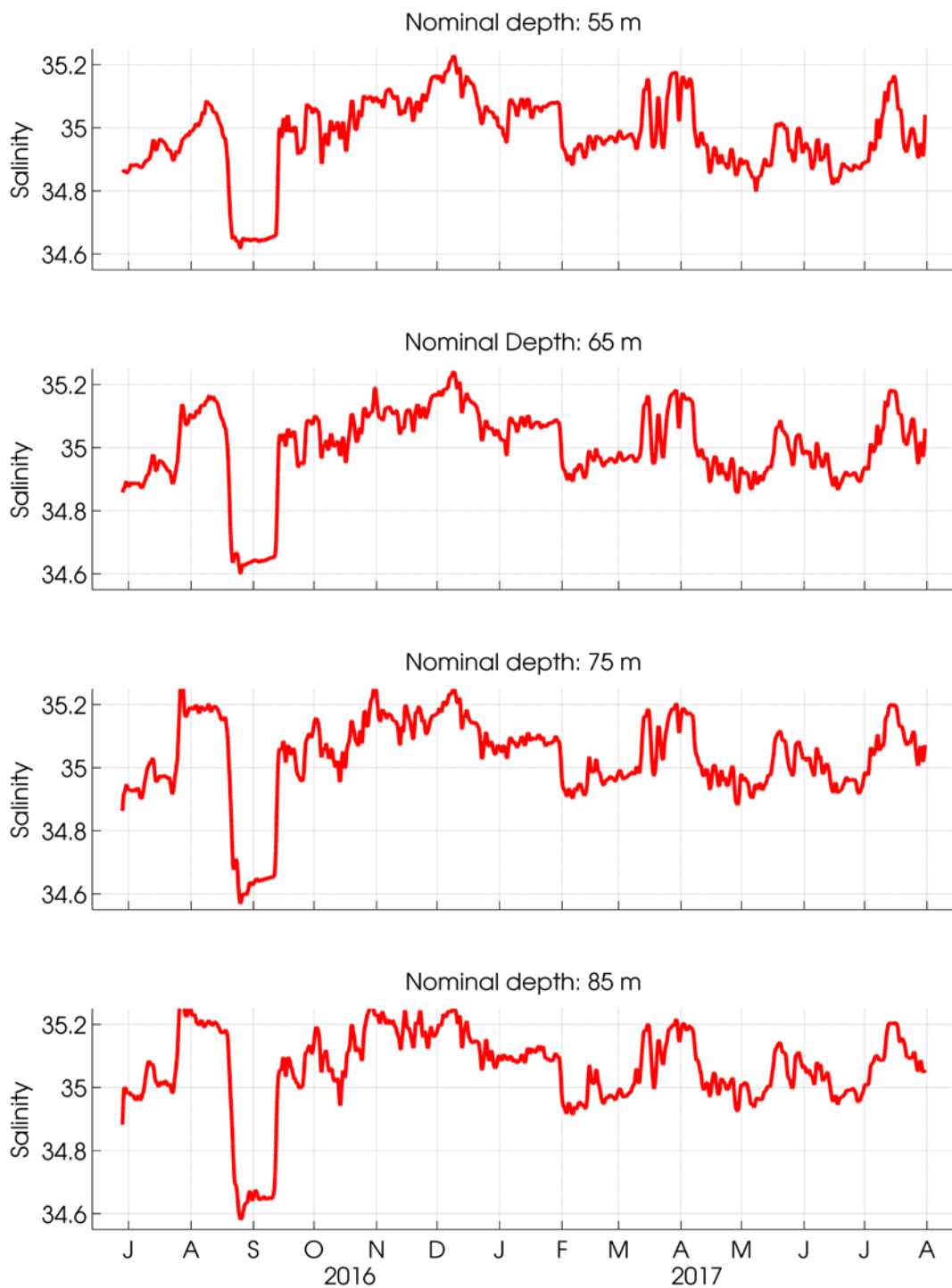


Figure 6-23. Same as in Figure 6-21, but at 55, 65, 75, and 85 m.

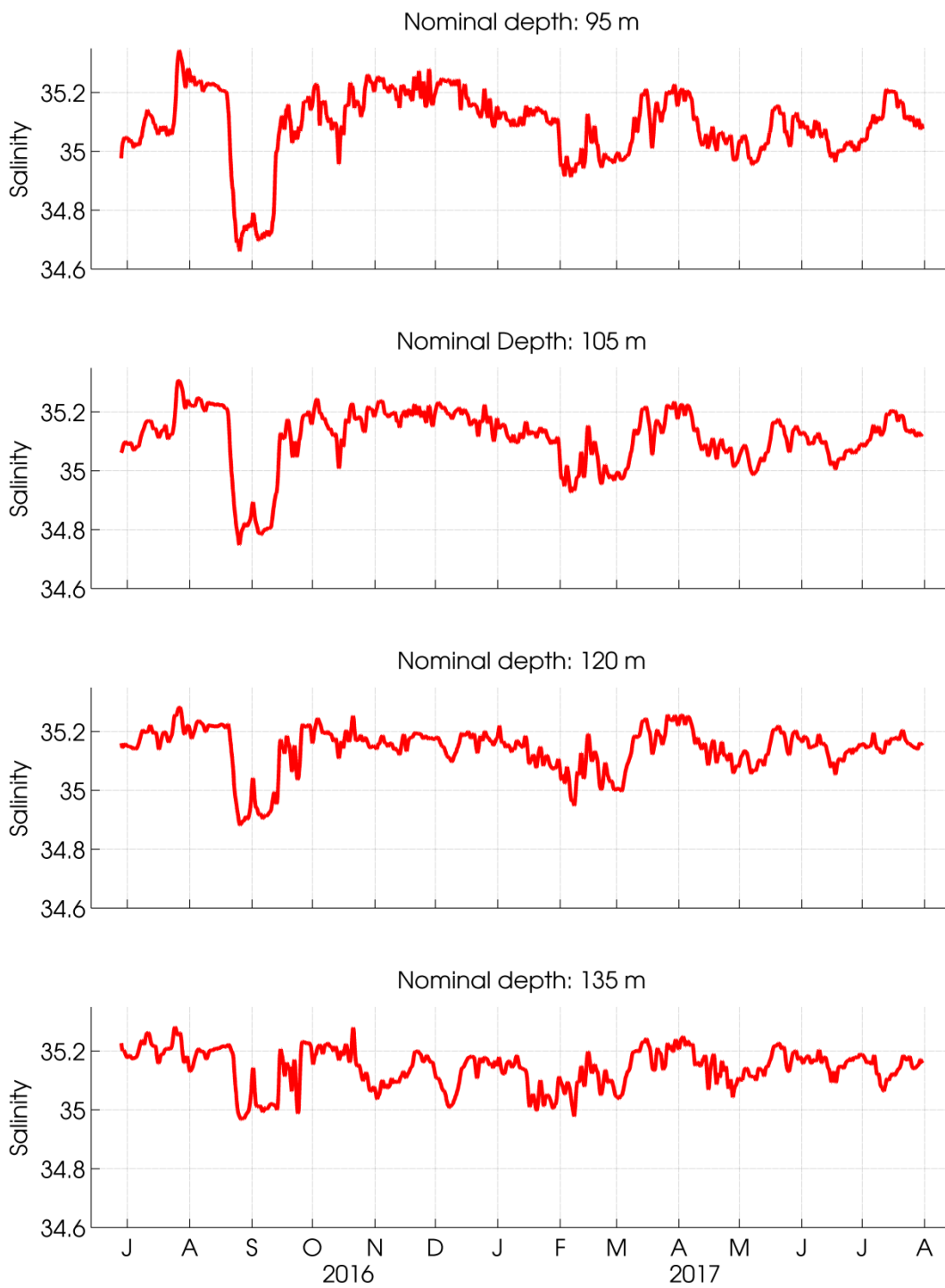


Figure 6-24. Same as in Figure 6-21, but at 95, 105, 120, and 135 m.

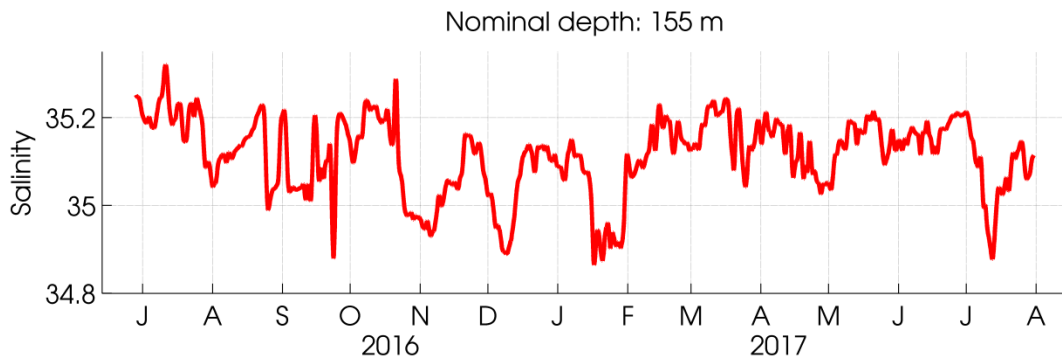


Figure 6-25. Same as in Figure 6-21, but at 155 m.

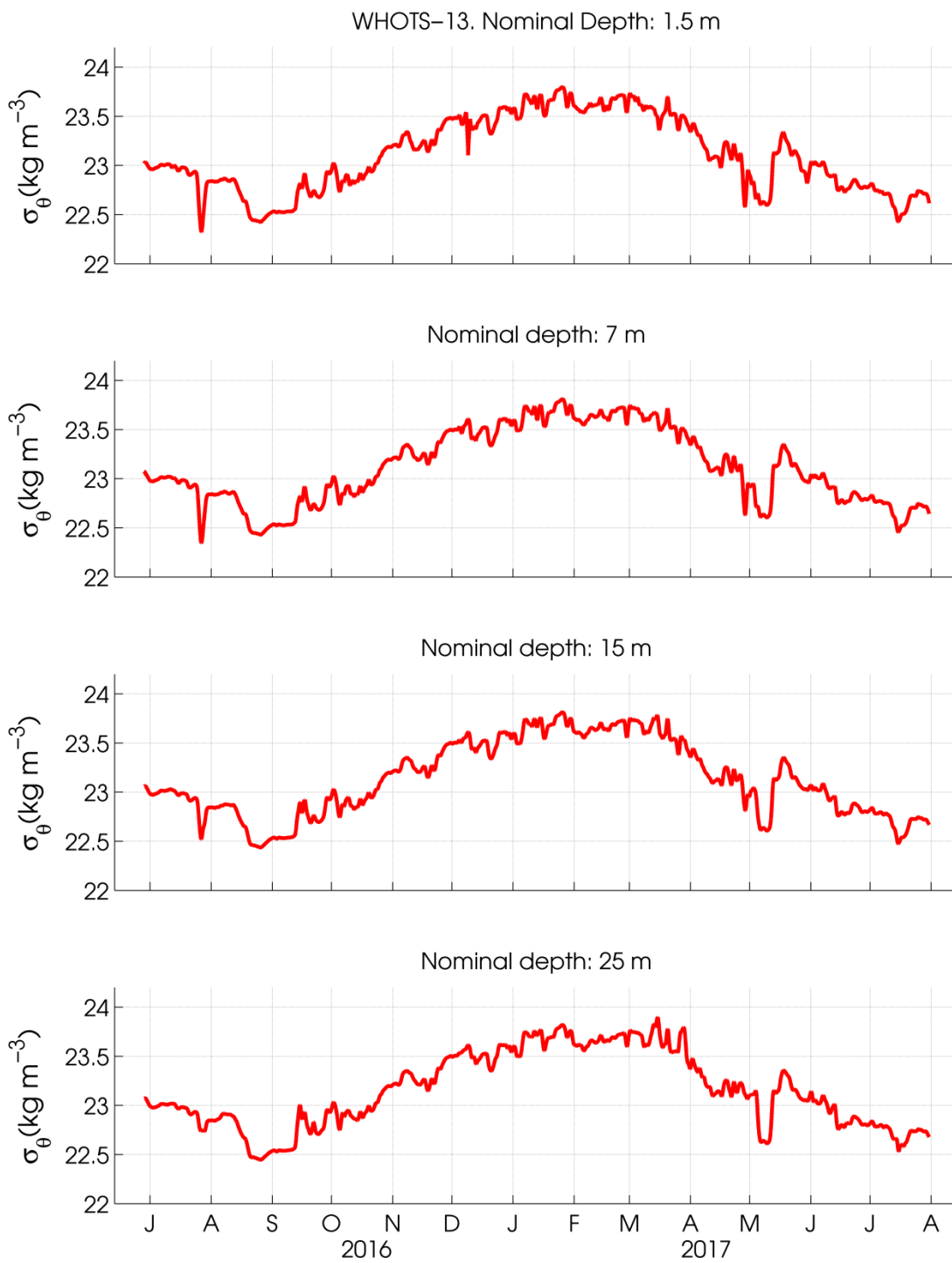


Figure 6-26. Potential densities (σ_θ) from MicroCATs during WHOTS-13 deployment at 1.5, 7, 15, and 25 m.

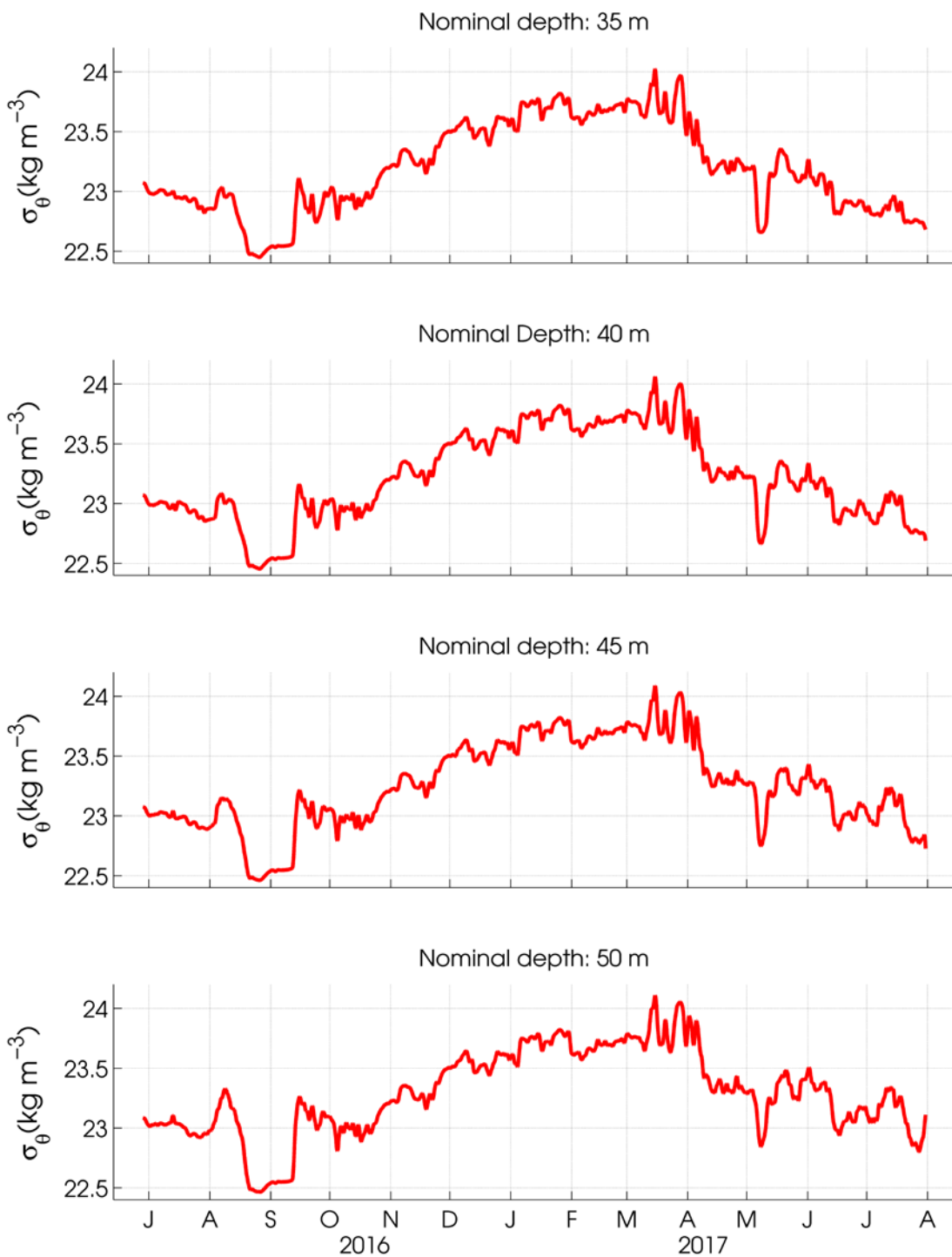


Figure 6-27. Same as in Figure 6-26, but at 35, 40, 45, and 50 m.

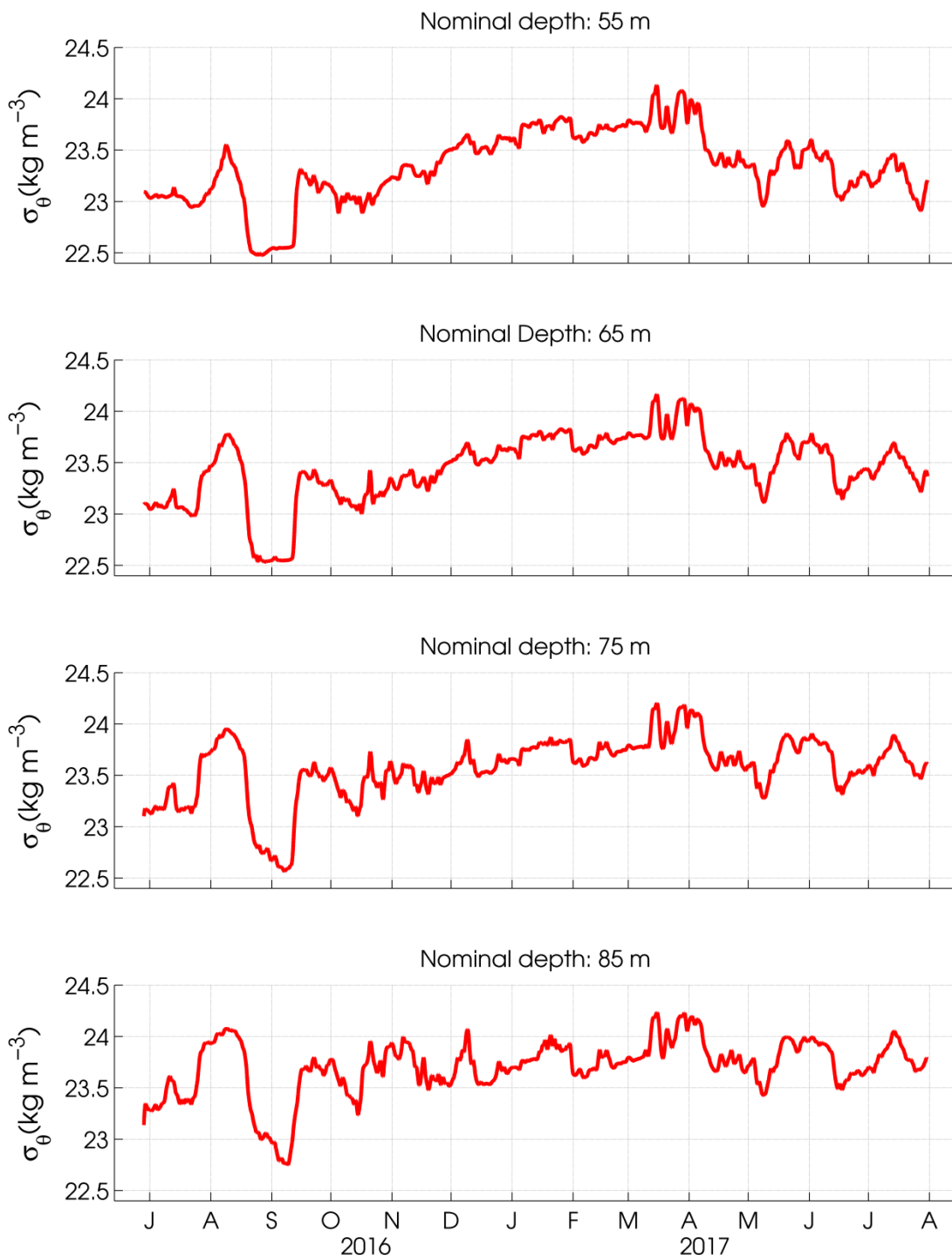


Figure 6-28 Same as in Figure 6-26, but at 55, 65, 75, and 85 m.

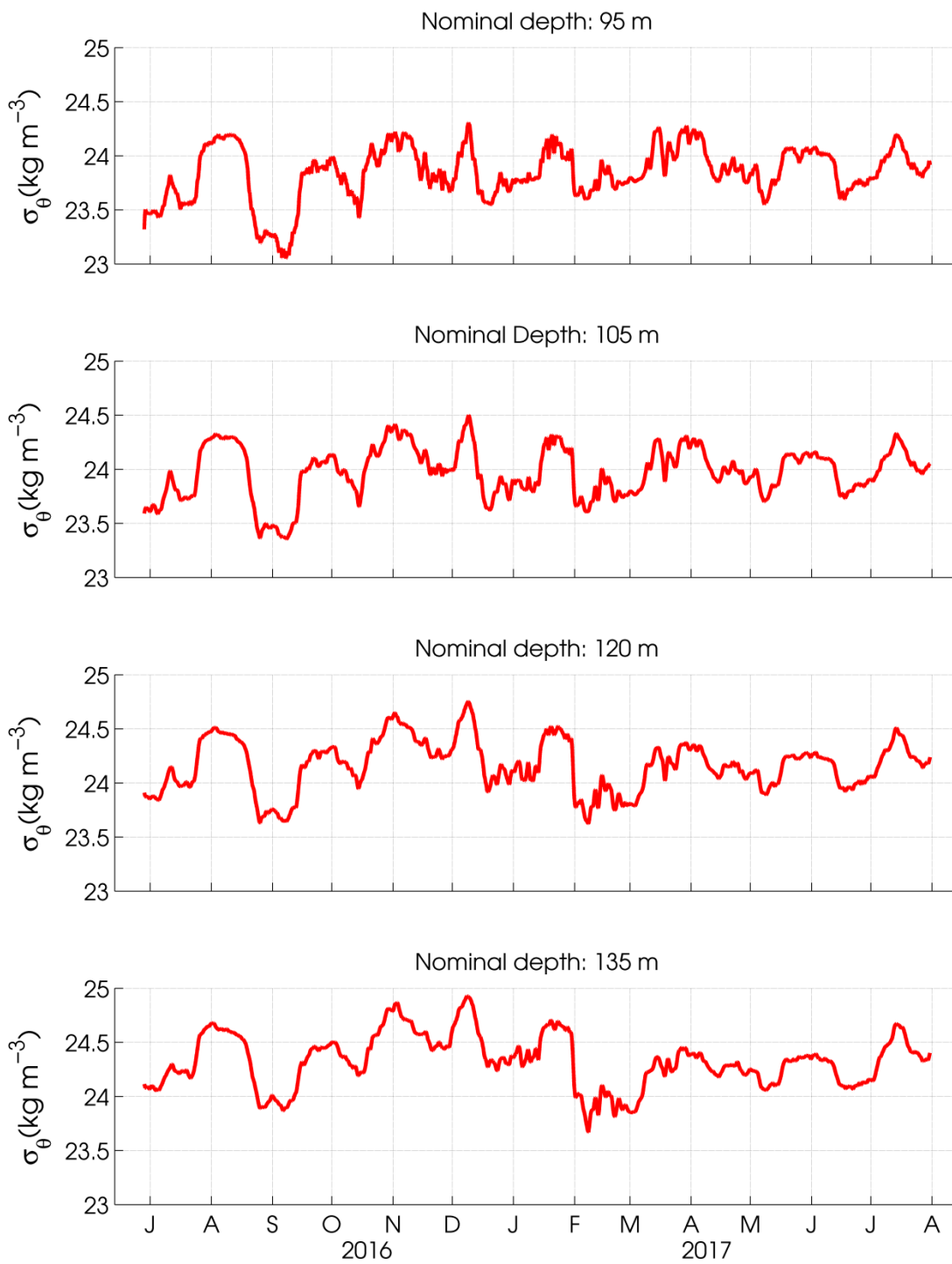


Figure 6-29 Same as in Figure 6-26, but at 95, 105, 120, and 135 m.

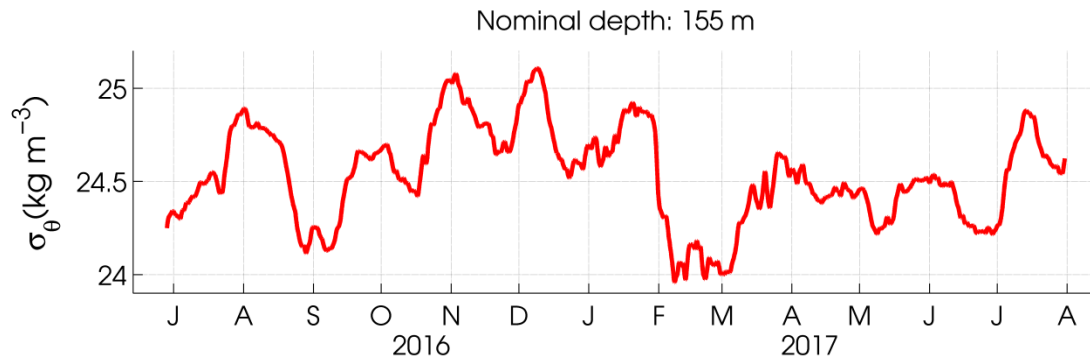


Figure 6-30. Same as in Figure 6-26, but at 155 m.

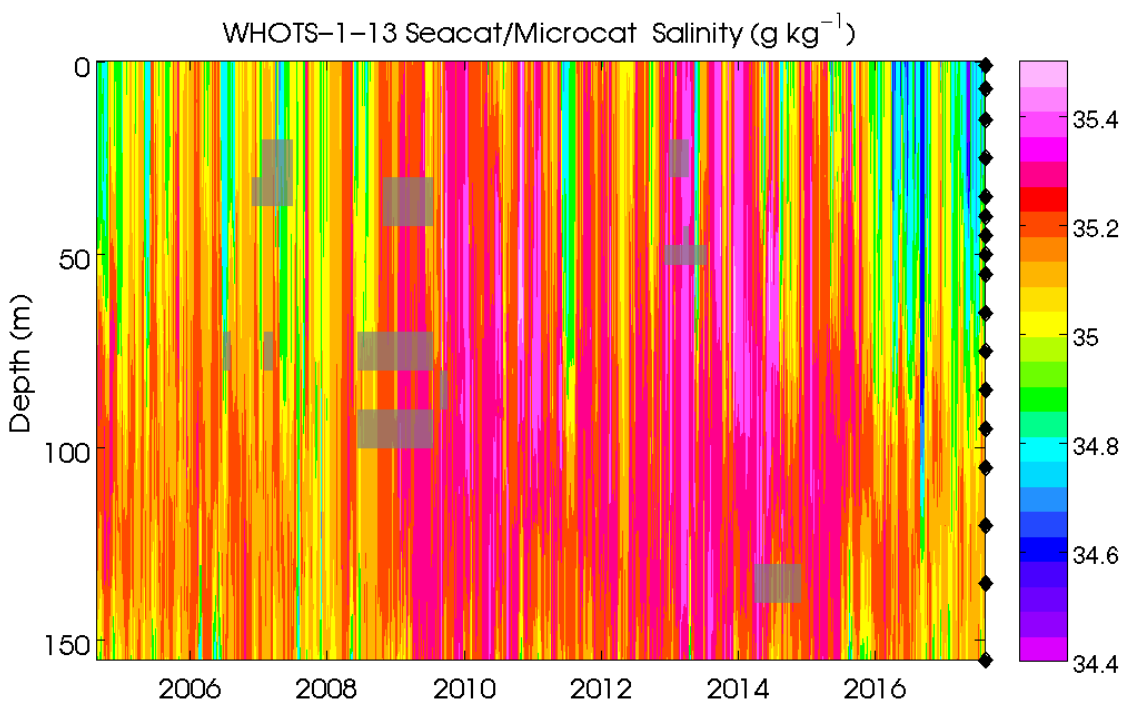
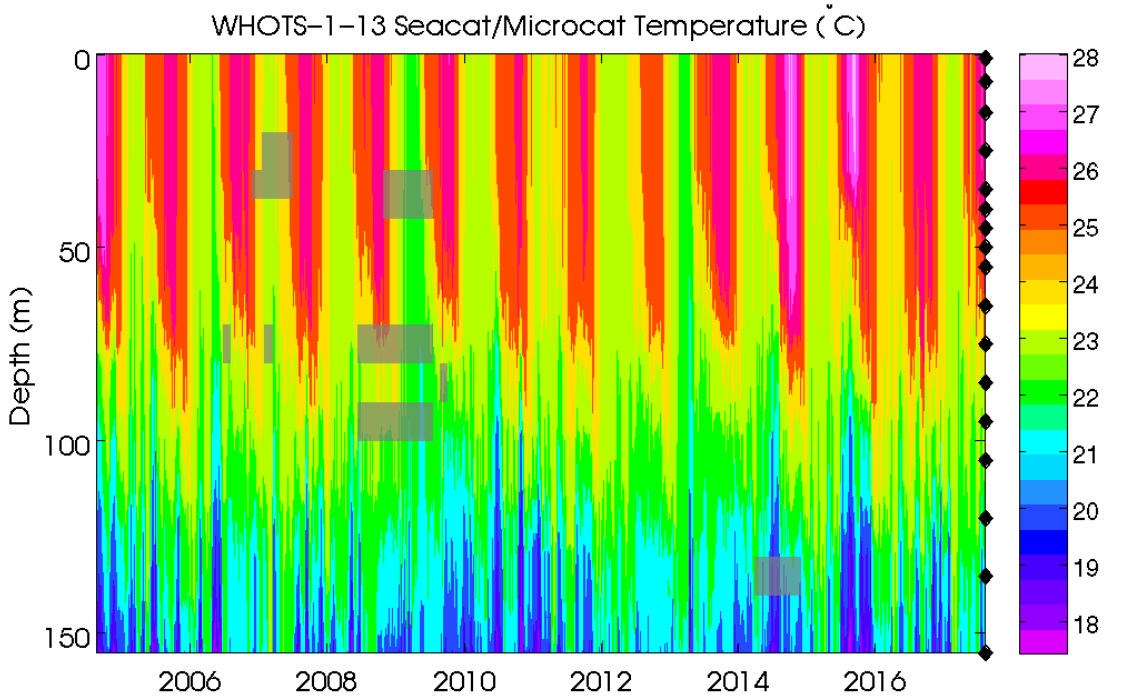


Figure 6-31. Contour plots of temperature (upper panel), and salinity (lower panel) versus depth from SeaCATs/MicroCATs during WHOTS-1 through WHOTS-13 deployments. The shaded areas indicate missing data. The diamonds along the right axis indicate the instruments depths.

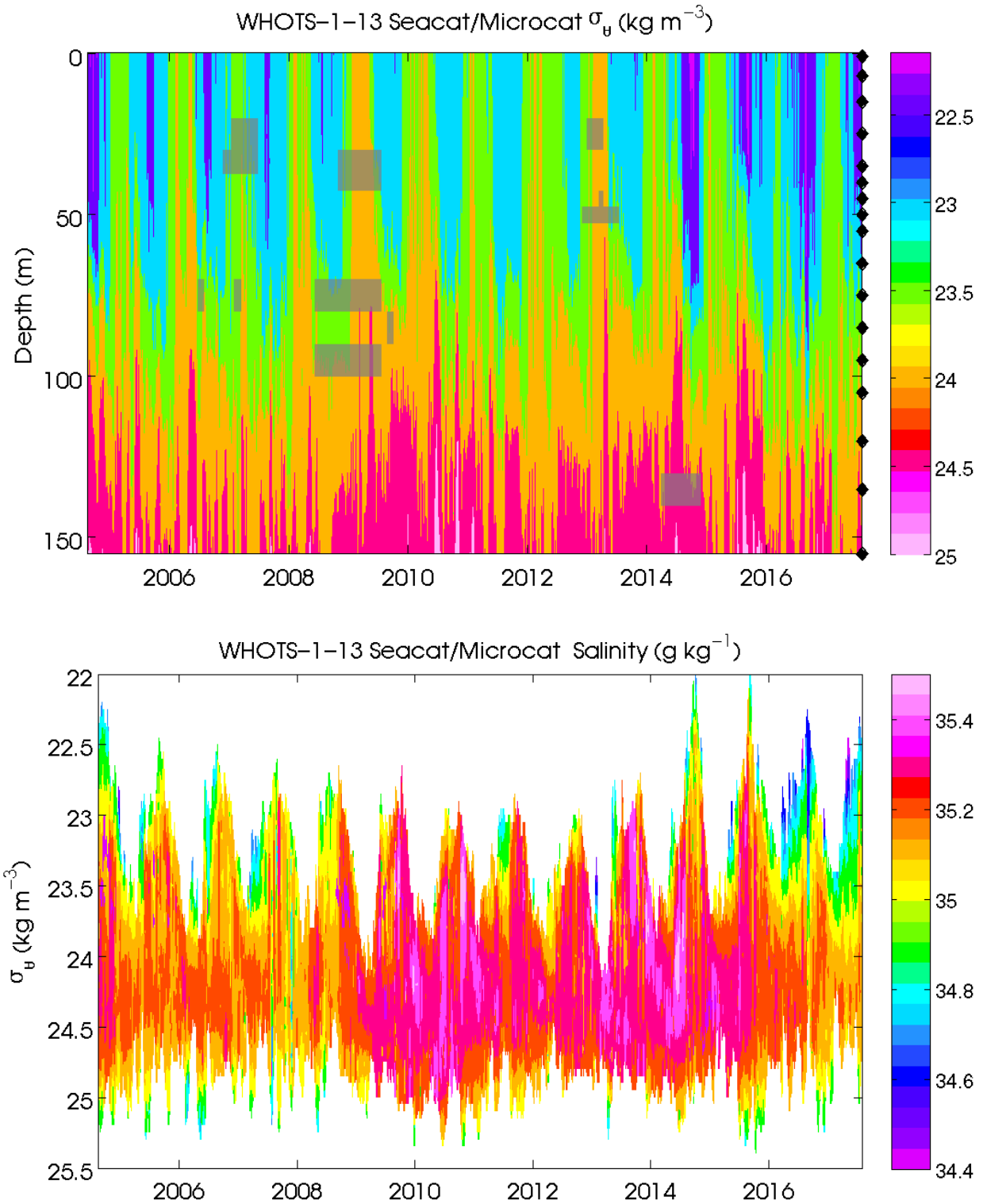


Figure 6-32. Contour plots of potential density (σ_{θ} , upper panel), versus depth, and of salinity versus σ_{θ} (lower panel) from SeaCATs/MicroCATs during WHOTS-1 through WHOTS-13 deployments. The shaded areas indicate missing data. The diamonds along the right axis in the upper figure indicate the instruments depths.

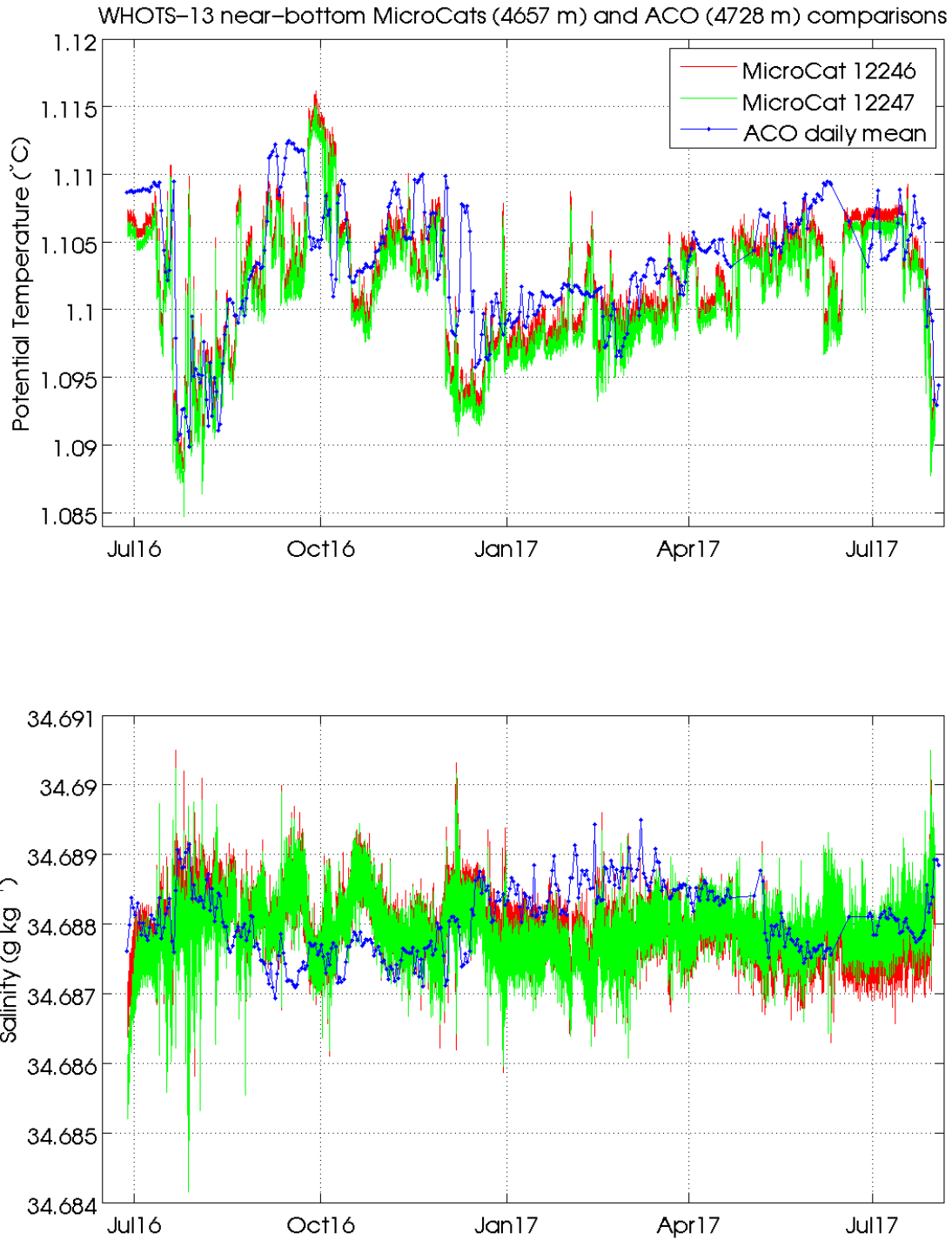


Figure 6-33 Potential temperature (upper panel) and salinity (lower panel) time-series from the ALOHA Cabled Observatory (ACO) sensors and from the WHOTS-13 MicroCATs 12246 and 12247.

D. Moored ADCP data

Contoured plots of smoothed horizontal (east and north component) and vertical velocity as a function of depth during the mooring deployments 1 through 13 are presented in Figures 6-34 through 6-36. A staggered time-series of smoothed horizontal and vertical velocities are shown in Figures 6-37 through 6-39. Smoothing was performed by applying a daily running mean to the data and then interpolating the data on to an hourly grid.

Contours of east and north velocity components from the Ship *Hi'ialakai's* Ocean Surveyor broadband 75 kHz shipboard ADCP, and the moored 300 kHz ADCP from the WHOTS-13 deployment as a function of time and depth, during the WHOTS-13 cruise are shown in Figures 6-40 and 6-41.

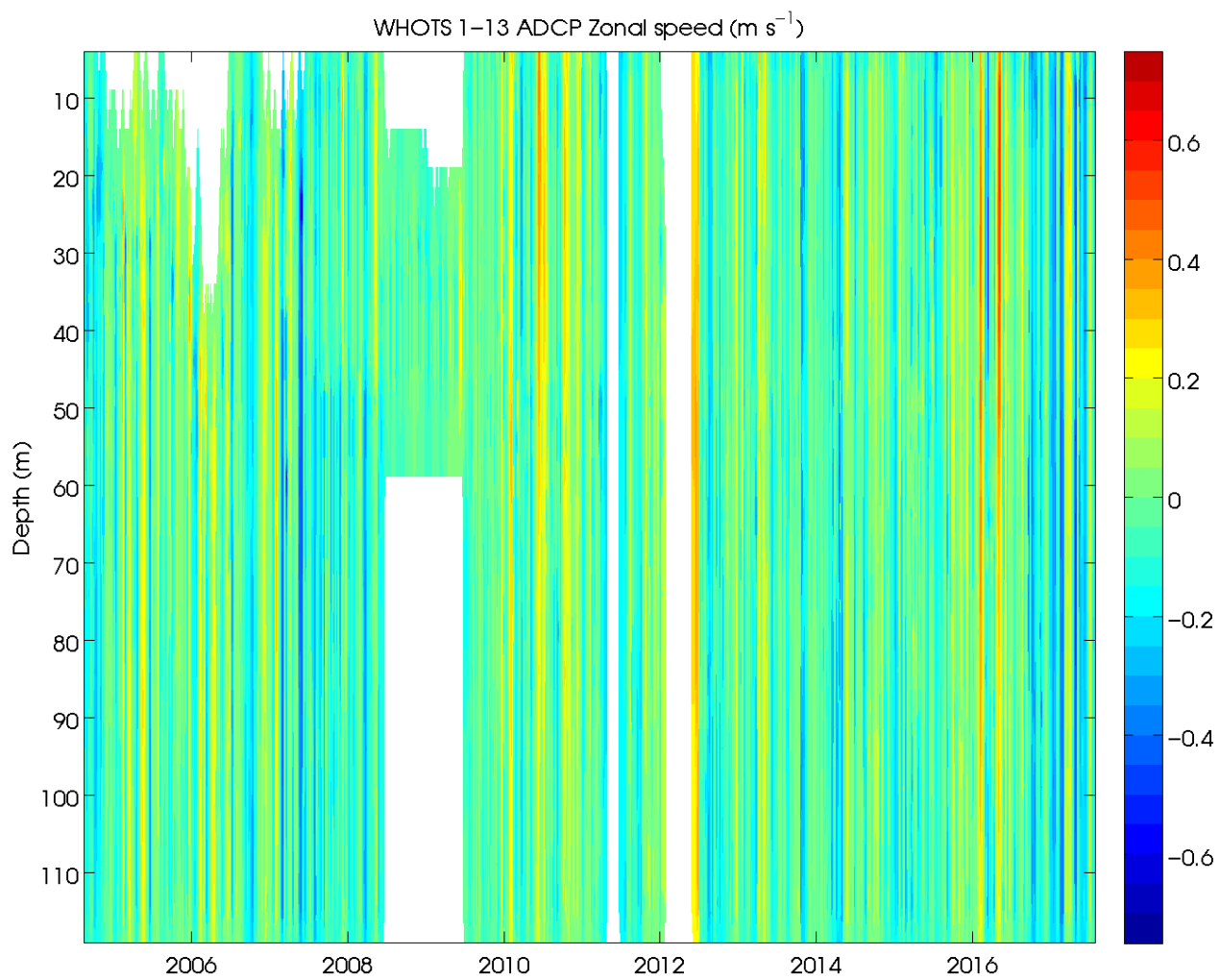


Figure 6-34. Contour plot of east velocity component ($m s^{-1}$) versus depth and time from the moored ADCPs from the WHOTS-1 through -13 deployments.

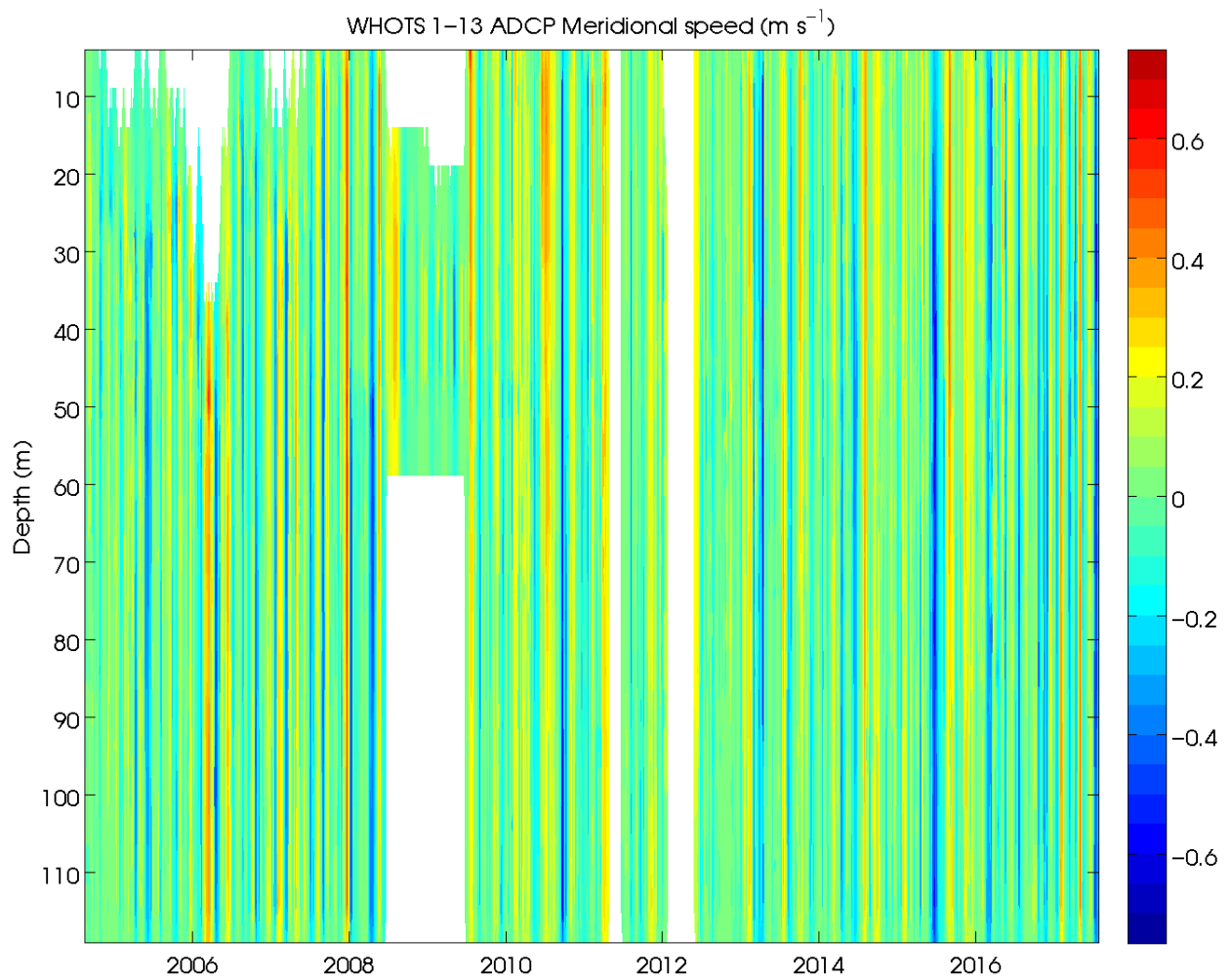


Figure 6-35. Contour plot of north velocity component ($m s^{-1}$) versus depth and time from the moored ADCPs from the WHOTS-1 through -13 deployments.

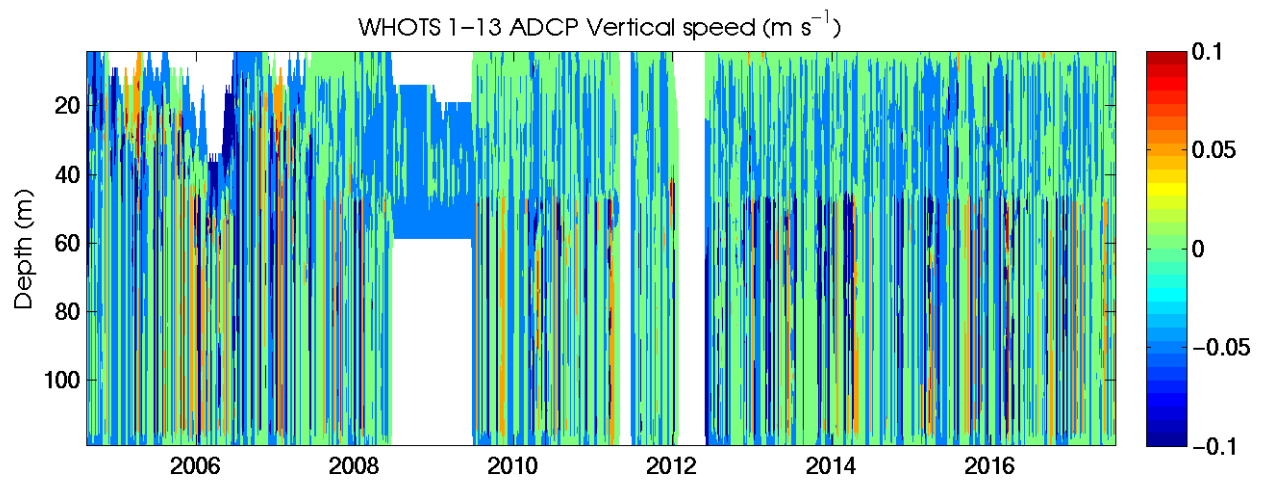


Figure 6-36. Contour plot of vertical velocity component (m s-1) versus depth and time from the moored ADCPs from the WHOTS-1 through -13 deployments.

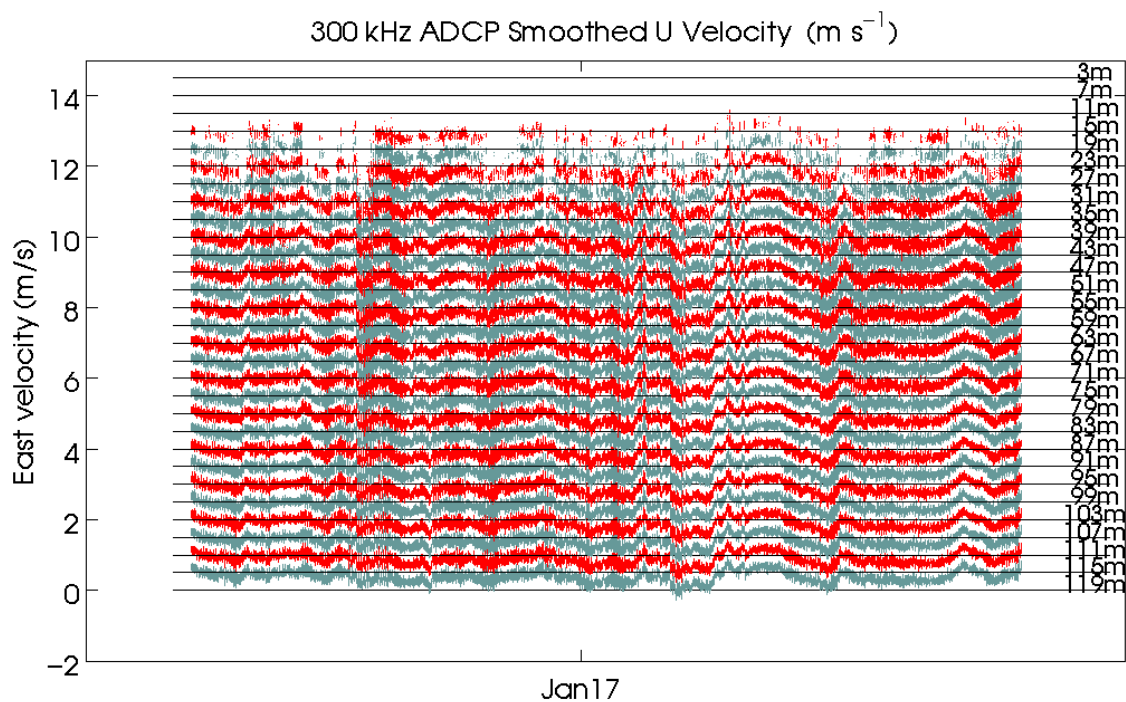
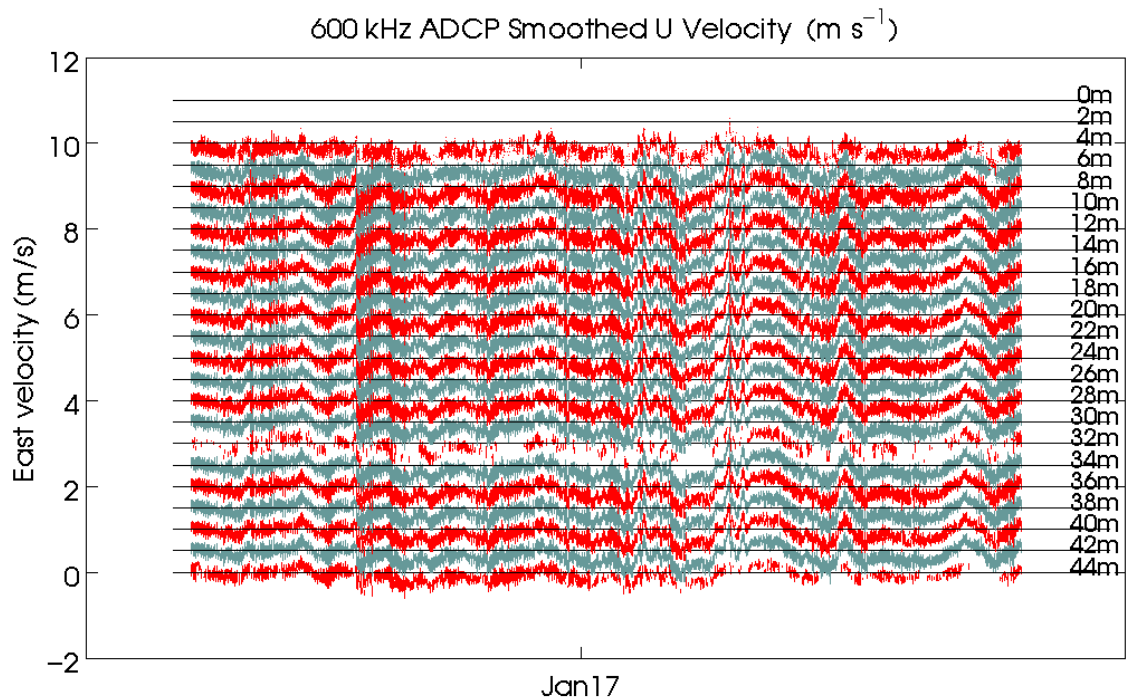


Figure 6-37. Staggered time-series of east velocity component (m s^{-1}) for each bin of the 600 kHz (upper panel), and 300 kHz (lower panel) moored ADCPs during WHOTS-13. The time-series are offset upwards by 0.5 m s^{-1} , the depth of each bin is on the right.

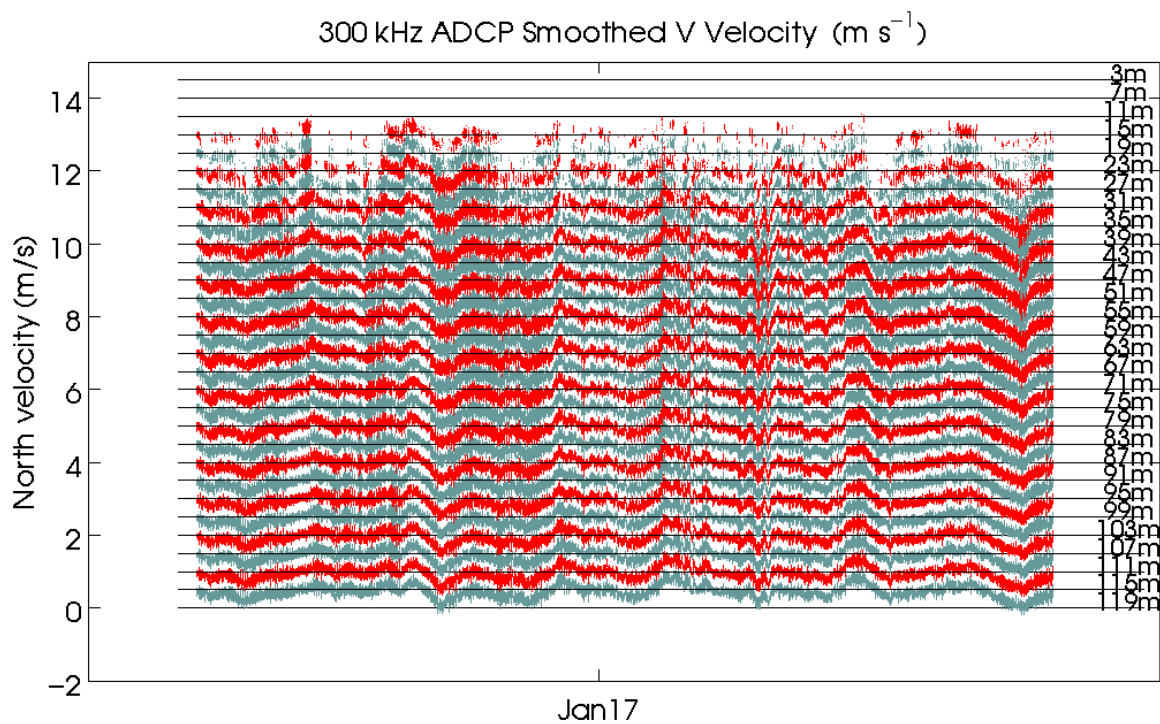
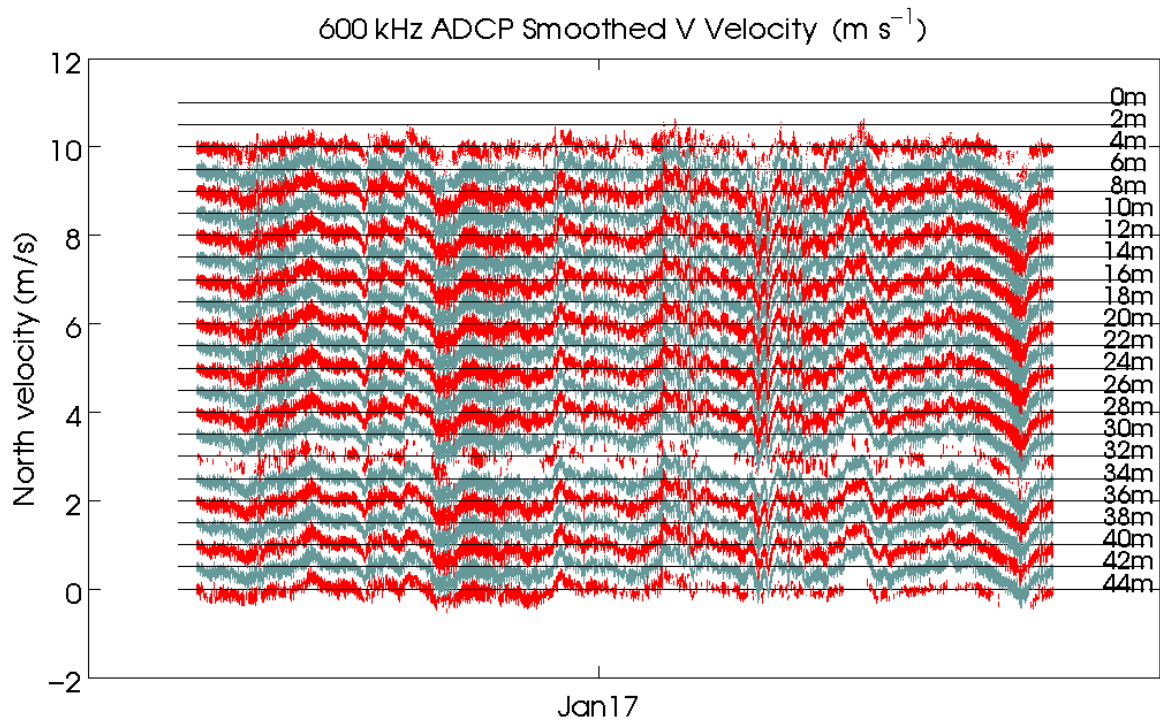


Figure 6-38. Staggered time-series of north velocity component (m s^{-1}) for each bin of the 600 kHz (upper panel), and 300 kHz (lower panel) moored ADCPs during WHOTS-13. The time-series are offset upwards by 0.5 m s^{-1} , the depth of each bin is on the right.

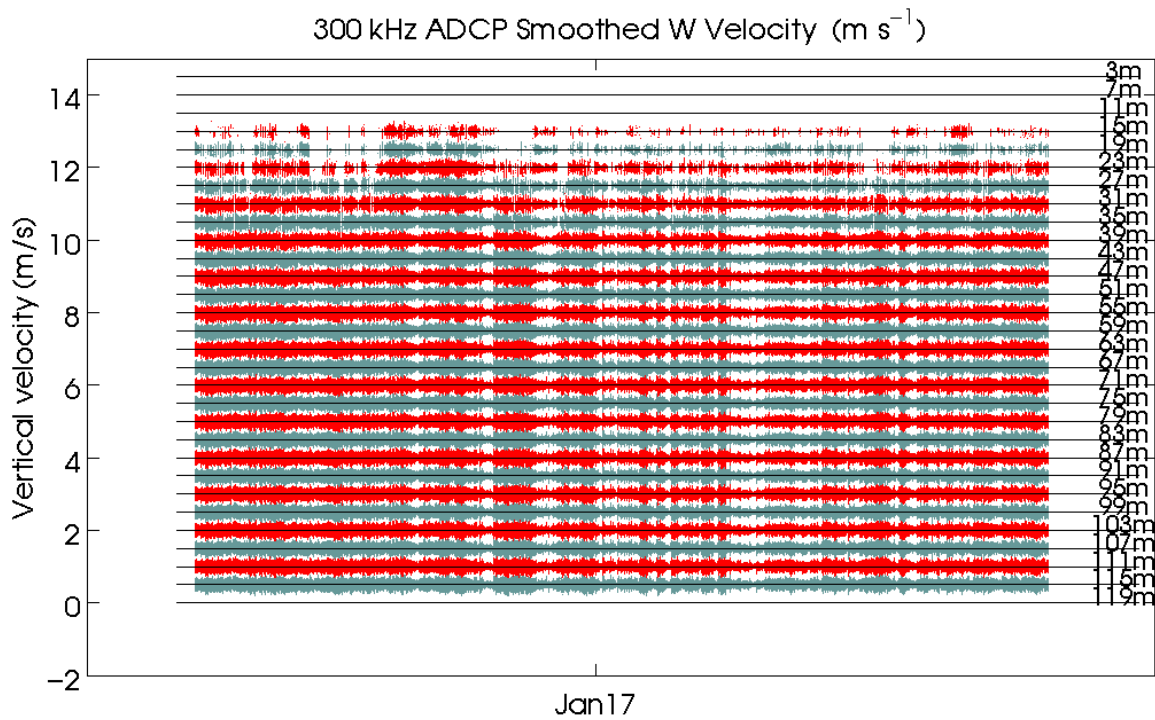
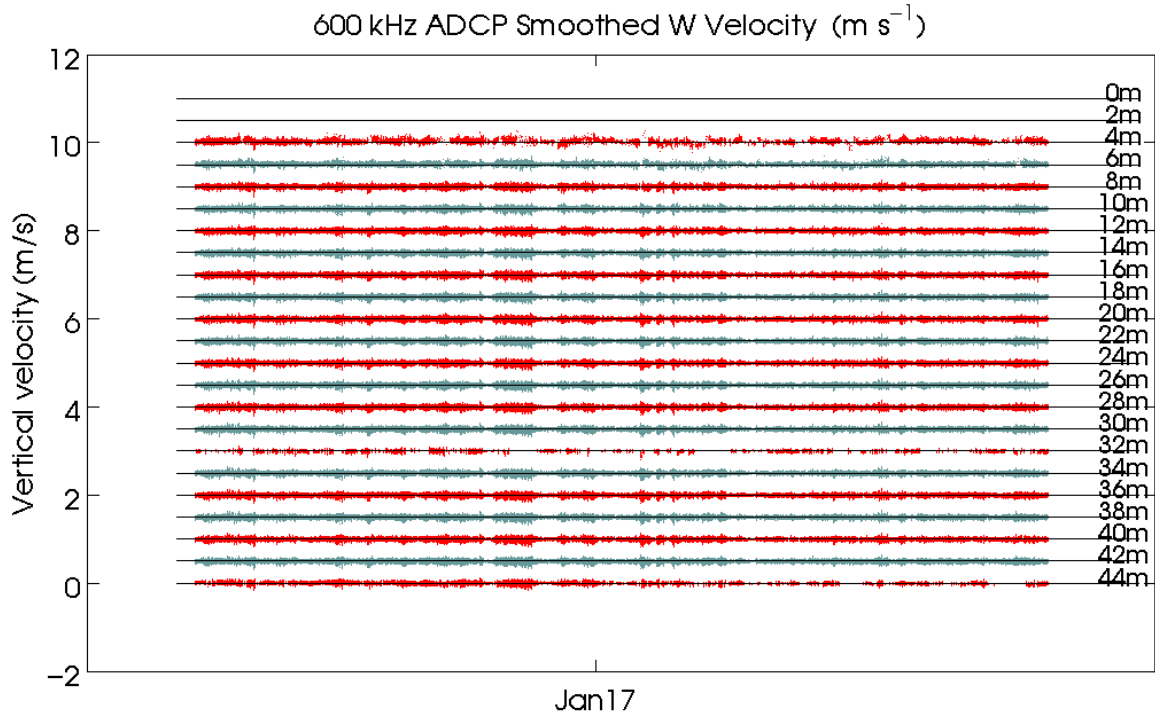


Figure 6-39. Staggered time-series of vertical velocity component (m s^{-1}) for each bin of the 600 kHz (upper panel), and 300 kHz (lower panel) moored ADCPs during WHOTS-13. The time-series are offset upwards by 0.5 m s^{-1} , the depth of each bin is on the right.

E. Moored and Shipboard ADCP comparisons

Contours of zonal and meridional current components from the Ship *Hi'ialakai's* Ocean Surveyor broadband 75 kHz shipboard ADCP, and the moored 300 kHz ADCP from the WHOTS-13 deployment as a function of time and depth, during the WHOTS-13 cruise are shown in Figures 6-40 and 6-41. Similar comparisons during the WHOTS-14 cruise are in Figures 6-42 and 6-43.

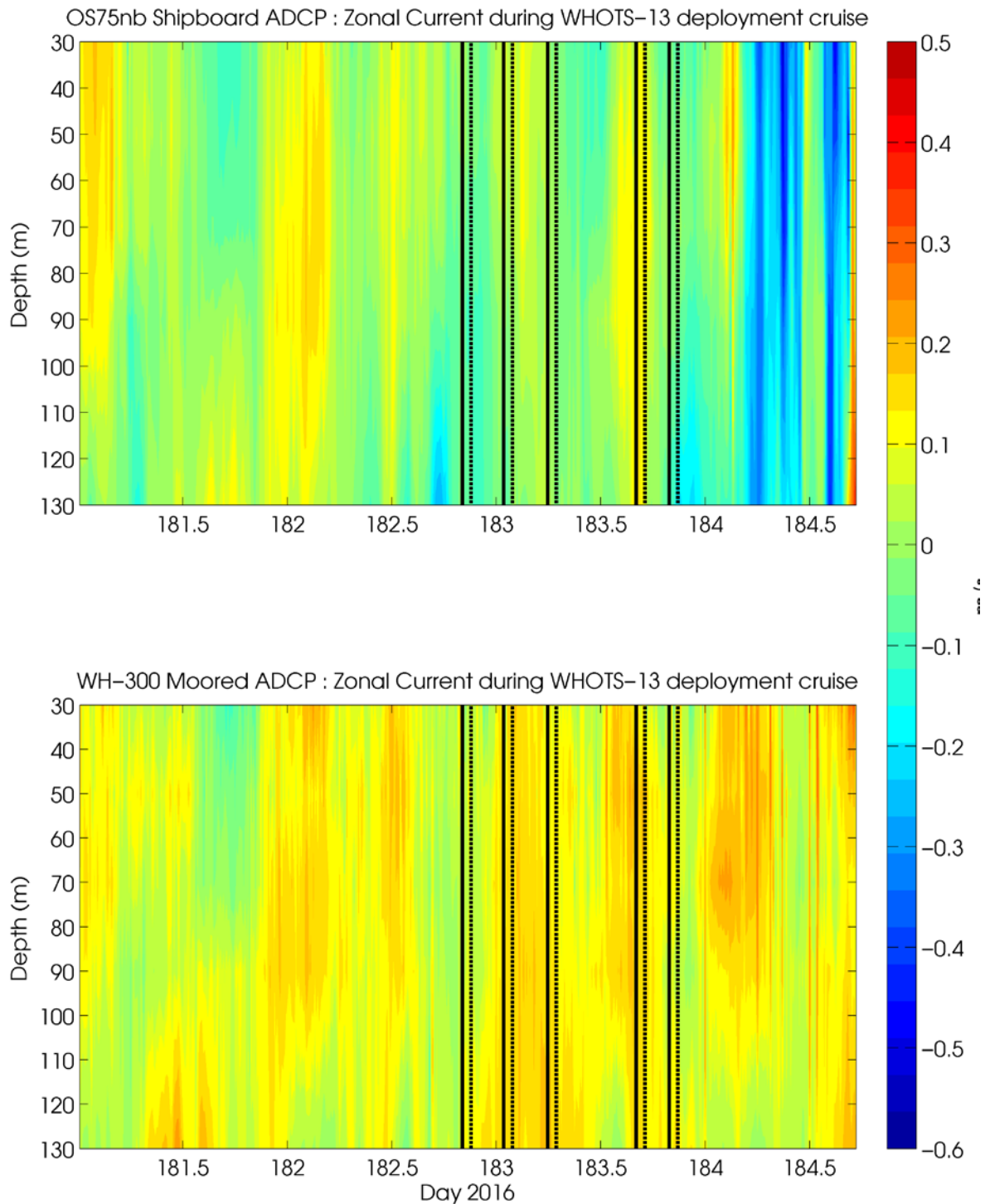


Figure 6-40. Contour of zonal currents ($m s^{-1}$) from the Ship Hi'ialakai's Ocean Surveyor narrowband 75 kHz shipboard ADCP (upper panel), and the moored 300 kHz ADCP from the WHOTS-13 mooring (bottom panel) as a function of time and depth, during the WHOTS-13 cruise. Times when the CTD rosette were in the water are identified between solid and dashed black lines.

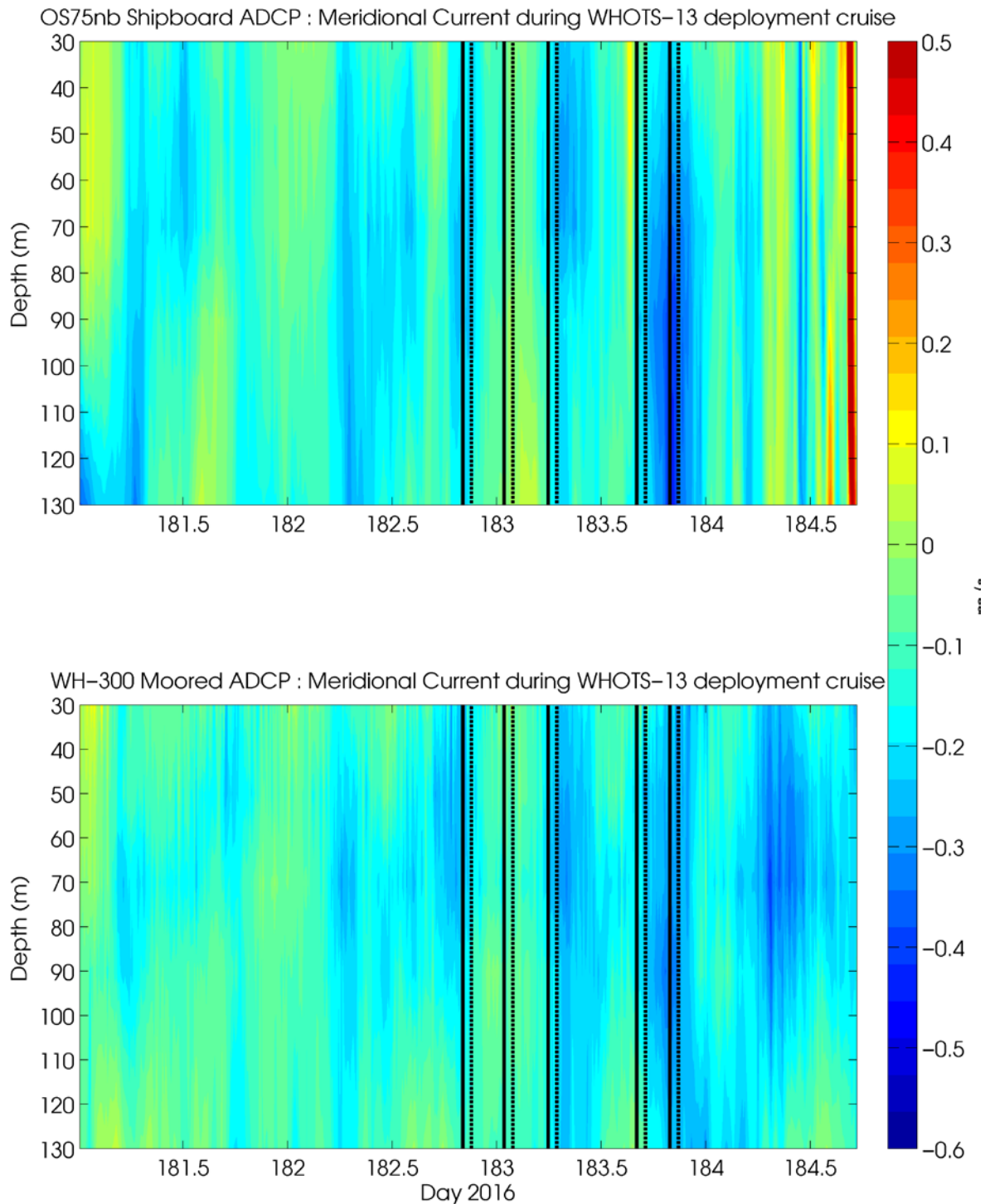


Figure 6-41. Contours of meridional currents ($m s^{-1}$) from the Ship *Hi'ialakai's* Ocean Surveyor narrowband 75 kHz shipboard ADCP (upper panel), and the moored 300 kHz ADCP from the WHOTS-13 mooring (lower panel) as a function of time and depth, during the WHOTS-13 cruise. Times when the CTD/rosette was in the water are identified between the solid and dashed black lines.

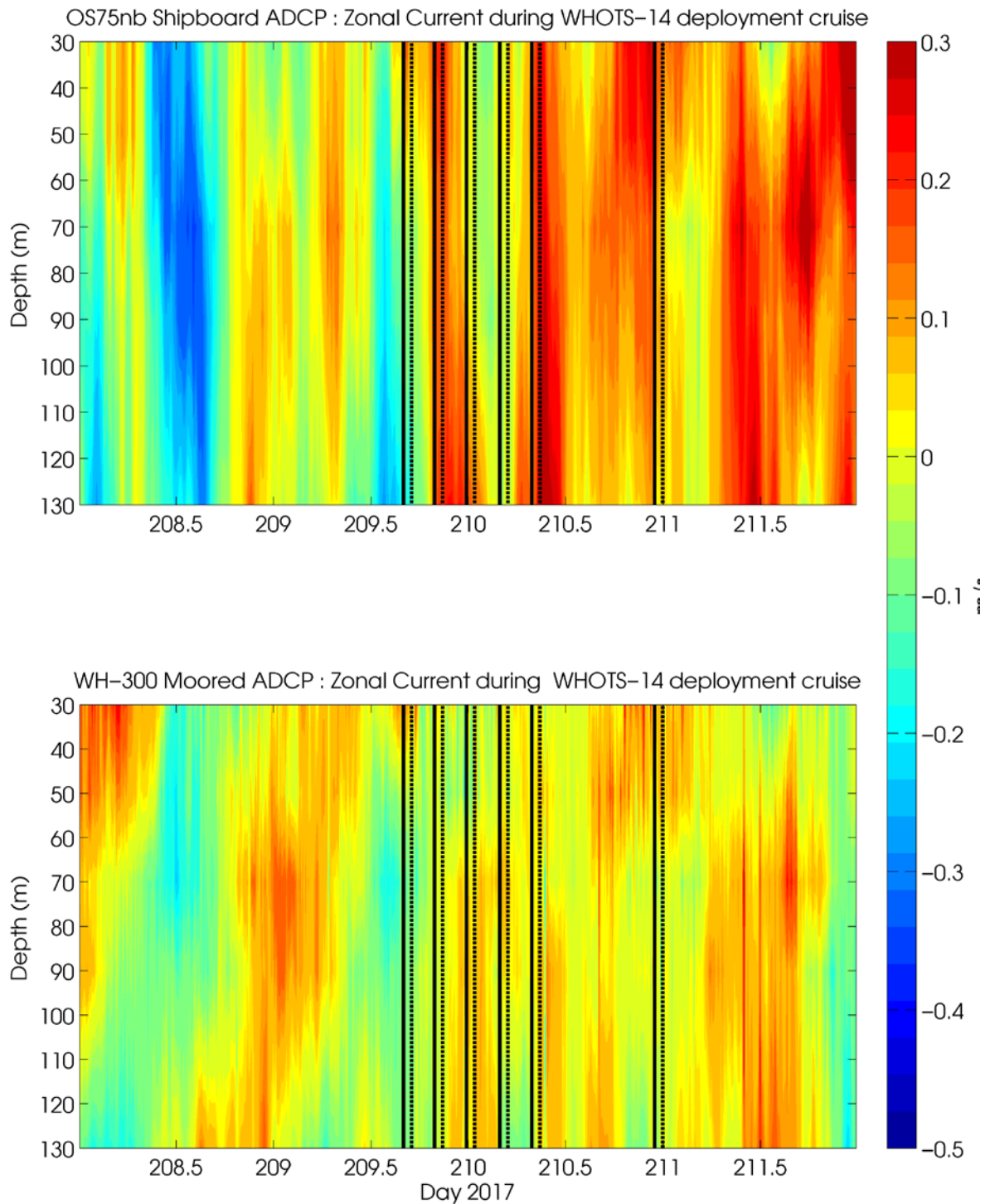


Figure 6-42. Contour of zonal currents ($m s^{-1}$) from the Ship Hi'ialakai's Ocean Surveyor narrowband 75 kHz shipboard ADCP (upper panel), and the moored 300 kHz ADCP from the WHOTS-13 mooring (bottom panel) as a function of time and depth, during the WHOTS-14 cruise. Times when the CTD rosette were in the water are identified between solid and dashed black lines.

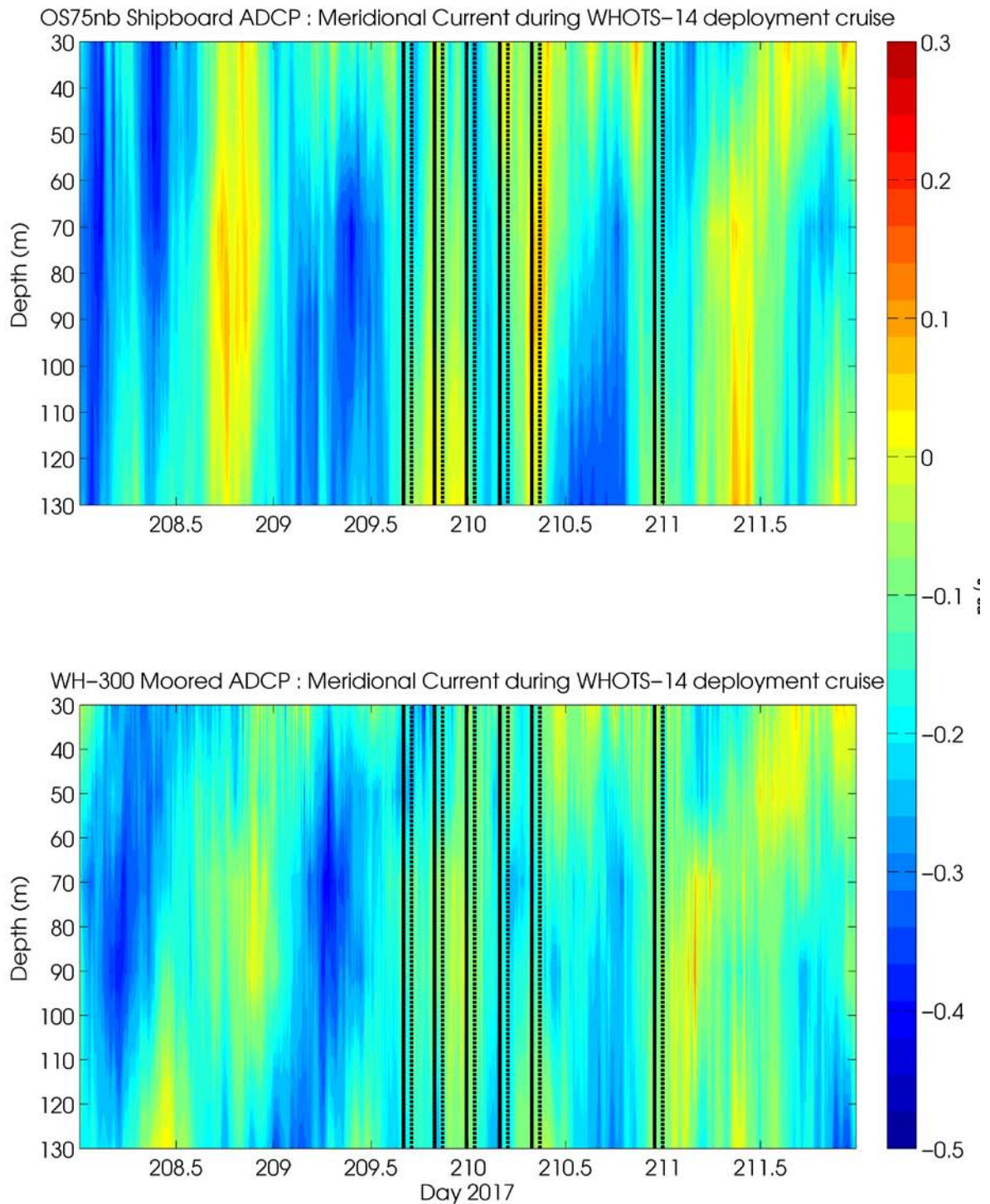


Figure 6-43. Contours of meridional currents ($m s^{-1}$) from the Ship *Hi'ialakai's* Ocean Surveyor narrowband 75 kHz shipboard ADCP (upper panel), and the moored 300 kHz ADCP from the WHOTS-13 mooring (lower panel) as a function of time and depth, during the WHOTS-14 cruise. Times when the CTD/rosette was in the water are identified between the solid and dashed black lines.

Comparisons between quality-controlled moored ADCPs during the WHOTS-13 deployment and available shipboard ADCP obtained during regular HOT cruises 285 to 294 and during the WHOTS-13 and -14 cruises are shown in Figure 6-44 for the 300 kHz ADCP, and Figure 6-45 for the 600 kHz ADCP. The shipboard profiles were taken when the ship was stationary, within 1 km of the mooring, and within 4 hours before the start and 4 hours after the end of the CTD cast conducted near the WHOTS mooring.

HOT cruises conducted on the R/V *Kilo Moana* (HOT-289 and 294) used data from a TRDI Workhorse 300 kHz ADCP (wh300) with 4 m bin size, reaching 100 m, and averaging ensembles every 2 minutes; and from a TRDI Ocean Surveyor 38 kHz operating in broad band mode (os38bb) with 12 m bin size, reaching 1200 m, with 5 minute ensemble averages, and in narrow band mode (os38nb) with 24 m bin size, reaching 1500 m and also with 5 minute ensemble averages. Data from the wh300 were used for the comparisons with the moored ADCP data, or from the os75bb if the wh300 data were not available. HOT cruises conducted on the R/V *Ka'Imikai-O-Kanaloa* (HOT-285-286 and 290-293) used data from a TRDI Workhorse 300 kHz ADCP (wh300) with 4 m bin size, reaching 100 m, and averaging ensembles every 2 minutes. HOT-287 was conducted aboard the R/V *Oceanus* using data from a wh300 with 4 m bin size, reaching 100 m, and averaging ensembles every 2 minutes; and from a TRDI Ocean Surveyor 75 kHz operating in broad band mode (os75bb) with 12 m bin size, reaching 1200 m, with 5 minute ensemble averages, and in narrow band mode (os38nb) with 24 m bin size, reaching 1500 m and also with 5 minute ensemble averages. Data from the wh300 were used for the comparisons with the moored ADCP data, or from the os75bb if the wh300 data were not available. HOT-288 was conducted aboard the R/V *Sikuliaq* using data from two TRDI Ocean Surveyors, in 75 kHz and 150 kHz, and both operating in broad band mode (os75bb/os150bb) with 12 m bin size, reaching 1200 m, with 5 minute ensemble averages, and in narrow band mode (os75nb/os150nb) with 24 m bin size, reaching 1500 m and also with 5 minute ensemble averages. Data from the os75bb were used for the comparisons with the moored ADCP data.

The moored ADCP data were collected from the upward facing 300 kHz ADCP located at 125 m and the upward facing 600 kHz ADCP located at 47.5 m over the same time period. Zonal (U), and meridional (V) current components from the shipboard and moored vertical profiles were interpolated to the profile resolution of the shipboard ADCP, and ensemble mean profiles were obtained for each data set to compute differences between them. Bins with less than 50% data were excluded.

WHOTS-13 300 kHz to HOT Shipboard ADCP Comparisons

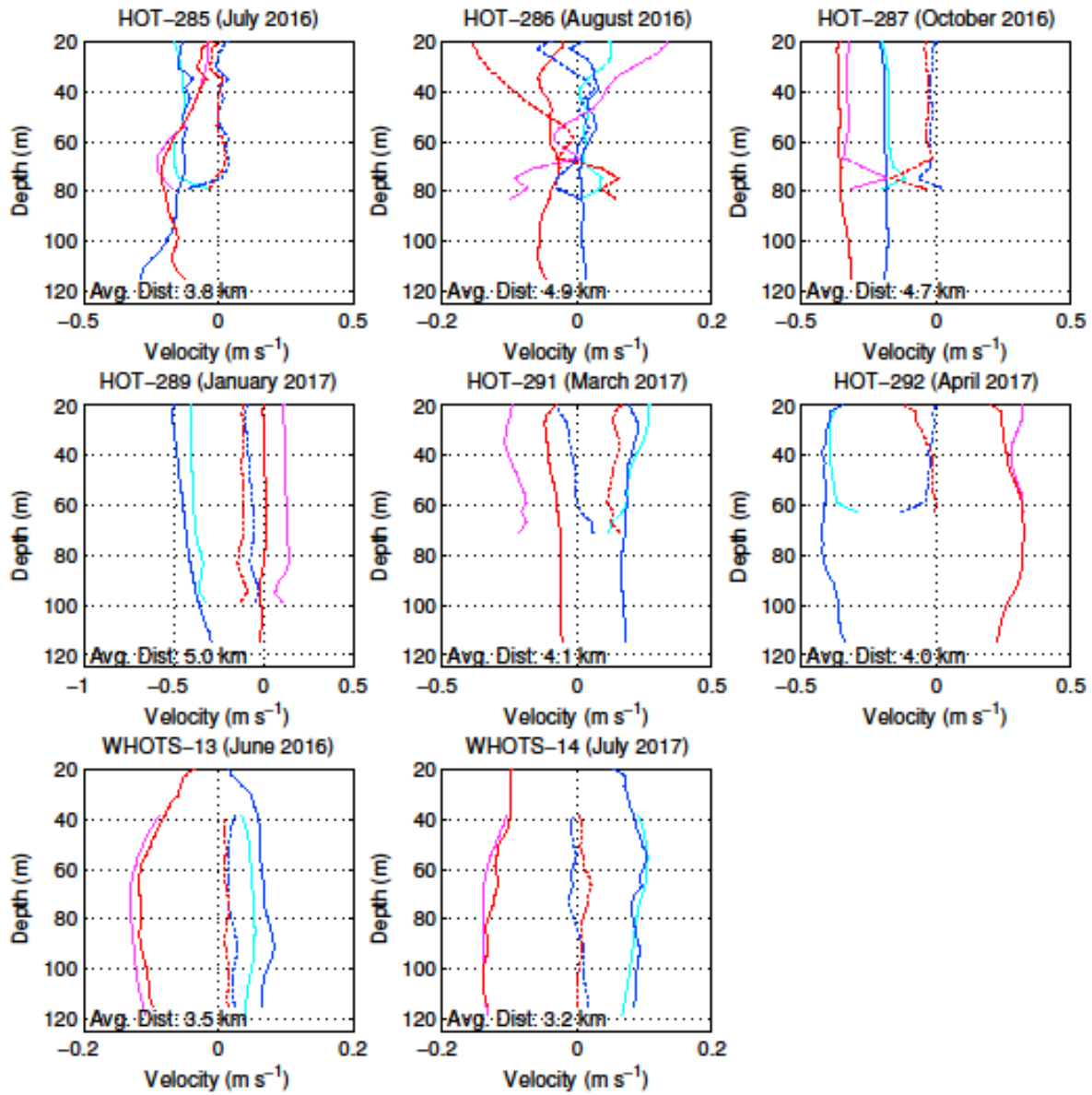


Figure 6-52. Mean current profiles during shipboard ADCP (cyan: zonal, magenta: meridional) versus moored 300 kHz ADCP (blue: zonal, red: meridional) intercomparisons from HOT-285 through HOT-292 and from WHOTS-13 and WHOTS-14 cruises. Moored minus shipboard ADCP differences shown in dotted lines (blue: zonal, red: meridional).

WHOTS-13 600 kHz to HOT Shipboard ADCP Comparisons

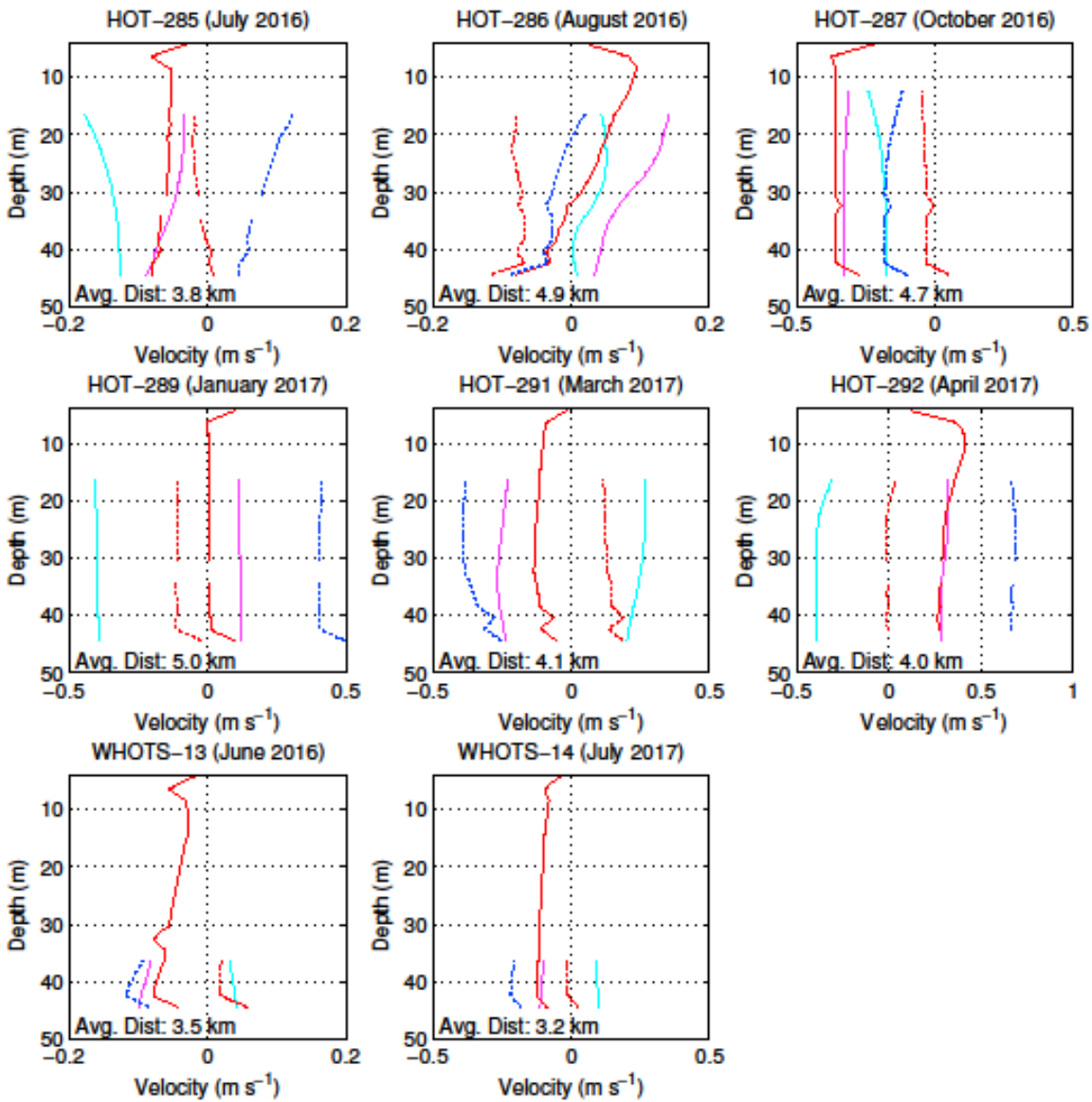


Figure 6-63. Mean current profiles during shipboard ADCP (cyan: zonal, magenta: meridional) versus moored 600 kHz ADCP (blue: zonal, red: meridional) intercomparisons from HOT-285 through HOT-292 and from WHOTS-13 and WHOTS-14 cruises. Moored minus shipboard ADCP differences shown in dotted lines (blue: zonal, red: meridional).

F. Next Generation Vector Measuring Current Meter data (VMCM)

Time-series of daily mean horizontal velocity components for the VMCM current meters deployed during WHOTS-13 at 10 m and 30 m are presented in *Figure 6-44*.

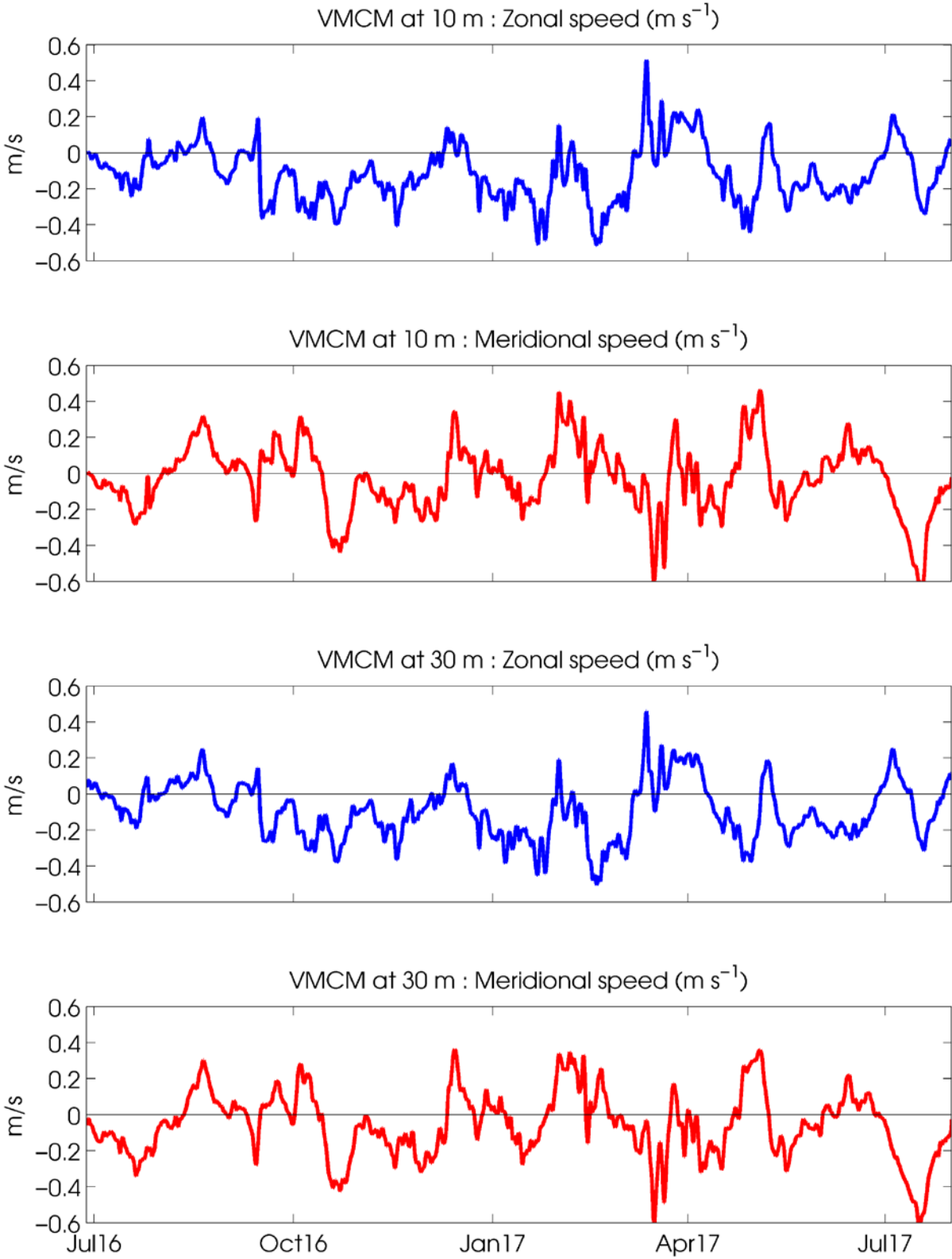


Figure 6-74. Horizontal velocity data (m/s) during WHOTS-13 from the VMCMs at 10 m depth (first and second panel) and at 30 m depth (third and fourth panel).

G. GPS data

Time-series of latitude and longitude of the WHOTS-13 buoy from GPS data are presented in Figure 6-45 and spectra of the time-series is shown in Figure 6-46.

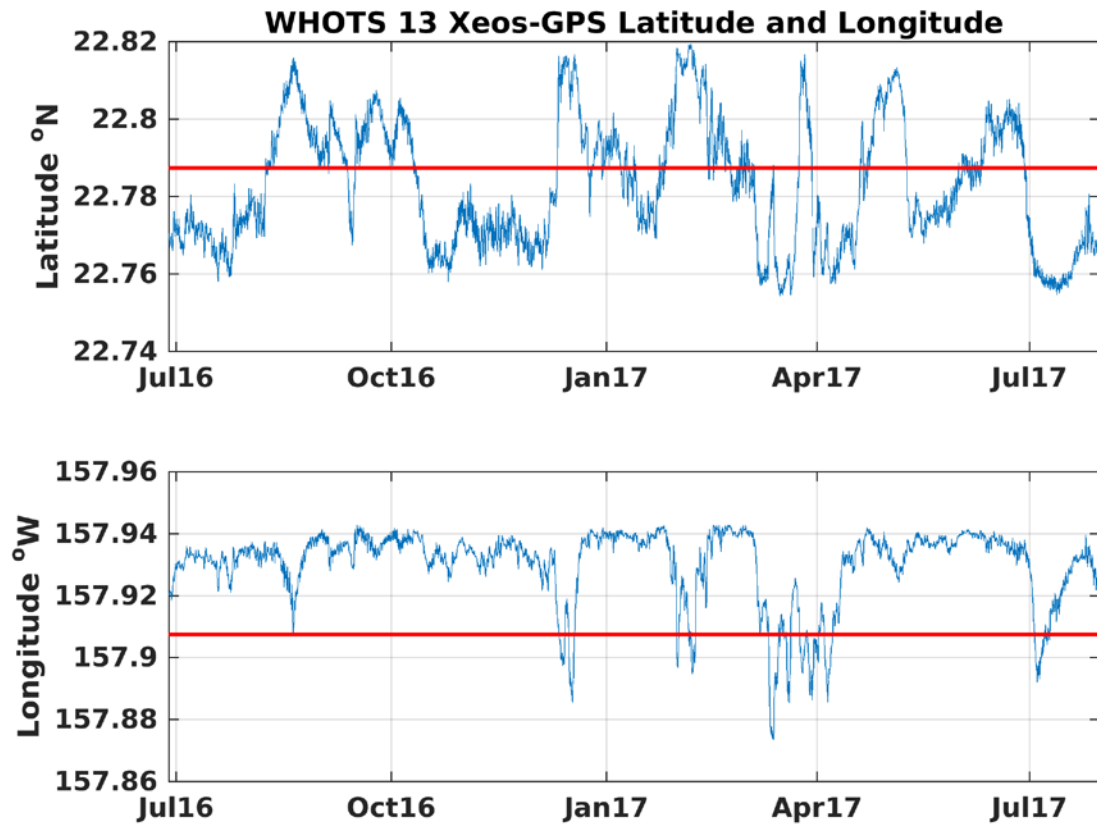


Figure 6-85. GPS Latitude (upper panel) and longitude (lower panel) time series from the WHOTS-13 deployment.

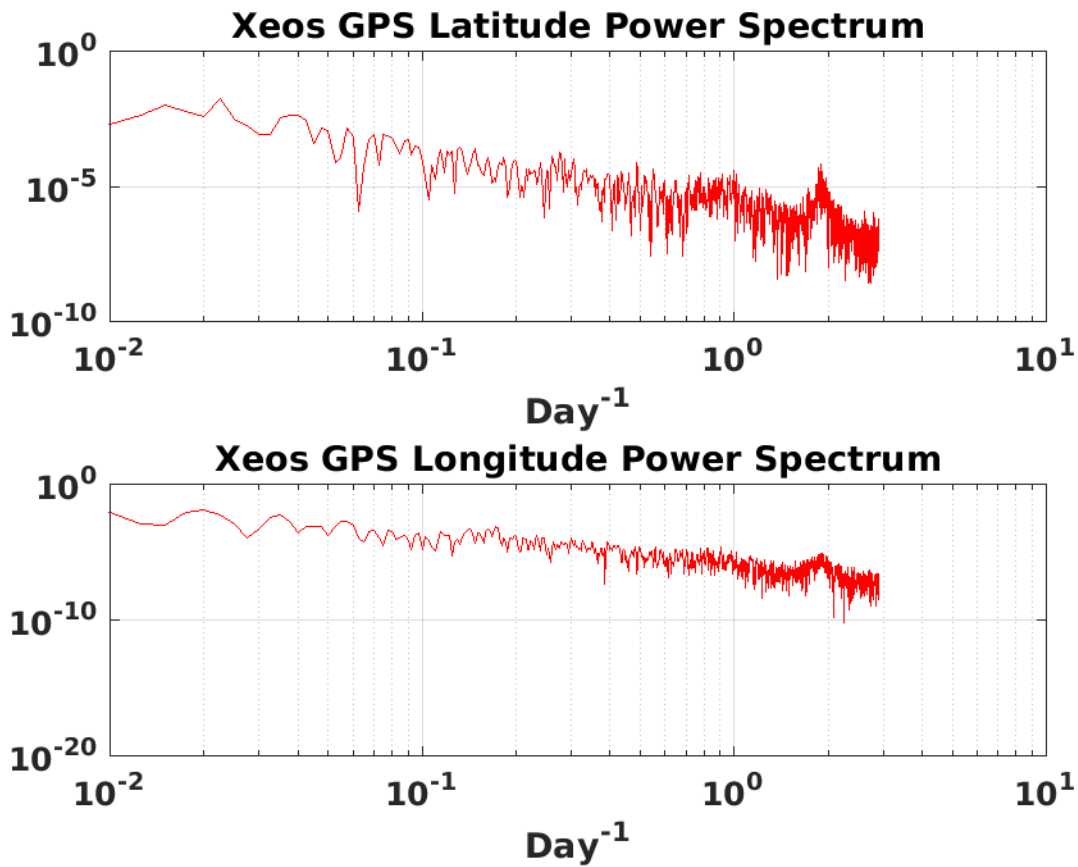


Figure 6-96. Power spectrum of latitude (upper panel) and longitude (lower panel) for the WHOTS-13 deployment.

H. Mooring Motion

The position of the mooring with respect to its anchor was determined from the ARGOS positions as shown in Section V.D. Additional information of the mooring motion was provided by the ADCP data of pitch, roll and heading, shown in this section.

Figure 6-47 shows the ADCP data of the instrument's tilt (a combination of the pitch and roll), plotted against the buoy's distance from its anchor (derived from ARGOS positions), for both WHOTS ADCP's. The red line in the plot is a quadratic fit to the median tilt calculated every 0.2 km distance bins. The figure shows that during both deployments, the ADCP tilt increased as the distance from the anchor increased. This tilting was caused by the deviation of the mooring line from its vertical position as it was pulled by the anchor. The tilting of the line also caused the rising of the instruments attached to the line.

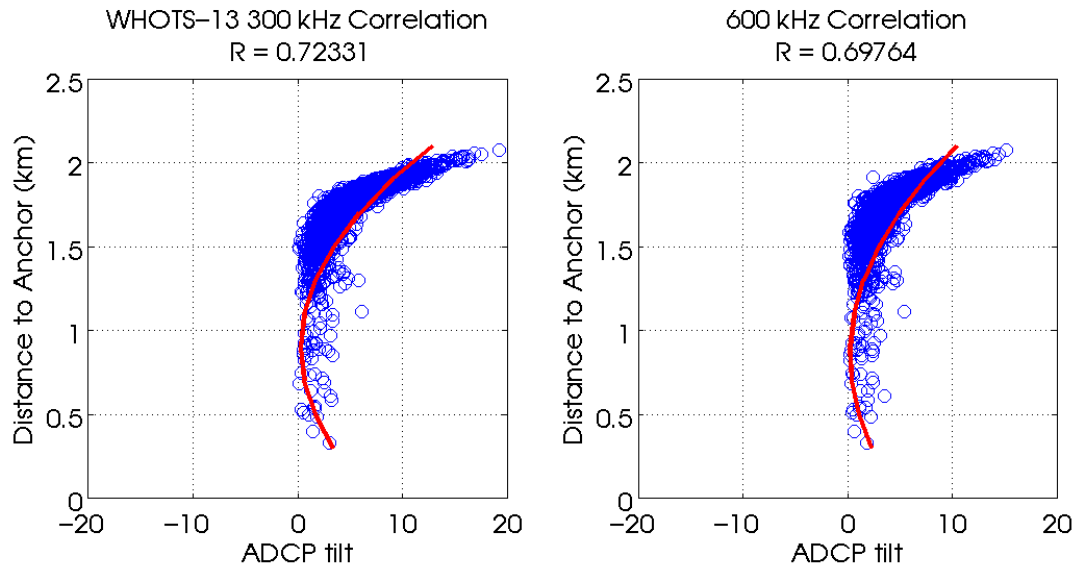


Figure 6-107. Scatter plots of ADCP tilt and distance of the buoy to its anchor during the WHOTS-13 deployment for the 300 kHz (left panel), and the 600 kHz ADCP deployments (right panel, blue circles). The red line is a quadratic fit to the median tilt calculated every 0.2 km distance bins.

VII. References

- Colbo, K., R. Weller, 2009. Accuracy of the IMET Sensor Package in the Subtropics. *J. Atmos. Oceanic Technol.*, 26, 1867-1890.
- Firing, E., 1991. Acoustic Doppler Current Profiling measurements and navigation. In *WOCE Hydrographic Operations and Methods*. WOCE Operations Manual, WHP Office Report WHPO 91-1, WOCE Report No. 68/91, 144pp.
- Freitag, H. P., M. E. McCarty, C. Nosse, R. Lukas, M. J. McPhaden, and M. F. Cronin, 1999. COARE Seacat data: Calibrations and quality control procedures. NOAA Technical Memorandum, ERL PMEL-115. 93 pp.
- Fujiaki et al 2019. HOT data report 29: 2017 (in preparation).
- Fujiaki L. A., F. Santiago-Mandujano, K. Rosburg, K. Trifonova, R. Lukas, and D. Karl, 2018. Hawaii Ocean Time-series Data Report 28: 2016. School of Ocean and Earth Sciences and Technology publication # 10564. 416 pp.
- Hosom, D. R. Weller, R. Payne, and K. Prada, 1995. The IMET (Improved Meteorology) Ship and Buoy Systems. *J. Atmos. Oceanic Technol.*, 12, 527-540.
- Howe, B. M., R. Lukas, F. Duennebieer, and D. Karl, ALOHA cabled observatory installation, *OCEANS 2011*, 19-22 Sept. 2011.
- Kara, A. B., P. A. Rochford, and H. E. Hulbert, 2000. Mixed layer depth variability and barrier layer formation over the North Pacific Ocean, *J. Geophys. Res.*, 105, 16,803–16,821.
- Lukas, R., F. Santiago-Mandujano, F. Bingham and A. Mantyla, 2001. Cold bottom water events observed in the Hawaii Ocean time-series: Implications for vertical mixing. *Deep-Sea Res.* I, 48 (4), 995-1021
- Owens, W. B. and R. C. Millard, 1985. A new algorithm for CTD oxygen calibration. *Journal of Physical Oceanography*, 15, 621-631.
- Plueddemann, A.J., R.A. Weller, R. Lukas, J. Lord, P.R. Bouchard, and M.A. Walsh, 2006, WHOI Hawaii Ocean Timeseries Station (WHOTS): WHOTS-2 Mooring Turnaround Cruise Report, Woods Hole Oceanographic Institution, Technical Report WHOI-2006-08, 68 pp.
- Santiago-Mandujano, F., J. Snyder, K. Rosburg, A. King, S. Natarov, K. Maloney, N. Howins, G. Hebert, and R. Lukas. 2017. UH Contributions to WHOTS-14 Cruise Report. School of Ocean and Earth Science and Technology, University of Hawaii. Internal Report , 54 pp. (http://www.soest.hawaii.edu/whots/proc_reports/WHOTS-13_CruiseRpt.html).

Santiago-Mandujano, F., D. McCoy, J. Snyder, R. W. Deppe, K. Rosburg, G. Carter, K. Berry, and R. Lukas. 2016. UH Contributions to WHOTS-13 Cruise Report. School of Ocean and Earth Science and Technology, University of Hawaii. Internal Report , 55 pp. (http://www.soest.hawaii.edu/whots/proc_reports/WHOTS-13_CruiseRpt.html).

Santiago-Mandujano, F., P. Lethaby, R. Lukas, J. Snyder, Weller, A. Plueddeman, J. Lord, S. Whelan, P. Bouchard, and N. Galbraith, 2007. Hydrographic Observations at the Woods Hole Oceanographic Institution (WHOI) Hawaii Ocean Timeseries (HOT) Site (WHOTS): 2004-2006. School of Ocean and Earth Science and Technology, University of Hawaii. (http://www.soest.hawaii.edu/whots/data_report1.html)

Tupas, L., F. Santiago-Mandujano, D. Hebel, R. Lukas, D. Karl, and E. Firing 1993. Hawaii Ocean Time-series Data Report 4, 1992, School of Ocean and Earth Science and Technology, University of Hawaii, 93-14, 248 pp.

Tupas, L., F. Santiago-Mandujano, D. Hebel, C. Nosse, L. Fujieki, E. Firing, R. Lukas, D. Karl, 1997. Hawaii Ocean Time-series Data Report 8, 1996, School of Ocean and Earth Science and Technology, University of Hawaii, 97-7, 296 pp.

UNESCO. 1981. Tenth Report of the Joint Panel on Oceanographic Tables and Standards. UNESCO Technical Papers in Marine Science, No. 36, UNESCO, Paris.

Whelan S., R. Weller, R. Lukas, F. Bradley, J. Lord, J. Smith, F. Bahr, P. Lethaby, J. Snyder, 2007. WHOI Hawaii Ocean Timeseries Station (WHOTS): WHOTS-3 Mooring Turnaround Cruise Report. Technical Report. Woods Hole Oceanographic Institution, WHOI-2007-03, 103 pp.

VIII. Appendices

A. Appendix 1: WHOTS-13 300 kHz ADCP Configuration

Program Version 50.4

System Frequency 300 kHz

Convex

Sensor Configuration #1

Transducer Head Attached TRUE

Orientation UP

Beam Angle 20 Degrees

Transducer 4 Beam Janus

Real Data

CPU Serial Number: 7637

False Target Threshold Maximum (WA) 70 counts

Bandwidth Control (WB) 0

Low Correlation Threshold (WC) 64 counts

Error Velocity Threshold, mm/s (WE) 2000 mm/s

Blank After Transmit, cm (WF) 176 cm

Minimum Percent Good (WG) 0

Water Reference Layer (WL) 003, 007, first bin, last bin

Mode (WM) 1

No. of depth cells (bins) (WN) 30

Pings per ensemble (WP) 40

Depth Cell Size (bin length), cm (WS) 400 cm

Ambiguity Velocity, cm/s radial (WV) 175 cm/s

Heading Alignment, deg (EA) 0.00 degrees

Heading Bias, deg (EB) 9.39 degrees

Coord Transform (EX) 00011111 Earth Coordinates

Sensor Source (EZ) 01111101 cdhprst

Sens Avail 00011101 cdhprst

Time per Ping, sec (TP) 00:04.00

Time per Ensemble, min (TE) 10:00.00

Hardware 4 Beams

Code Reps. 9

Lag Length 0.49 m

Xmt Length 4.42 m

1st Bin 6.22 m

B. Appendix 2: WHOTS-13 600 kHz ADCP Configuration

Program Version 50.4
 System Frequency 300 kHz
 Convex
 Sensor Configuration #1
 Transducer Head Attached TRUE
 Orientation UP
 Beam Angle 20 Degrees
 Transducer 4 Beam Janus

Real Data
 CPU Serial Number: 7637
 False Target Threshold Maximum (WA) 70 counts
 Bandwidth Control (WB) 0
 Low Correlation Threshold (WC) 64 counts
 Error Velocity Threshold, mm/s (WE) 2000 mm/s
 Blank After Transmit, cm (WF) 088 cm
 Minimum Percent Good (WG) 0
 Water Reference Layer (WL) 003, 007, first bin, last bin
 Mode (WM) 1
 No. of depth cells (bins) (WN) 25
 Pings per ensemble (WP) 80
 Depth Cell Size (bin length), cm (WS) 200 cm
 Ambiguity Velocity, cm/s radial (WV) 175 cm/s

Heading Alignment, deg (EA) 0.00 degrees
 Heading Bias, deg (EB) 9.39 degrees
 Coord Transform (EX) 00011111 Earth Coordinates
 Sensor Source (EZ) 01111101 cdhprst
 Sens Avail 00011101 cdhprst
 Time per Ping, sec (TP) 00:02.00
 Time per Ensemble, min (TE) 10:00.00

Hardware 4 Beams
 Code Reps. 9
 Lag Length 0.25 m
 Xmt Length 2.21 m
 1st Bin 3.11 m